MASTER THESIS SPRING 2012

for

Stud. Techn. Jon Marius Aasheim

Conceptual Design of Surface Buoy for Arctic Conditions

Konseptuel prosjektering av overflatebøye for arktiske strøk

Hydrocarbon exploration and exploitation in arctic regions are expected to increase substantially in the years to come. Potential reserves are often located at a significant water depth, making bottom supported installations practically unfeasible. An alternative is to install floating production units or sub sea installations, possibly assisted by surface floaters for power supply and/or maintenance work. The floaters may be assisted by ice management, e.g. by means of icebreakers, but they may also be designed to resist the actions of ice drifting on the platforms.

The ice actions depend heavily on the layout of the structure at the sea surface. The forces may be significantly reduced if the structure has a conical shape as opposed to a vertical side, so as to enable breaking of ice flows rather than crushing. This layout may however have significant draw-backs with respect to wave induced motions. At the conceptual design stage it is essential to balance the various conflicting requirements in a systematic manner, e.g by performing parametric studies of the governing design parameters. As an aid to decision making in the conceptual design stage a tool for fast analysis should be developed.

The purpose of the work is to contribute to the development of the assessment tool. The starting point for the development are the master thesis of Nils Gunnar Viko and Einar Bernt Glomnes and existing software based on MATLAB, and model tests of a conical surface buoy carried out for Force Technology in 2006.

The work is proposed carried out in the following steps

1. Review of laboratory sea keeping tests for the icebreaking buoy carried out by Force Technology. Perform statistical analysis of selected response histories. On the basis of the results discuss the motion characteristics of the buoy

2. On the basis of a critical review of the MATLAB program developed by Viko/Glomnes decide whether a new code should be included, where the static and dynamic pressure form the sea are integrated numerically. Alternatively, modify the existing software to improve its behaviour for large sea states. To appropriately account for wave nonlinearities, the hydrodynamic forces should be integrated up to actual surface level, and also take into account any exceedance of the conical side and or the freeboard. A flowchart of the program shall be developed, and the code shall be properly documented/commented. It is advised to start with pure heave motion before addressing combined pitch/heave motion. Modelling of mooring lines shall be considered.

3. Establish a model of the buoy for WASIM analysis. Modelling of mooring lines shall be considered.

4. Verify and calibrate model parameters by comparison with selected test results. Simulate all or a number of the tests with the simplified program and WASIM. Compare time series as well as the statistical properties of the most important response terms for both programs and the tests.

5. Discuss the applicability of the buoy with respect to open water behaviour. To the extent needed supplementary simulations should be carried out.

6. If time permits develop an algorithm for ice forces for buoy in level ice based on Croasdale's method. Simulate the behaviour of the buoy under normal and extreme level ice conditions.

7. Conclusions and recommendation for further work

Literature studies of specific topics relevant to the thesis work may be included.

The work scope may prove to be larger than initially anticipated. Subject to approval from the supervisors, topics may be deleted from the list above or reduced in extent.

In the thesis the candidate shall present his personal contribution to the resolution of problems within the scope of the thesis work.

Theories and conclusions should be based on mathematical derivations and/or logic reasoning identifying the various steps in the deduction.

The candidate should utilise the existing possibilities for obtaining relevant literature.

Thesis format

The thesis should be organised in a rational manner to give a clear exposition of results, assessments, and conclusions. The text should be brief and to the point, with a clear language. Telegraphic language should be avoided.

The thesis shall contain the following elements: A text defining the scope, preface, list of contents, summary, main body of thesis, conclusions with recommendations for further work, list of symbols and acronyms, references and (optional) appendices. All figures, tables and equations shall be numerated.

The supervisors may require that the candidate, in an early stage of the work, presents a written plan for the completion of the work. The plan should include a budget for the use of computer and laboratory resources that will be charged to the department. Overruns shall be reported to the supervisors.

The original contribution of the candidate and material taken from other sources shall be clearly defined. Work from other sources shall be properly referenced using an acknowledged referencing system.

The report shall be submitted in two copies: - Signed by the candidate - The text defining the scope included - In bound volume(s) - Drawings and/or computer prints which cannot be bound should be organised in a separate folder.

Ownership

NTNU has according to the present rules the ownership of the thesis. Any use of the thesis has to be approved by NTNU (or external partner when this applies). The department has the right to use the thesis as if the work was carried out by a NTNU employee, if nothing else has been agreed in advance.

Thesis supervisors

Prof. Jørgen Amdahl and Sverre Steen

At Force Technology, Sandvika: Marc LeFranc

Deadline: June 10, 2012

Trondheim, January 15, 2012

Jørgen Amdahl

Preface

This thesis is culmination of my work in the final semester at the Department of Marin Technology at the Norwegian University of Science and Technology. The master thesis counts for 30 credits in the tenth semester of the Master of Science in Marin Technology.

The work on this thesis has been very challenging due to the programming part of the task. The most time consuming was to find the simplest allowable theory i could apply. The success of the thesis work has largely depended on my ability to produce a working code. Luckily, I managed to get started with the programming early in the semester, because even though the bulk of the programming was completed in good time before the deadline I struggled with the pitch motion until 2 weeks before the deadline. At that point I had been working for several weeks trying to find errors in the code which could be the cause of the bad results and I had almost resigned myself with not completing. Unfortunately, this also resulted in loss of valuable time which could have been used to improve and rewrite some old functions.

I would like to thank my supervisor professor Jørgen Amdahl for his support and encouragement through the thesis work, Marc Lefranc at Force Technology for allowing me access to the model test results, and Einar B. Glomnes and Gunnar Viko for their previous work which gave me a much needed head start without which the code would not have worked. I would also like to thank my fellow students for various input and help, particularly with the LaTeXcoding.

And finally I would like to thank my girlfriend and my family for being supportive through these 5 years of studying.

Trondheim, 8 June 2012

Jon Marius Aasheim

Summary

Due to a rising interest in oil exploration in Arctic areas several new platform designs have been introduced to combat the problems with level ice loads. This has led to research into ice strengthening and how this affects the open water behaviour. One of the new designs, called the Total Buoy, has a slanted hull in the waterline intended to deflect level ice down and around the structure, but this hull design introduces a geometrical non-linearity. This non-linearity causes problems in the design of these types of structures, because most hydrodynamic program cannot handle the rapid change of geometry in the waterline. This has inspired several attempts to write a simple numerical model to handle the calculation, and avoid costly model tests in the pre-design.

A large part of this thesis presents the theory and methods used in the development of this new numerical model. This is meant to document the thought process in a way which can allow others to continue the development. The numerical model was developed to calculate motion results from regular waves in the three symmetric motions; Surge, Heave and Pitch. In addition to this a very simple ice calculation was included as a starting point for further development.

As part of this work on a new numerical model a parallel study of an alternative commercial program was done. This is to test the usability of an (expensive) commercial program in relation to this non-linear problem. The DNV program Wasim was selected for this purpose, and the modelling has also been documented and the input files are included in the electronic appendix.

After documenting the basis of the numerical model and Wasim model it was necessary to do a comprehensive comparison study of the models. To help with the comparison Force Technology allowed the use of model tests results which were performed on the Total Buoy concept in 2006. The comparisons showed that while the numerical model was showing some large responses around the heave natural period in both heave and pitch the results were in general close to the model tests. The Wasim model did not show the same correlation in surge and pitch, but the heave results were shown to be close, but the use of the Wasim program is believed to be unwise on this type of problem.

Finally, an assessment of the Total Buoy's open water and level ice behaviour was done. This assessment showed that the Total buoy would most likely have problems with large pitch motions. This was shown to be true in both the Norwegian Sea and the Eastern Barents Sea, the Norwegian Sea was found to be a unlikely deployment area due to the lack of level ice. The pitch motion was so large that it would make year round human habitation impossible, and it was advised that the buoy should not be used for this purpose, and only in the eastern Barents Sea. Finally, it was found that the ice theory which was applied for the ice calculation could not give a true assessment of the level ice capabilities of the buoy, and the lack of other alternative solutions made the assessment impossible.

Sammendrag

På grunn av en økende interesse for oljeleting i Arktis, så har man kommet med nye designer på offshore plattformer som er beregnet for å håndtere is laster. Dette har ført til forskning på nye måter å bryte isen på, og hvordan disse nye designene påvirker oppførselen til strukturene i åpent vann. Ett av disse nye designene er Total bøyen som er en konisk overflatebøye som skal være mer effektiv i håndteringen av is. Problemet med dette designet er at den koniske formen introduserer en ikke-linearitet på grunn av stor forandring i vannlinjen. Dette gjør at de fleste beregningsprogram ikke klarer å håndtere problemet. Denne masteroppgaven har som mål å starte utviklingen av en enkel beregningsmodell for å håndtere hydrodynamikk for ikke-lineær geometri og islaster.

En stor del av denne oppgaven brukes til å presentere den teoretiske basisen som brukes i beregningsmodellen, og oppbygningen av selve programmet. Dette er ment til å gi andre innsikt i tankeprosessen slik at de kan bruke programmet, og eventuelt utbedre det som mangler. Beregningsmodellen er i første omgang laget for å håndtere regulære bølger, og beregne bevegelsene for Jag, Hiv og Stamp. I tillegg til dette har det også blitt laget en enkel ismodul som et startpunkt for videre utvikling.

Parallelt med arbeidet på den numeriske modellen, så har det også blitt gjort et forsøk på å modellere problemet i et kommersielt hydrodynamisk program. Programmet som ble brukt er DNVs Wasim, som er en del av Sesam pakken. Dette var for å undersøke om et alternativt kommersielt program kunne løse oppgaven, og eventuelt brukes for å hjelpe til med utviklingen av beregningsmodellen. Modelleringen har derfor også blitt dokumentert i oppgaven samt inkludert i form av input filer i appendiks.

Ved hjelp av modellforsøk på Total bøyen gjennomført av Force Technology i 2006, så ble det mulig å sammenligne modellene. Sammenligningen viste at selv om den numeriske modellen hadde noen store responsamplituder, i både hiv og stamp, nær egensvingeperioden i hiv, så var resultatene ellers veldig nære modellforsøkene. Wasim modellen hadde ikke samme korrelasjon med modellforsøkene i jag og stamp, men heller en lineærrelasjon. Hivbevegelsen derimot viste større likhet med modellforsøkene. Dette var fremdeles ikke nok til at Wasim kan anbefales til fremtidig arbeid med dette problemet.

Helt til slutt ble det gjort en utredning av Total bøyens oppførsel i bølger og i is. Denne utredningen viste at Total bøyen mest sannsynlig vil ha problemer med stampebevegelser. Dette på tross av at bøyen sannsynligvis er ment til å bli brukt i det østre Barentshavet som har mye mildere sjøtilstander enn i Norskehavet. Stampebevegelsene viste seg å være såpass store in noen tilfeller at det ikke kan anses som forsvarlig for mennesker å oppholde seg der året rundt. Det anbefaltes derfor at bøye, dersom den skal brukes, benyttes som en ubemannet installasjon mesteparten av tiden. I forsøket på å vurdere iskapabiliteten til bøyen, så ble det oppdaget at det fantes svært lite i form av dokumentasjon på metoden som ble brukt til isberegningen og ellers få alternative løsninger til sammenligning. Det ble derfor umulig å gjøre en skikkelig utredning av iskapabiliteten til Total bøyen.

Contents

List of Figures

List of Tables

Nomenclature

Abbreviations

BEM	Boundary Element Method
CFD	Computational Fluid Dynamics
GUI	Graphical User Interface
RAO	Response Amplitude Operator
SWL	Still Water Level

Greek Symbols

λ	Wave length
ϕ	Velocity potential
ζ_d	Damping ratio
ω	Wave Frequency
ρ	Density of Sea Water
ζ	Wave Elevation
ζ_a	Wave Amplitude

Roman Letters

$(T_H)_M$	Mean Horizontal Tension
δV	Change of Volume
A	Added Mass coefficient
C	Restoring coefficient
d	Depth
F	Force
g	Gravity constant
H	Wave height
l	Total Length of Mooring Line
l_s	Length of Free Span of Mooring Cable
M	Mass
T	Wave Period
T_H	Horizontal Tension
U	Ursell number
w	Submerged Weight of Cable
$\vec{a}$	Acceleration Vector
$\vec{F}_{FK}$	Froude-Krylov Force
$\vec{s}$	Displacement Vector
$\vec{v}$	Velocity Vector
d	Water Depth

ds	Line Segment
k	Wave Number
p	Pressure
p_{dyn}	Dynamic Pressure
S_w	Underwater Area
t	Time Operator
x	Surge Coordinate
z	Heave Coordinates
z'	Wheeler Modified vertical Coordinate
B	Damping Coefficient
Hs	Significant Wave Height
Tp	Peak Period
V	Volume

Chapter 1

Introduction

In the last few decades there has been a rising interest for oil exploration in the Arctic regions. This area gives rise to new challenges in the design of offshore structures, in particular the challenge of Ice loading, great water depths and harsh climate in general. As part of this interest in the Arctic region a few new designs of ice strengthened offshore structures have been proposed. This thesis will focus on spar buoy platforms with a waterline designed to deflect ice. An example of this can be seen in figure 1.1. This design has been examined by previous students in both their project thesis and master thesis, and in the process a MATLAB program was developed which uses hydrodynamic theory to calculate motions and forces. The most important work was done by Nils Gunnar Viko in his master thesis(Viko, 2006) and Einar B Glomnes in his project(Glomnes, 2006) and master thesis(Glomnes, 2007)

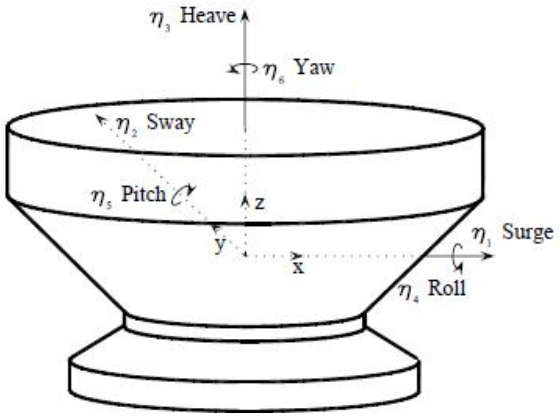

Figure 1.1: Total buoy (Glomnes, 2006)

A preliminary study of the numerical model was made before the start of this thesis, and the results of this study was such that it was deemed necessary to attempt to write another numerical model with a different theoretical basis. The main comparisons of the previous numerical model have been included in appendix A. In addition to this an appendix highlighting the problematic areas of the previous numerical mode has also been added (appendix B). It should be noted that these comparisons were made before

the model tests from Force Technology was made available, and the model test results which are used are only the ones which were available through Glomnes (2006) and Glomnes (2007). These have been added to show the background for this thesis. They can also give valuable insight into the workings of the previous numerical model, and an understanding of problems which needed to be solved in this numerical model.

The main objective in this thesis is to start the development of another MATLAB program which will use a simple theory as basis. The aim of the program is to keep it as simple as possible, and also keeping the programming understandable. This means that the theory applied will be explained in detail in this thesis, and the program code will have comments explaining the different steps in the code. Specifics of the theory will be kept to a minimum in the code itself to keep the code readable. If it is possible code from the previous attempts by Glomnes and Viko will be reused, however due to the general lack of comments and some poor code structuring, there will still be much work to be done. These functions will also be verified, but a description or explanation of all the theory will not be featured in this thesis. All codes used will be credited in the header comments of each function. If the programming progresses quickly effort will be made to rewrite or change the old code, but the focus in this thesis is first and foremost to get working non-linear motion analyses.

To test the results from the new program some comparisons will be made between the new program, and model tests of the total buoy, which have been made available through Force Technology. The numerical model will also be compared to a commercial program. The commercial program is Wasim, which is part of the HydroD in DNVs SESAM package.

Finally an assessment of the Open Water Behaviour and the Ice Behaviour of the Total Buoy will be performed. This is to give an actual assessment on the buoy design.

As it is not expected that the new numerical model will be perfect, some effort will be made to point out areas which will need further development. This is the point of the extensive comparisons which will feature a large part of this thesis

Chapter 2

Theory

This chapter contains a description of the theory which is applied in the new program. Specific programming related theory and a short description of the different functions will be the subject of chapter 3.

2.1 Wave Theory

One of the key points in this program is pressure force integration to the true surface, and this requires the wave kinematics to be changed as regular airy waves are only accurate to the SWL, which means that it is only valid for infinitesimal waves. (see section 4.1 for the specifics of the airy theory or see (Faltinsen, 1990)) To avoid using higher order theory it is possible to apply simplified methods.

2.1.1 Extrapolated Airy

The first and simplest method is the extrapolated airy. In this method the normal airy kinematics are used from the sea bottom to the wave through. The parts of the structure which are in a wave through will simply be excluded from the force integration. As for the wave crest one simply uses the pressure value at SWL as a constant value in the entire wave crest. The method is shown in figure 2.1.

A problem with this method is that an error of second order is introduced in the wave through. This is due to the dynamic pressure at that point, which is zero. The static pressure at that point however is non zero and the result is a non zero total pressure in a point which should be zero. This is further shown in figure 2.2.

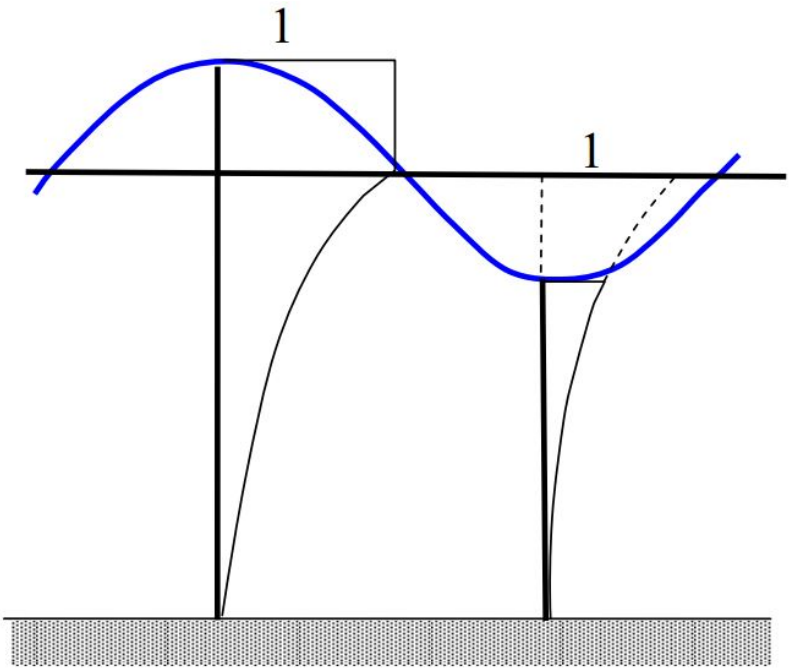

Figure 2.1: Illustration of extrapolated Airy (Amdahl, 2010)

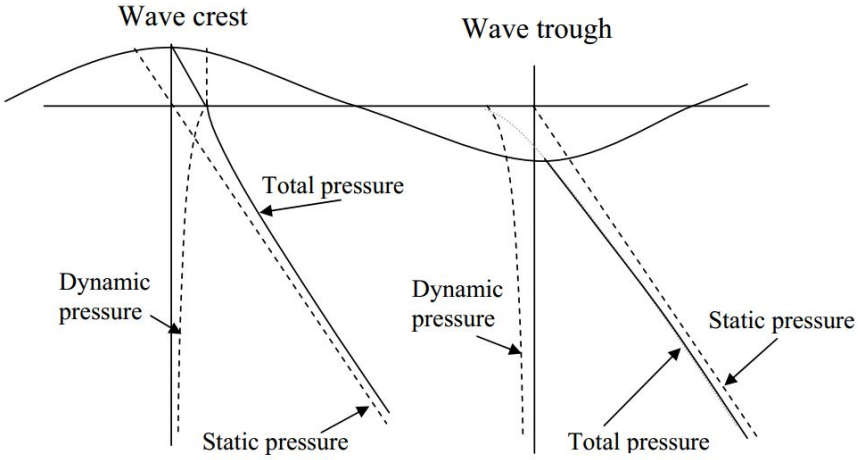

Figure 1.8 Hydrodynamic pressures in wave crests and wave troughs

Figure 2.2: Hydrodynamic pressures in wave crests and wave trough (Faltinsen, 1990)

2.1.2 Wheeler Stretching

Another method which can be used is Wheeler Stretching. The point is to extend the validity of the wave kinematics above the SWL, and to do it in a better way than just keeping the pressure in the wave crest constant. The method is similar to regular Airy theory except that the entire wave column is included by stretching the airy theory to include the instantaneous wave height. An illustration of this method can be seen figure 2.3.

$$z' = (z - \zeta)\frac{d}{d + \zeta} \tag{2.1}$$

Where $\zeta = \zeta_a sin(\omega t - kx)$

With this modification one can simply exchange the z in the normal Airy kinematics equations to gain the stretched kinematics. The dynamic pressure equation is of particular interest in this program, as it is the basis for the pressure calculation which is the key to the motion calculation.

$$p_{Dyn,Airy} = \rho g \zeta_a e^{kz} sin(\omega t - kx) \tag{2.2}$$

which becomes

$$p_{Dyn,Wheeler} = \rho g \zeta_a e^{k(z-\zeta)\frac{d}{d+\zeta}} sin(\omega t - kx) \tag{2.3}$$

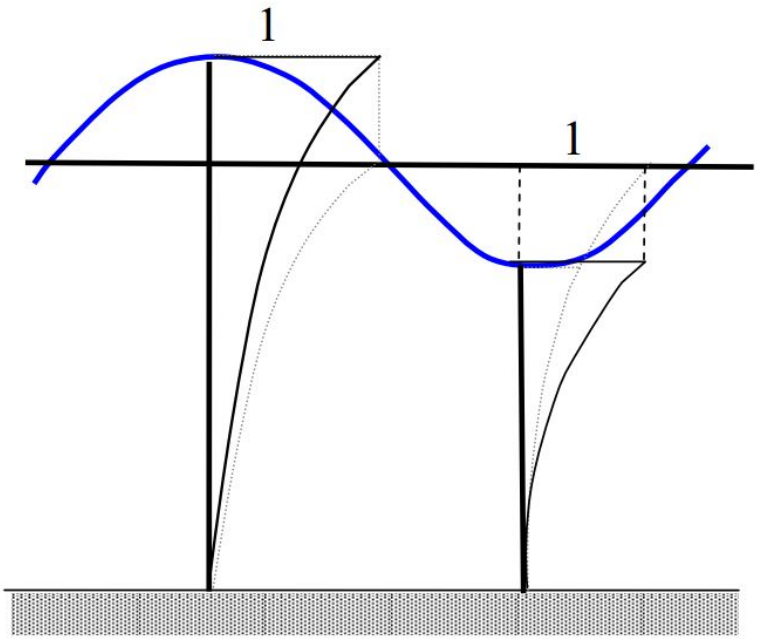

Figure 2.3: Illustration of Wheeler Stretching (Amdahl, 2010)

2.1.3 Differences Between Methods

There are some differences in the wave kinematics of the methods, however the difference is mainly for drag dominated structures i.e. affected by velocity. For mass dominated structures, i.e. affected by acceleration, the difference is not that large. In the case of a platform type spar buoy, it is generally considered to be a mass dominated structure because of the size, so it should not matter whether wheeler or extrapolated airy is chosen for this analysis.

2.2 Motion Theory

As previously mentioned the motion calculations are going to be as simple as possible. The previous programs did try to solve an equation of motion system with three degrees of freedom. (see equation 2.4)

$$(M + A)\vec{a} + B\vec{v} + C\vec{s} = \vec{F} \tag{2.4}$$

The problem with trying to solve this system of equations is that it requires a comprehensive time integration scheme which may have some problems with accuracy and slow solution. This problem increases when including coupling effects and thereby increasing the size of the matrix.

One of the key points of the new program is to increase the solution speed, and also to increase the accuracy compared to the old program. This must be done by introducing some simplifications to the problem. The main idea is to calculate the acceleration for each time step, and calculate the damping and restoring terms as forces on the right side of the equation system. The calculations must be done for each time step, and we can use the previous time step values for the velocity and displacement (see equation 2.5]. This would, of course, require the time step to be relatively small to keep the error which is introduced by this method small.

$$\vec{a}_{t+1} = \frac{\vec{F}_{FK} - B\vec{v}_t - C\vec{s}_t}{M + A} \tag{2.5}$$

2.2.1 Froude-Krylov force

An important part of this calculation is the Froude-Krylov force. (See equation 2.6) This force is calculated from the undisturbed pressure field on the structure. It includes both the dynamic pressure, which is related to the waves passing the structure as if it was not there, and the static pressure, which is the water pressure. This pressure is then integrated over the submerged area of the structure and also multiplied with the normal vector according to which force direction is desired. A more detailed account of the Froude-Krylov force can be found in (Faltinsen, 1990)

$$\vec{F}_{FK} = -\iint_{S_w} p\ \vec{n}\ ds, \tag{2.6}$$

2.2.2 Added Mass

The added mass used in this program is limited slightly as it is quite complicated to calculate, or find correct added mass for a structure as it often requires either comprehensive CFD calculation or model tests. The added mass is therefore not dependent on the wave frequency as it should be. The added mass can still be calculated but will be independent on frequency, one way of doing this is by using tables of similar shapes which can be found in different rules or recommended practices e.g DNV RP-H103. Added Mass coefficients can also be found using a forced oscillation test (Steen and Aarsnes, 2010). Added mass will then usually be found to be a multiple of the mass, and this is the form which is used in this program.

2.2.3 Damping

Damping has much of the same problems as the added mass with respect to calculation. The simplest way to actually find how large the structure damping is, is to do a free oscillation test (Steen and Aarsnes, 2010). Normally one finds the damping as a percentage of the critical damping of the structure. When this has been found one can find the actual damping coefficient by equation 2.7 (Ivar Langen, 1979) where the damping percentage is given by ζ_d.

$$B = 2\zeta_d\sqrt{(M+A)C} \tag{2.7}$$

2.2.4 Restoring Force

The restoring force is needed to get the structure to right itself after the initial displacement. There are different ways of calculating this according to what type motion it is, translation or rotation, and also whether the motion is connected to the buoyancy of the structure or mooring lines. Generally Surge, Sway and Yaw are only affected by mooring lines with respect to restoring force. Heave, Roll and Pitch on the other hand are mostly affected by the buoyancy of the structure, but they are also affected by mooring lines if the mooring line characteristics are defined in that manner.

Surge Restoring Force

As mentioned previously surge is only affected by the mooring lines with respect to restoring force. A good way of modelling mooring lines is to consider the lines as inelastic cables, this means that the simple catenary equations can be used. The entire

derivation of eq 2.9 in (Faltinsen, 1990). Figure 2.4 shows the geometric relations from which equation 2.8 can be found.

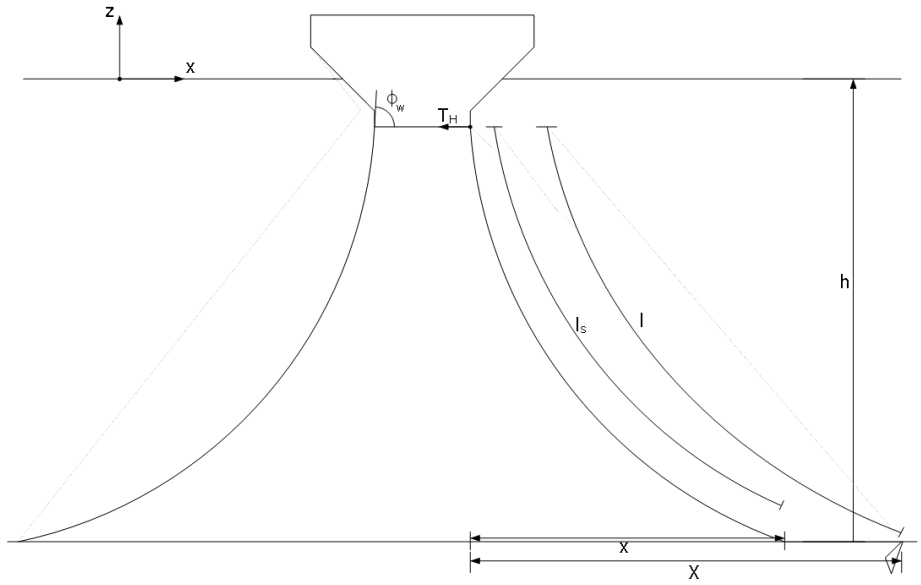

Figure 2.4: Mooring Lines on the Total Buoy

$$X = l - l_s + x \tag{2.8}$$

$$X = l - h\sqrt{1 + 2\frac{T_H}{wh}} + \frac{T_H}{w} cosh^{-1}(1 + \frac{hw}{T_H}) \tag{2.9}$$

where $h = \frac{T_H}{w}[cosh(\frac{xw}{T_H}) - 1]$ and $T_H = Tcos\phi_w$

With these equations it is possible to find the restoring coefficient for surge. An analytical expression can be found by differentiating equation 2.9. The resulting expression is equation 2.10.

$$C_{11} = \frac{dT_H}{dX} = w\left[\frac{-2}{\sqrt{1 + \frac{(T_H)_M}{wh}}} + cosh^{-1}(1 + \frac{hw}{(T_H)_M})\right]^{-1} \tag{2.10}$$

Where $(T_H)_M$ is the average horizontal force from the anchor line on the vessel.

Heave Restoring Force

This restoring force is based on the Archimedes principle. The buoyancy of the structure will change with the oscillation due to change in the draft. This force can therefore be

found from equation 2.11. In the program the δV is comprised of both the both the change in draft and the influence of the waves on the hull.

$$F_3^R = \rho g(V + \delta V) \tag{2.11}$$

Pitch Restoring Moment

This is also based on the buoyancy of the structure, but it is the force couple between the buoyancy forces and the mass which is gives rise to this moment as is shown i figure 2.5. The expression for the restoring moment will then be as shown in equation 2.12

$$M_5^R = \frac{GZ}{2}G + \frac{GZ}{2}B \tag{2.12}$$

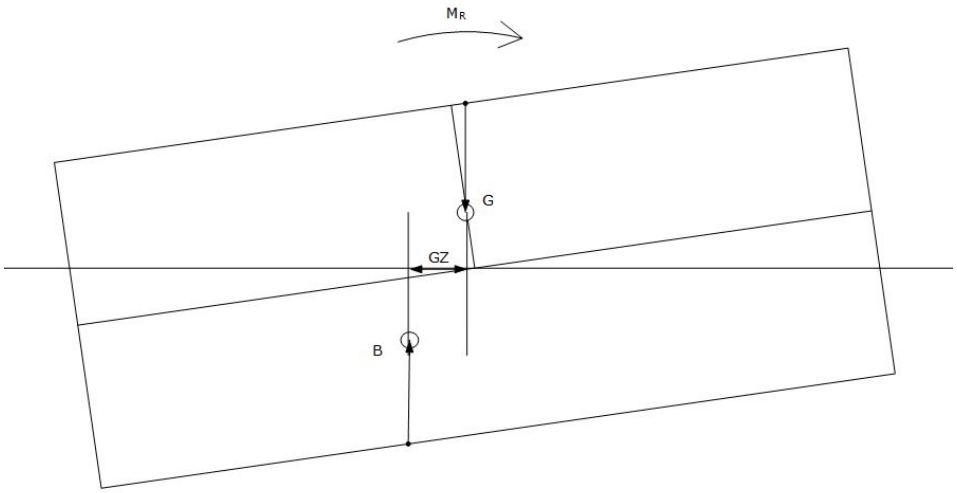

Figure 2.5: Restoring Moment

2.2.5 Numerical Integration

After calculating the different coefficients and finding the acceleration we need to find the velocity and displacement of the structure. There are different numerical integration theories which can be used for this purpose, but it is a stepwise integration method which is necessary in this case.

The Newmark-β numerical integration method has be selected for this purpose. The Newmark-β method is a good choice because the method is very easily customised, and if the right parameters are chosen it can be unconditionally stable. The full derivation of the Newmark-β method can be seen in (Newmark, 1959).

$$v_{k+1} = v_k + (1 - \gamma)ha_k + \gamma ha_k + 1 \tag{2.13}$$

$$s_{k+1} = u_k + hv_k + (\frac{1}{2} - \beta)h^2 a_k + \beta h^2 a_{k+1} \tag{2.14}$$

The numerical model uses the constant average acceleration variation on equation 2.13 and 2.14, with $\beta = \frac{1}{4}$ and $\gamma = \frac{1}{2}$.

β is the parameter deciding the acceleration slope between each time step. γ is governing whether the method has artificial damping, i.e. if the method will damp out free oscillation. A γ value larger than 0.5 gives artificial damping, a value of exactly 0.5 gives no damping, and a value less than 0.5 results in negative damping.

2.3 Ice Theory

Level ice loads on structures is a relatively new area of study, at least compared to other disciplines within structural and hydrodynamics. Much of the field focuses on empirical formulas created from model tests and full scale measurements.

2.3.1 Ice Parameters

Ice is a very complex load to consider because it has several different components which can influence the total load. The different types of ice also make the calculations more difficult because of the large difference in properties. In fact an ice sheet will probably have several different types of ice features which may hit the structure, some of the different types of ice features which need to considered are shown in table 2.1

These are still not all the parameters which influence the ice actions on structures however. The rest can be seen in figure 2.6 and this is the reason why ice actions are so difficult to calculate.

2.3.2 Ice Forces

From the ice parameters it is possible to find the most important forces from the ice action.

Type	Subdivision
Level Ice	Sea ice which is unaffected by deformation.
Deformed Ice	A general term for ice which has been squeezed together and in places forced upward or downwards.
Rafted Ice	Type of deformed ice formed by one piece of ice overriding another.
Ridge	A line or wall of broken ice forced up by pressure. May be fresh or weathered. The submerged part of the ridge is termed an ice keel. Parts of the keel may be consolidated. A ridge is formed by pressure or shear. Some types of ridges are: >New ridge: Ridge with sharp peaks and slopes of sides usually about 40^o >Weathered ridge: Ridge with peaks slightly rounded and slope of sides usually $30 - 40^o$. Individual fragments are not discernible. >Very Weathered ridge: Ridge with peaks very rounded, slope of sides usually $20 - 30^o$ >Aged Ridge: Ridge which has undergone considerable weathering >Consolidated ridge: A ridge in which the upper parts of the ridge has frozen together
Rubble	Ice piles haphazardly one piece over another in the form of ridges or walls
Hummock	A hillock of broken ice which has been forced upwards by pressure. May be fresh or weathered.

Table 2.1: Typical ice features (S. Loset, 2006)

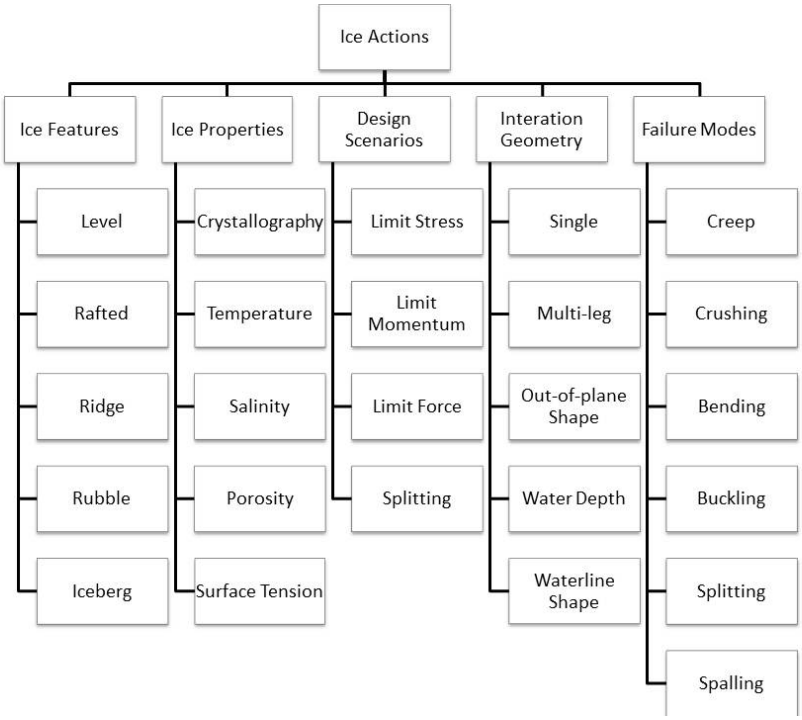

Figure 2.6: The major parameters affecting the ice action (S. Loset, 2006)

- Breaking Force
- Friction Force
- Submergence Force (Buoyancy Force)

Breaking Force

The first force is the force required to break ice when it hits the structure. As can be seen in figure 2.6 there are several different ways to break the ice. The difference in terms of the force required is quite large, but it is breaking ice by bending which is considered to be the mode which requires the least amount of force (S. Loset, 2006).

Friction Force

The friction force comes from ice which slides along the structure and is influenced by the surface roughness of the ice and the abrasiveness. These things can vary over a wide range of values within a single ice floe. The frictional forces are simply calculated from the Coulomb friction equation. This force is related to the other two forces as it is dependent on the normal force. The surface roughness and abrasiveness influences the force by changing the friction coefficient μ

$$F_{\mathrm{f}} \leq \mu F_{\mathrm{n}} \tag{2.15}$$

Submergence Force or Lifting Force

This force is really only relevant to structures which are slanted in the waterline i.e either pushes the ice upwards or downwards. These types of solutions are often used in dealing with ice, as it helps to break the ice in bending rather than crushing as previously mentioned. Instead the ice will subject the structure to the reaction force from either being pushed down into the water, or lifted up and often piled on the hull depending on which way the slanted hull pushes the ice.

2.3.3 Methods for Calculation

This leads us to the methods of calculation. In the case of the Total Buoy it is necessary to use a method which considers downwards slanting waterline geometry. However an upwards slanting method will be included as well.

Croasdale's method (S. Loset, 2006)

This is an empirical method developed by Croasdale and it is a two dimensional loading model on a plane slope. This method is for upwards slanted structures. An important

part of this method is that it includes the force required to push the ice blocks up the slope. The horizontal component of the force is:

$$F_H = C_1 D R_f \left(\frac{\rho_{water} g h^5}{E}\right)^{0.25} + C_2 D h_r h \rho_{ice} g \tag{2.16}$$

C_1 and C_2 are coefficients depending on the slope inclination and the ice dynamic friction on the structure surface. Other important parts of the equations are h, which is the level ice thickness, and h_r which is the rubble height. The coefficients can be found from the following relations.

$$C_1 = 0.68\frac{\zeta_1}{\zeta_2} \tag{2.17}$$

$$C_2 = \zeta_1(\frac{\zeta_1}{\zeta_2} + cot(\alpha)) \tag{2.18}$$

where

$\zeta_1 = sin(\alpha) + \mu cos(\alpha)$

$\zeta_2 = cos(\alpha) + \mu sin(\alpha)$

The ice rubble height is given from a formula which was developed by looking at rubble height at the confederation bridge in Canada. (S. Loset, 2006) This is really not relevant in the case of the total buoy as the ice floes will be pushed down and past the body.

$$h_r = 7.6h^{0.64} \tag{2.19}$$

This method was later modified by Croasedale and others, making it a 3D model instead of a 2D model. The new solution includes many additional factors that are important for the ice action. The new horizontal force includes the following force contributions.

- Ice Breaking Force
- Ice Sheet Pushing Force
- Ice Friction Force
- Ice Rubble Lifting Force i.e the force required to push the rubble up.
- Ice Block Turning Force

$$F_H = F_B + F_P + F_R + F_L + F_T \tag{2.20}$$

$$F_B = C_1 D R_f \left(\frac{\rho_{water} g h^5}{E}\right)^{0.25} \left[1 + (\frac{\pi^2 l}{4D})\right] \tag{2.21}$$

where l is the characteristic length of an ice sheet given by:

$$l = \left(\frac{Eh^3}{12\rho_{water} g(1-\nu^2)} \right)^{0.25} \tag{2.22}$$

The next force is the due to rubble from ice which has been pushed back onto the ice sheet from the structure and then pushes back on the ice sheet (see figure 2.7).

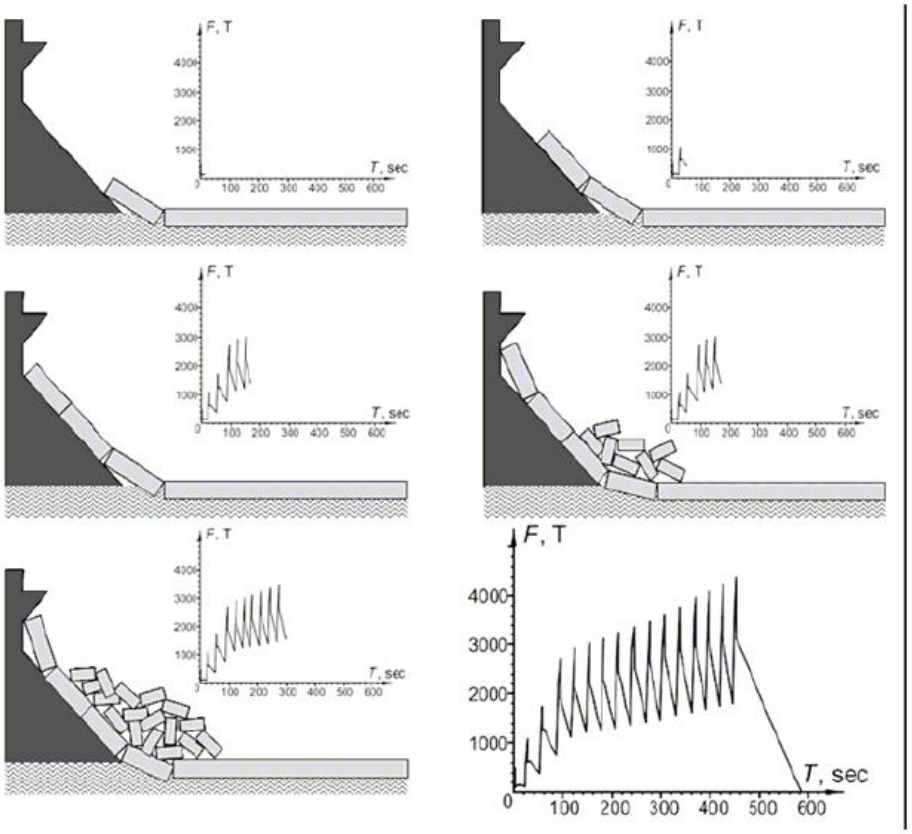

Figure 2.7: Ice sheet rubble build up (S. Loset, 2006)

$$F_P = Dh_r^2 \mu_i g(1-\eta) \left(1 - \frac{tan(\theta)}{tan(\alpha)}\right)^2 \left(\frac{1}{2tan(\theta)}\right) \tag{2.23}$$

After breaking the ice blocks will continue to slide upwards until they fall back onto the ice sheet as shown in figure 2.7. This sliding causes friction forces and is given by:

$$F_R = DP \left[\frac{1}{cos(\alpha) - \mu_i sin(\alpha)} \right] \tag{2.24}$$

where

$$P = 0.5(\mu_{ice} + \mu_s)\rho_{ice}g(1-\nu)h_r^2 \left[\mu_{ice}sin(\alpha)\left(\frac{1}{tan(\theta)} - \frac{1}{tan(\alpha)}\right)\left(1 - \frac{tan(\theta)}{tan(\alpha)}\right) + cos(\alpha)\left(\frac{1}{tan(\alpha)}\right)\left(1 - \frac{tan(\theta)}{tan(\alpha)}\right)\right] + hh_r\rho_{ice}g(1 + \mu_s cot(\alpha)) \tag{2.25}$$

The next force is the additional force required to lift and shear through the ice rubble which has failed and piled on top of the ice sheet. This force is only until the ice sheet has been pushed up enough that it breaks in bending.

$$F_L = 0.5Dh_r^2\rho_{ice}g(1-\eta)\zeta[(cot(\theta) - cot(\alpha))(1 - tan(\theta)cot(\alpha)) + tan(\phi)(1 - tan(\theta)cot(\alpha))^2] + \zeta cDh_r(1 - tan(\theta)cot(\alpha)) \tag{2.26}$$

Finally when the ice blocks (the broken pieces of the ice sheet) have been pushed to the top of the structure and begin to turn backwards a turning force will affect the structure.

$$F_T = 1.5h^2\rho_{ice}gD\left[\frac{cos(\theta)}{sin(\theta) - \mu_s cos(\theta)}\right] \tag{2.27}$$

2.3.4 Timco Correction

The Croasdale method was modified by G. W Timco (1997) to be applied on structures like the Total Buoy which has downwards slanted hull. One needs to consider effects which are related to buoyancy of the ice how this affects the friction forces and rotation of the ice blocks. The main changes are that the inclination angle, α which is negative here and the rubble height becomes rubble depth. The equation is similar to the original 2D Croasdale equation but instead some elements of the 3D Croasdale is introduced (the first expression is from equation 2.19).

$$F_B = C_3DR_f\left(\frac{\rho_{water}gh^5}{E}\right)^{0.25}\left[1 + (\frac{\pi^2 l}{4D})\right] + C_4Dh(\rho_{water} - \rho_{ice})g \tag{2.28}$$

$$C_3 = 0.68\frac{\zeta_3}{\zeta_4} \tag{2.29}$$

$$C_4 = \zeta_3(\frac{\zeta_3}{\zeta_4} - cot(\alpha)) \tag{2.30}$$

where

$\zeta_1 = \mu cos(\alpha) - sin(\alpha)$

$\zeta_2 = \mu sin(\alpha) + cos(\alpha)$

Chapter 3

Program Theory

The theory which was the topic of chapter 2 must be transformed into a programming language to be usable. This chapter's topic will be the different approximations and methods which are applied in the program, and should help in understanding the choices which have been made. Some effort will be made to point out intentional errors (where applicable) and simplifications which are necessary to get the program to function.

3.1 Program Description

This numerical mode is an attempt to solve the problem of a non-linear geometry within a reasonable time. The previous numerical model had problems with unstable solutions, noise and slow calculation. The theory applied in that version is sound but the solution of a large coupled matrix proved to be problematic. The old numerical model also had different solution options for the motion, such as frequency domain and linear time domain solutions (A diagram showing the functions of the old program can be seen in figure 3.1). This new attempt only has non-linear motion solution and it also has a basic ice calculation solution (the new diagram can be seen in figure 3.2)

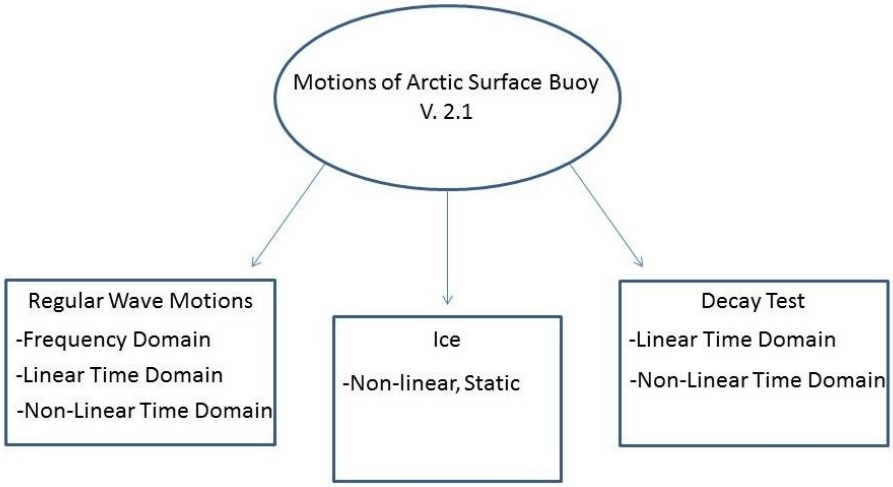

Figure 3.1: Functionality of the previous program

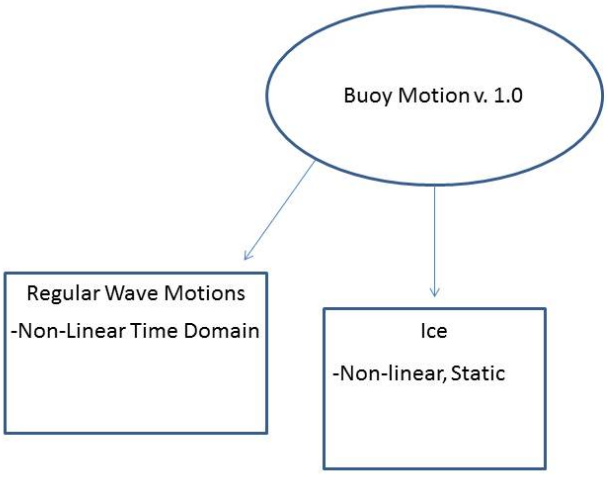

Figure 3.2: Functionality of the new program

3.2 Program Structure

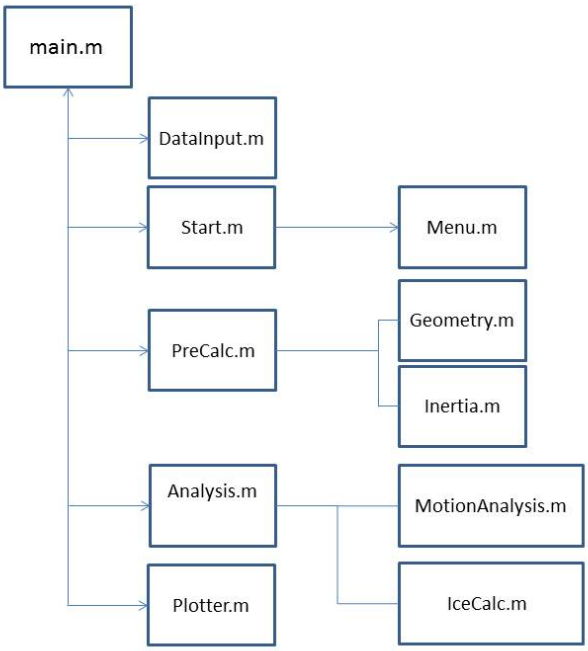

Figure 3.3: Flow diagram with main subroutines

main

This is the Main call function of the program, its main purpose is to coordinate the different subroutines of the program, and pass variables between them. It is essentially the back bone of the program.

DataInput

The DataInput subroutine is basically the general input file. This is where all the information about the buoy geometry, environment parameters and mooring characteristics. The main idea of having the input file as an m-file rather than a normal text file is to be able to have comments. This will help new user to understand how to input other values.

Start

This subroutine helps to extract and assign values from the graphical user interface (GUI) function. This mostly helps to keep the code structured.

Menu

This subroutine connects the GUI to the program itself. It contains different functions which are activated e.g. when buttons are pressed, inputs are confirmed etc. The menu has been created such that only the input panels which are visible will run if the start button is pressed. (see figure 3.4 and 3.5) The GUI takes input from the user through the input text boxes. After the input has been confirmed i.e the user has pressed enter or tab, then the number next to the text box will change. The user can also choose amongst several plots.

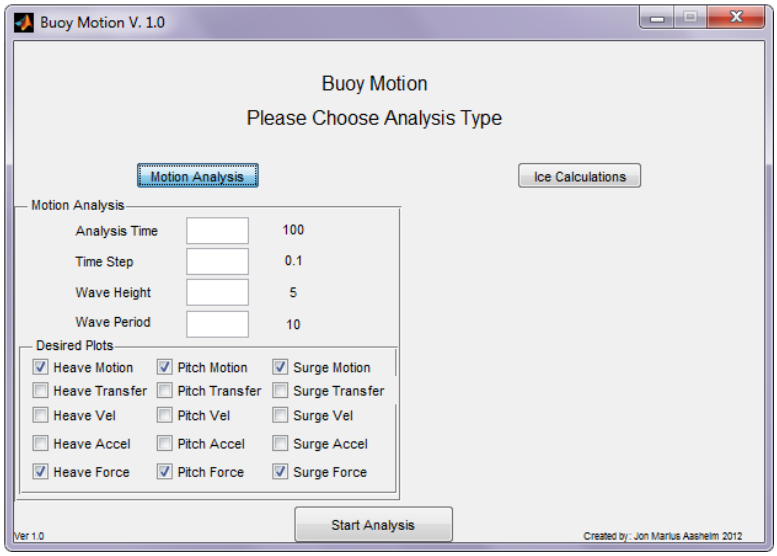

Figure 3.4: Motion analysis option

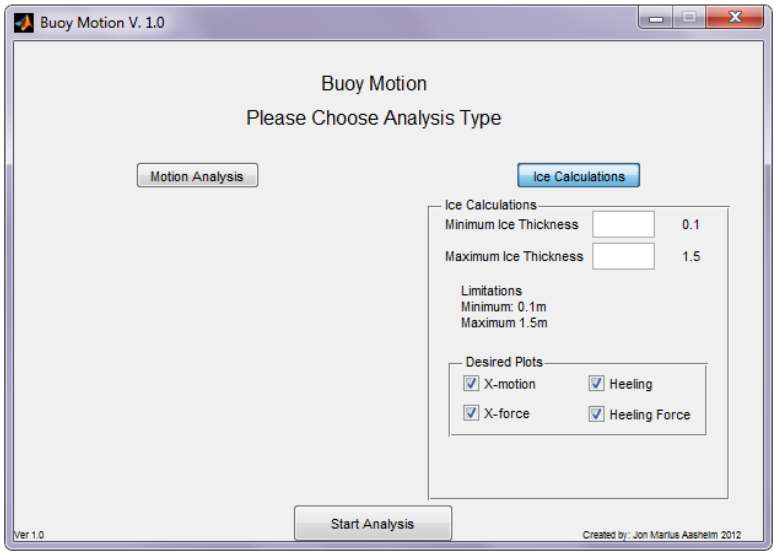

Figure 3.5: Ice calculation option

PreCalc

This subroutine controls calculations which must be done in order to be able to do the analysis. Once again it is only necessary for structuring of the code.

Geometry

This function creates the buoy geometry from the input values. It actually does several things which is related to the buoy geometry, it generates a figure (see figure 3.6) and a panel model with all coordinates in the Cartesian-coordinate system. It also calculates the area of each panel and translates all coordinates from the corners of each panel to the midpoint. This function is essential for the analysis later.

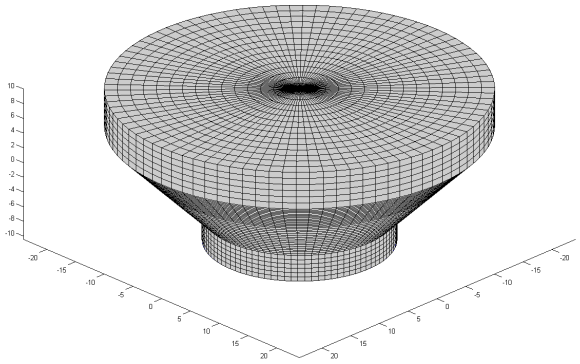

Figure 3.6: Panel model created by Geometry

Inertia

This function calculates the mass and added mass of the structure based on the geometry and added mass values defined in the input. Added mass is calculated as a factor times the mass of the structure as it would be to complex to actually calculate the added mass.

Analysis

This function is connected to the GUI as the analysis choice will determine if Motion-Analysis or IceCalc or both will run.

MotionAnalysis

This is the motion analysis function, it is based on the theory which was presented in section 2.2. The calculation procedure is performed as shown in figure 3.7

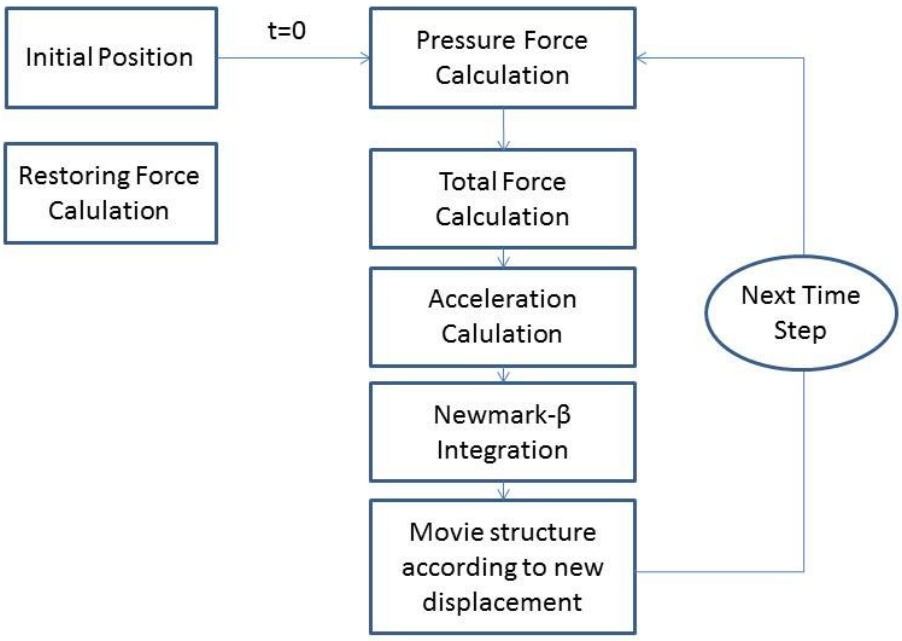

Figure 3.7: Diagram of motion analysis

The restoring calculation was written by Glomnes (2006) and Viko (2006) and it utilizes conic sections to do an approximation of the restoring moment for pitch, the heave restoring is not used in this program as that is calculated by using the static pressure calculation. The other factor which is calculated is the restoring coefficient due to the mooring lines. This part of the program was initially intended to be updated each time step, but it was slowing the program down significantly, so finally the calculations were done before the time calculations.

The pressure calculation uses the panel area and the panel midpoint coordinates to calculate the force on each panel over the structure. A built-in MATLAB function can be used to find the normal vectors of each panel, which makes it possible to calculate the separate motion directions with ease. The pressure calculations are done for both dynamic pressure and static pressure. (not interesting for surge) The pressure is calculated to the true surface and should therefore be able to handle the rapid changes in the geometry near the water line.

After these quantities have been calculated it is possible to calculate the total force by summing all the forces. The restoring forces and the damping forces normally needs to be calculated simultaneously as the acceleration but in order to simplify the program the velocity and displacement are from the previous step instead. This is, of course,

not correct, but the error should be small and will be dependent on the size of the time step.

By using the simplification above it is very simple to calculate the acceleration for the next step, and by using the Newmark-β integration method it is also very simple to find the velocity and displacements.

After the displacements have been found the coordinates which are used in the calculations are displaced accordingly. This results in a change in the pressure forces and the displacements are also used to find the new restoring coefficients.

IceCalc

This function is actually very simple and it follows the description which can be seen in the section 2.3. As these methods are based on coefficients the calculations are just based on calculating the coefficients and finding the force of the level ice on the structure. The complication is that as this method is for fixed structures and not floating structures it is necessary to iterate with the restoring forces of pitch and surge. The iteration is done by moving the structure step by step until the restoring force is equal to the ice force (within an error rate which is set to a low value). At that point the heeling and drift-off is saved. This is done for all the ice thicknesses which have been input in the GUI.

Plotter

This is the result plotting function. The function has a simple layout and different plots will be generated depending on the selections made in the GUI. Each plot has also been written in a way which improves the figures which are created, by adding lines and expanding the borders of the figure itself.

Chapter 4

Modelling of Spar in Wasim

The focus of this chapter will be on the most important theory and assumptions which are applied in the modelling of the structure in Wasim. The aim is to attempt to model the buoy as closely as possible to the numerical model. This should give results which are comparable. Another point is to highlight the differences in the modelling which could highlight inaccuracies in the numerical model.

4.1 Sea model

From the model tests by Force Technology presented by (Glomnes, 2006), and also the limitations of the numerical models capabilities regular waves are used in the calculations also in Wasim. The details of the design locations is not known, so a few parameters have just been picked out from the numerical model and also from the thesis of (Glomnes, 2006).

4.1.1 Location Parameters

Some of the most important physical parameters in this case are the water depth, proximity to land, and other possible disturbances. The last two cases have simply been ignored in the modelling, so the structure is assumed to be in an area which has a flat bottom and open seas.

Water Depth	300 m
Kinematic viscosity	1.025 Kg/m^3
Density of Water	1.462e-005 m^{2}s

Table 4.1: Main Location Parameters

4.1.2 Waves

In the Wasim analysis there are two possible choices regarding non-linear wave theory which can be applied to the structure. These are:

- Airy waves
- 5th order stokes waves

Airy wave theory

Airy wave theory is a linearised wave theory which describes the motion and velocity of the wave particles with potential flow or velocity potential. The theory is derived from the Navier-Stokes equation using the assumptions of an irrotational, incompressible and inviscid fluid. Even with the limitations these assumptions impose on the airy waves, the result is still fairly accurate. However the airy theory does not have the required physical description in this case. The main reason for this can be seen in the derivation of the airy wave theory which can be seen in full in chapter 2 of (Faltinsen, 1990) but the most critical component in this derivation comes from the simplifications of the kinematic (equation 4.1) and dynamic free surface (equation 4.2) conditions which are applied on the free surface.

$$\frac{\partial \zeta}{\partial t} + \frac{\partial \phi}{\partial x}\frac{\partial \zeta}{\partial x} + \frac{\partial \phi}{\partial y}\frac{\partial \zeta}{\partial y} - \frac{\partial \phi}{\partial z} \; on \; z = \zeta(x, y, t) \tag{4.1}$$

$$g\zeta + \frac{\partial \phi}{\partial t} + \frac{1}{2}(\left(\frac{\partial \phi}{\partial x}\right)^2 + (\frac{\partial \phi}{\partial y})^2 + (\frac{\partial \phi}{\partial z})^2) \; on \; z = \zeta(x, y, t) \tag{4.2}$$

These boundary conditions are non-linear but in linear theory they are linearised by doing a Taylor expansion. This enables the transfer of the boundary conditions from the free-surface position $z = \zeta(x, y, t)$ to the mean free-surface $z = 0$. In the linear theory all higher order terms in the Taylor expansion are neglected and the result is (Kinematic and dynamic respectively):

$$\frac{\partial \zeta}{\partial t} = \frac{\partial \phi}{\partial z} \; on \; z = 0 \tag{4.3}$$

$$g\zeta + \frac{\partial \phi}{\partial t} = 0 \; on \; z = 0 \tag{4.4}$$

The problems with this simplification is shown in figure 4.1 which shows the pressure variation under a wave crest. The pressure variation is correctly defined up to the mean free surface but is assumed constant in the remaining distance to the actual free surface. The free surface of a single airy wave is a sinusoidal which can be represented on the form as equation 4.5. A sinusoidal does not represent the real shape of a wave so a higher order theory is needed.

$$\zeta(x, t) = \zeta_a sin(\omega t - kx) \tag{4.5}$$

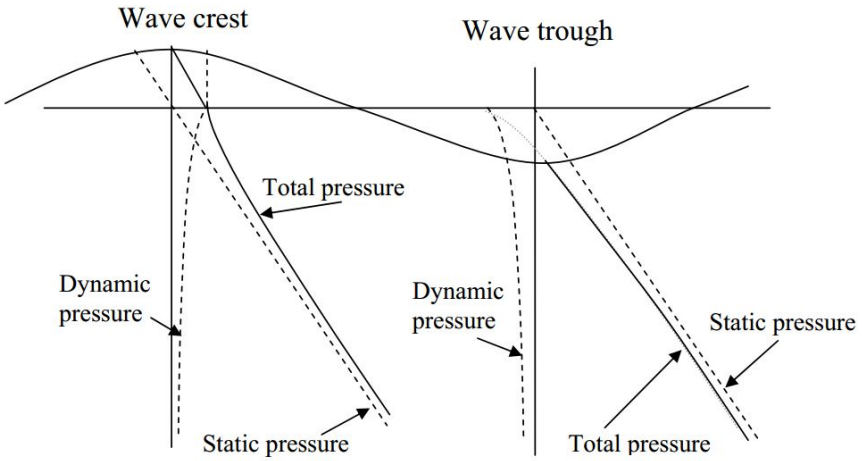

Figure 1.8 Hydrodynamic pressures in wave crests and wave troughs

Figure 4.1: Pressure variation under wave crest(Faltinsen, 1990)

4.1.3 Stokes 5th order waves

The Stokes 5th order waves are derived in the same way as Airy waves, which actually corresponds to a 1st order stokes wave. The difference lies in the order of the Taylor expansion which is included in the derivation of the free surface boundary conditions. The advantage of this is that the wave kinematics are defined to the instantaneous free surface i.e. the wave particle speed and acceleration. This results in a different wave profile compared to the airy wave theory (see figure 4.2). The details of the derivations can be seen in (Fenton, 1990)

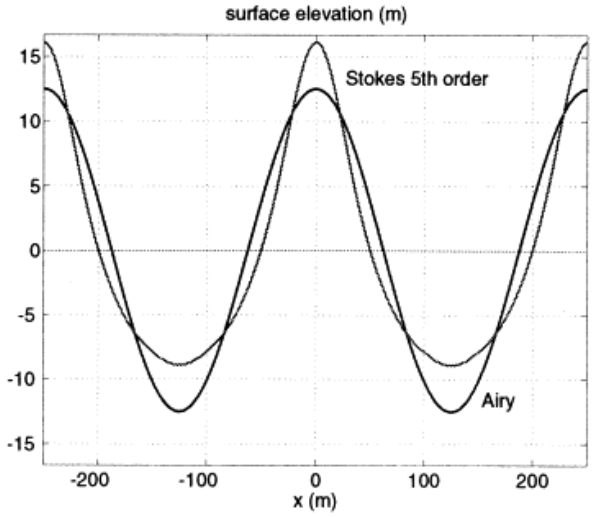

Figure 4.2: Linear wave versus 5th order stokes wave profile(Ditlevsen, 2002)

This wave was chosen for the simulations of the buoy motions in Wasim. This impacts the responses of the model by increasing the amplitudes. This is due to the shape of the buoy and the waves interacting.

4.1.4 Validity of Wave Theory

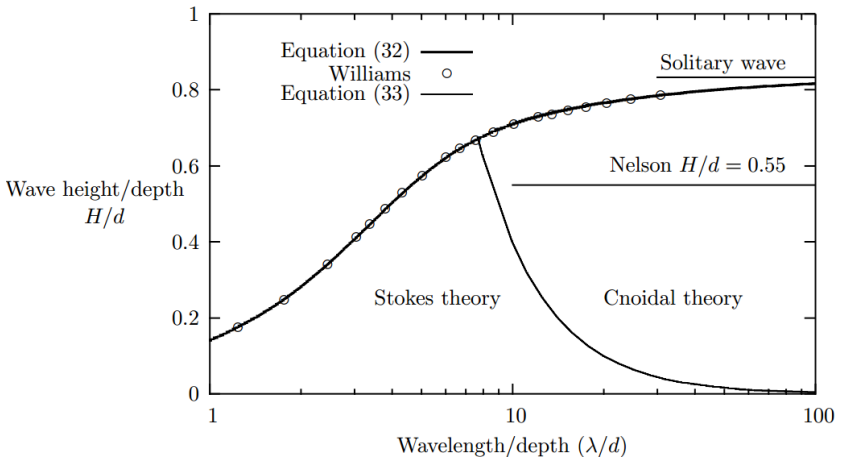

Figure 4.3: Validity Range of Wave Theories(Fenton, 1990)

It is important to note the limitations of the theory. According to (Fenton, 1990), for shallow water "contributions of the higher order terms will tend to dominate, and results obtained will not be accurate". Thus it is important to check the validity of this theory in the selected range. There are a few ways to check the validity range of the different theories(e.g figure 4.3). One of the simplest however is the Ursell number.

$$U = \frac{H/d}{(d/\lambda)^2} = \frac{"Nonlinearity"}{"Shallownes"} \tag{4.6}$$

A boundary between Stokes theory(Including Airy) and the alternative shallow water theory was shown by (Hedges, 1995)

$$U = \frac{H\lambda^2}{d^3} = 40 \tag{4.7}$$

And the Stokes Theory is valid for U<40. By using the highest order of Stokes Theory available the validity range will be as large as possible (Due to the fact that the higher orders will be more "correct" than Airy Theory)

Wave Height	Wave Period	H/d	λ/d	Ursell Number
3	6	0.01	0.187	0.0003
6	6	0.02	0.187	0.001
6	12	0.02	0.749	0.0168
10.5	10.7	0.035	0.595	0.0124
9	13.4	0.03	0.9344	0.026
3	15	0.01	1.17	0.0087
19.5	14.6	0.065	1.11	0.0.08
9	20	0.03	2.08	0.1297

Table 4.2: Ursell Numbers and Wave Parameters of Chosen Sea States

As shown in table 4.2 and figure 4.3 the chosen periods and wave heights are well within the validity range of the Stokes Wave theory.

4.2 Structure Modelling

Wasim uses a non-linear Rankine Panel Method to solve the motions of the structure. This method requires meshing of the structure as well as the sea surface. The modelling of the structure could be done in 2 different ways either as close to reality as possible or as close to the numerical model as possible. The first alternative is very time consuming and the results might not be possible to compare with the numerical model. This results in the following model characteristics:

- Limited to 3 degrees of freedom; Surge, Heave and Pitch
- Critical damping percentages from model tests are utilized
- No mooring specified

4.2.1 Main Dimensions

In the model tests done by Force Technology(Technology, 2006) they test the total buoy with damping skirts to see how the buoy motion is affected. In the preliminary study (see appendix A) only a few model test results were available through the thesis written by Glomnes (2006). In those tests the buoy configuration which was used is shown in figure 4.4. The Buoy has been fitted with a damping skirt to reduce the motions of the buoy. This damping skirt was included in the modelling in the preliminary study, however after the model tests were made available it was possible to ignore this and only include the effects.

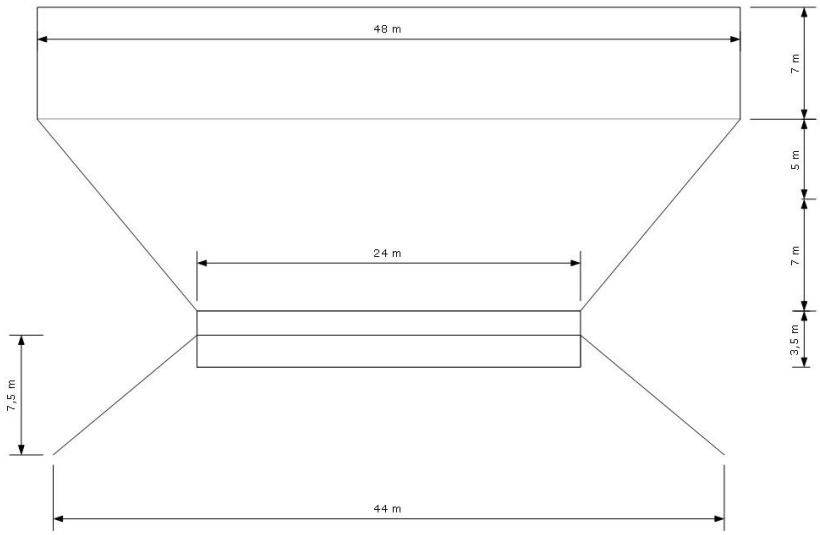

Figure 4.4: Main dimensions of model with damping skirt

4.2.2 Damping

As mentioned the damping is modelled by a percentage of critical damping. The values have been found from decay model tests performed by Force Technology. The values in table 4.3 are taken from (Glomnes, 2006)

Damping Ratio	[%]
Surge	4.3
Heave	6.8
Pitch	3.6

Table 4.3: Critical Damping Ratios from Decay tests

The damping coefficients can be found from equation 4.8

$$C = 2\zeta_d\sqrt{(M+A)K} \tag{4.8}$$

Where ζ_d is the damping ratio. By using this approach we will only obtain the diagonal terms of the damping matrix, which means that there is no coupling between the different motions of the buoy. This is a necessary assumption as the damping term in the equation of motion is often very difficult to model, due to multiple higher order effects. e.g. viscosity and vortex-shedding

4.2.3 Rankine Panel Method

As previously mentioned Wasim uses the Rankine Panel Method which is a Boundary Element Method (BEM). This particular BEM uses Rankine sources to calculate the green functions. The method requires a meshing of the sea surface as well as the structure and this makes it possible to integrate Froude-Krylov force and hydrostatics over the exact wetted surface. The Added mass of the structure is also most likely found using the same methods, although the exact method is not known as it has not been possible to find the exact documentation. The methods are described in Faltinsen (1990) and it should be possible to use them to find a usable added mass estimate.

Chapter 5

Review of Model Tests

Force Technology has been so kind as to allow access to some model tests which were performed on the Total Buoy in 2006. In a preliminary study of the previous work done by Glomnes and Viko some of the model test results were available through their theses, and these were used to test the previous numerical model and a Wasim model which was created as an alternate comparison due to the lack of more model tests(these comparisons can be seen in appendix A).

This chapter will be a review of the model tests, but results will not be presented here. The model test setup can be seen in figure 5.1.

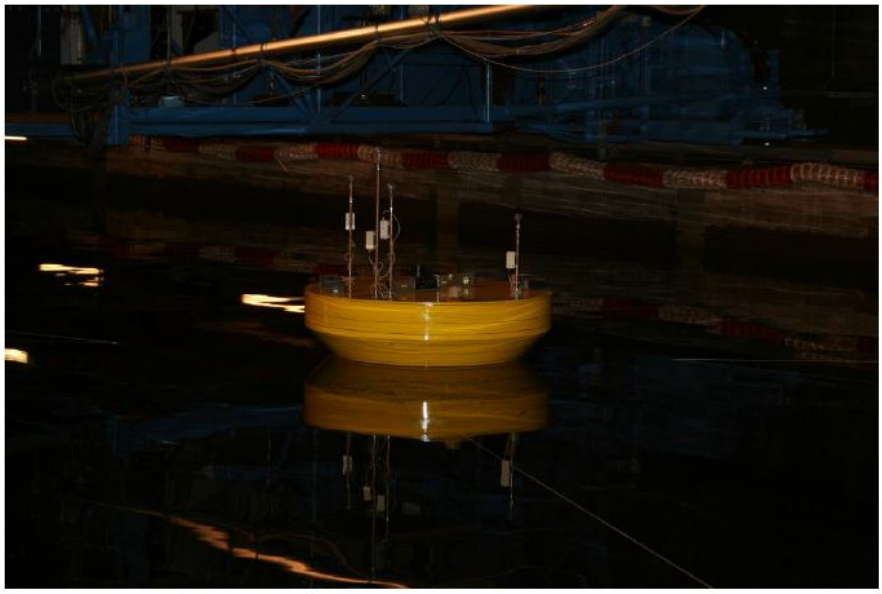

Figure 5.1: Model Test Setup

5.1 Model Test Parameters

5.1.1 Model

The model was made in 1:40 scale and the model itself was made of 45 kg/m^3 foam. The damping skirt was made from a 2 mm steel plate. The hull does not have any deck structures, risers or other hull appendages. The dimensions of the model can be seen in figure 5.2

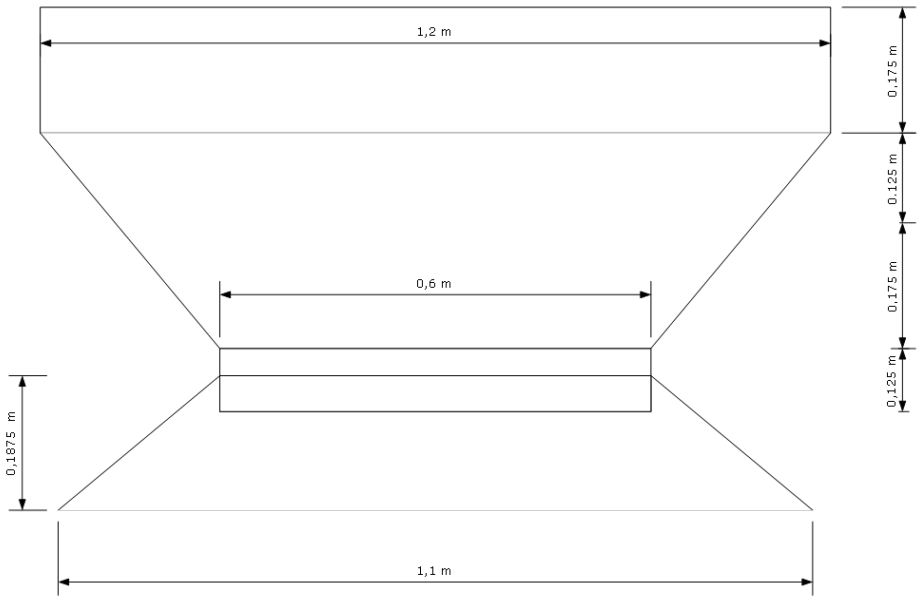

Figure 5.2: Total buoy in 1:40 scale

5.1.2 Mooring System

The model is moored to keep it from drifting but the mooring is designed to give very little contribution to pitch and heave restoring forces. As can be seen in figure 5.3, there are four mooring lines, and they are connected at the height of the center of gravity and at the rotation center in pitch. Unfortunately the mooring system is not possible to replicate as it is connected to the edges of the model basin and there is no information about the surge restoring force in the information supplied by Force Technology. This means that the surge results will probably not by comparable.

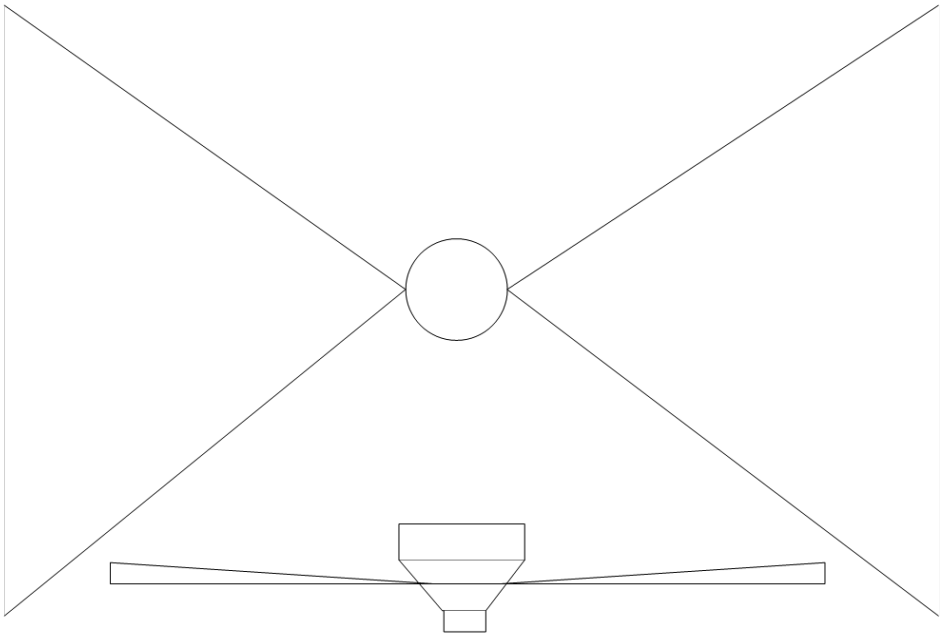

Figure 5.3: Model test mooring setup

5.1.3 Model Test Runs

The model test had several different sessions with different configurations of the Total Buoy, these sessions also had a varying amount of runs. An overview of the different sessions can be seen in table 5.1

Of course for the new numerical model it will not be necessary to compare with the irregular wave sessions so these can be ignored. As we have one session (Original skirt, High VCG) in particular with more runs than any other this is a good choice for the comparisons.

Configuration of Total Buoy	Wave type	Number of runs
Original skirt, High VCG	Irregular waves	5
Original skirt, High VCG	Regular waves	19
No skirt, High VCG	Irregular waves	3
Original skirt, Medium VCG	Irregular waves	4
Original skirt, Medium VCG	Regular waves	4
Original skirt, Low VCG	Irregular waves	4
Original skirt, Low VCG	Regular waves	4
Second skirt, Medium VCG	Irregular waves	4
Second skirt, Medium VCG	Regular waves	5

Table 5.1: Overview of model test sessions

Original skirt, High VCG in regular waves

The largest session in the model test has 19 runs with the parameters shown in table 5.2. This means that there is many to choose from, but it should not be necessary to use them all in the comparisons. A good way to test check the program is to compare several different wave periods and wave heights. Ideally one should have more runs to make the comparisons statistically significant, but a good impression of the solutions can be seen if one makes a wide selection of wave heights and periods within the available model tests. For this reason the runs selected for the comparison will cover the entire period range in the model tests, and additional runs might be chosen to point out a problematic area in the numerical model results.

Run	Wave height[m]	Wave period [s]
2001	3	6
2002	5	9.9
2003	9	9.9
2004	10.5	10.7
2005	13.5	12.10
2006	16.5	13.4
2007	21	16.3
2008	7.5	9
2009	4.5	7
2010	9	13.4
2011	12	11.4
2012	15	12.8
2013	18	14
2014	9	20
2015	19.5	14.6
2016	4.5	7
2017	5	9.9
2018	5.15	16.3
2019	9	20

Table 5.2: Overview of Wave Heights and Wave Periods

Chapter 6

Comparisons

It is necessary to check the results of the new numerical model against other alternative solutions to verify the results. Fortunately, this time the model tests on the Total Buoy are available. In addition to comparing the numerical model with the model test results, effort will be made to compare with Wasim which is a commercial program. Wasim could be used in place of the numerical model, but the accuracy of Wasim on this type of problem is really not known. Therefore it is a good idea to check this at the same time as it could turn out to be a waste of time if the results are bad.

This chapter will contain many figures to give a significant amount of comparison basis. This is important to check the validity of the numerical model and Wasim model.

6.1 Model Test Run 2001

The first run chosen was 2001, it is a mild "sea state" with regular waves of wave height 3 meters and wave period 6 seconds. In the following section the results from the model tests, the numerical model and Wasim are shown. The symmetric motions are compared separately.

Surge

In the following figures, we can see the result motion of surge in the model tests (figure 6.1), the new numerical model (figure 6.2) and the wasim model (figure 6.3). One important point with the surge motion is that the model tests have another mooring setup. (which is not possible to replicate in a good way, see section 5.1 for an explanation) Due to this problem it will be necessary to analyse the results carefully. One important difference might be the amount of static drift-off which is seen i.e. how far the buoy drifts before the mooring lines restricts motion. Another important factor might be low frequency oscillations due to the surge restoring stiffness, but these oscillations must be proved to have similar oscillation periods to be comparable between the models.

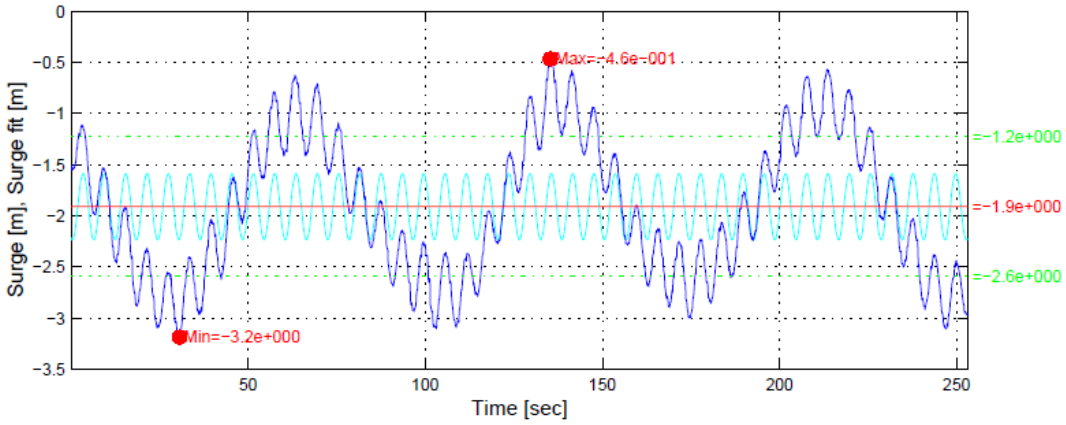

Figure 6.1: Model test surge results with H=3m and T=6s

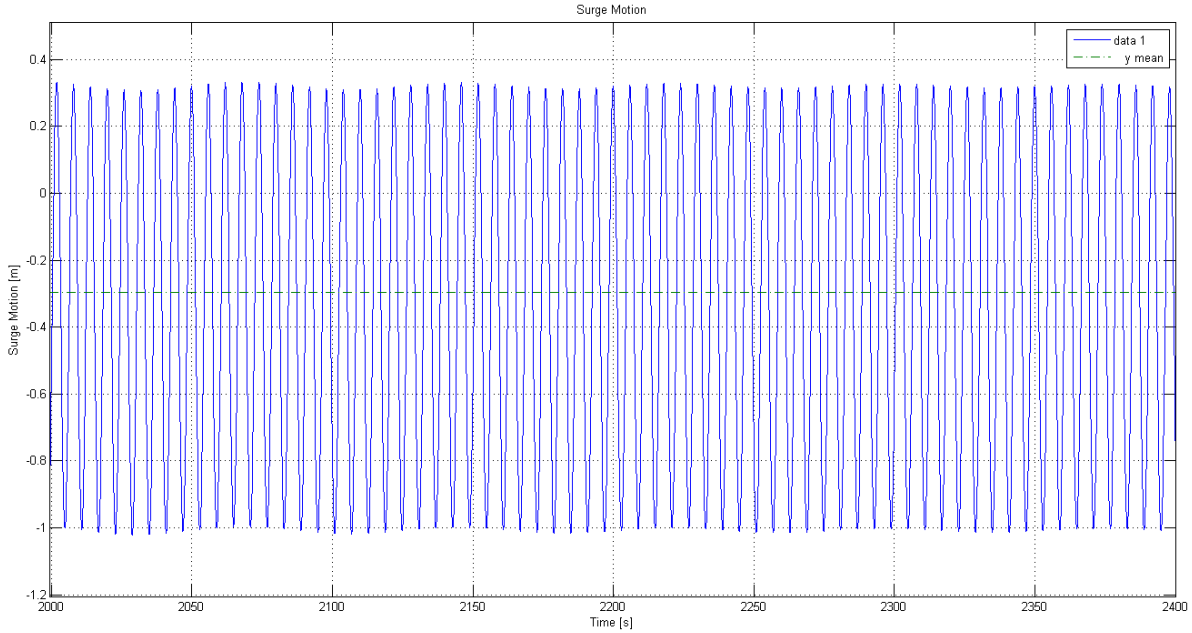

Figure 6.2: Matlab surge results with H=3m and T=6s

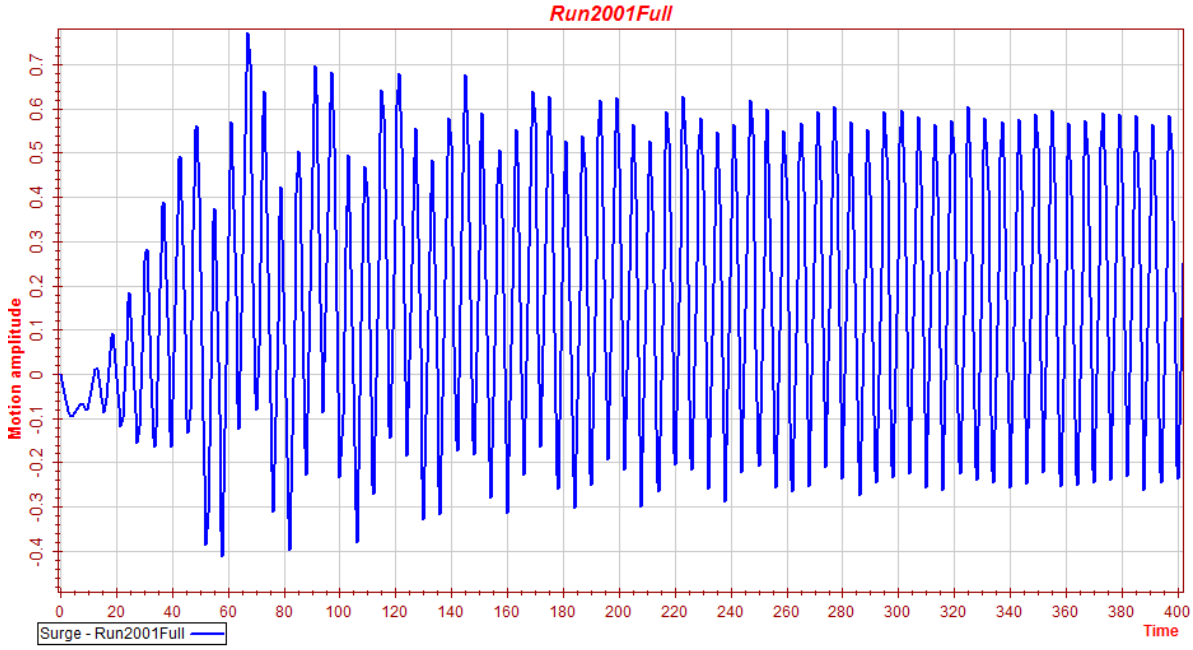

Figure 6.3: Wasim surge results with H=3m and T=6s

The model test is oscillating around -1.9 m ± 1.3 m in surge, and in addition there is a high frequency oscillation which is oscillating ± 0.7 m. By counting the number of peaks and dividing by the time we see that the low frequency oscillation has a period of 66.6 seconds, and the high frequency oscillation has a period of approximately 6 seconds

While the numerical model does start out with a slow oscillation like the model tests it is damped out after a while. It ends up oscillating around -0.3, with ± 0.65 m, and as in the model tests this is a high frequency oscillation. When looking at the oscillation period in the same way as the model tests, we see that the period of this high frequency oscillation is approximately 6 seconds.

Finally we have the Wasim simulation, which has a very simple mooring setup based on the mooring system used in the numerical model. It simply has an additional restoring matrix with the surge restoring coefficient which can be calculated from the equations shown in section 2.2. We see that there is an oscillation of ± 0.4 m around 0.2 m. The oscillation period is approximately 6 seconds. The static drift-off here is positive; though this might only be due to a difference in the coordinate system between the Wasim model and the other models.

There is good agreement between the model test and the numerical model in this case, while the Wasim model also is seen to be in the same range it does deviate more. When looking at the high frequency oscillation period of the models we see that they are all approximately 6 seconds, but the model test is the only with steady low frequency oscillations as well. This low frequency oscillation and the static drift-off difference is the most likely due to the difference in the mooring as mentioned previously.

Heave

In the following figures (figures 6.4, 6.5 and 6.6) we can see the results of heave simulations. Surge results were a little difficult to compare, but the heave results should be more comparable. As this "sea-state" is relatively mild there should be little response from the buoy. Also it is worth noting that the mooring should not be affecting heave in any of the models.

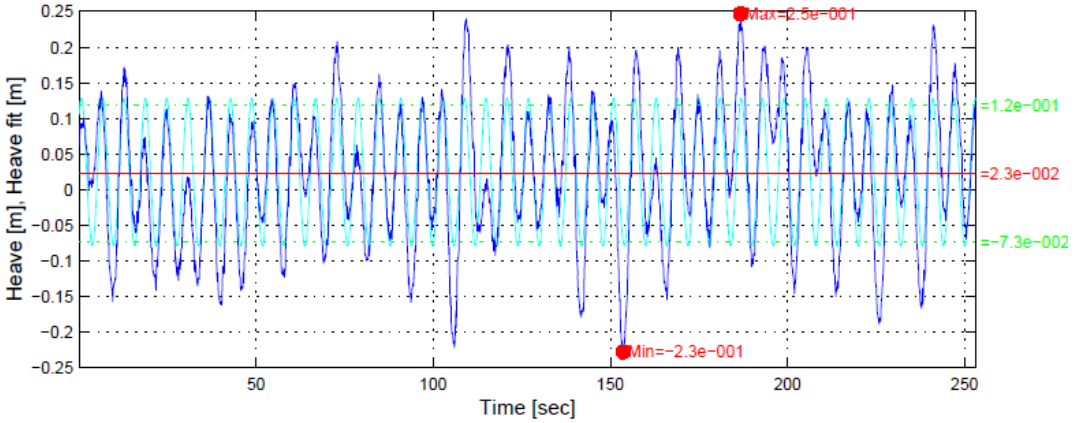

Figure 6.4: Model test heave results with H=3m and T=6s

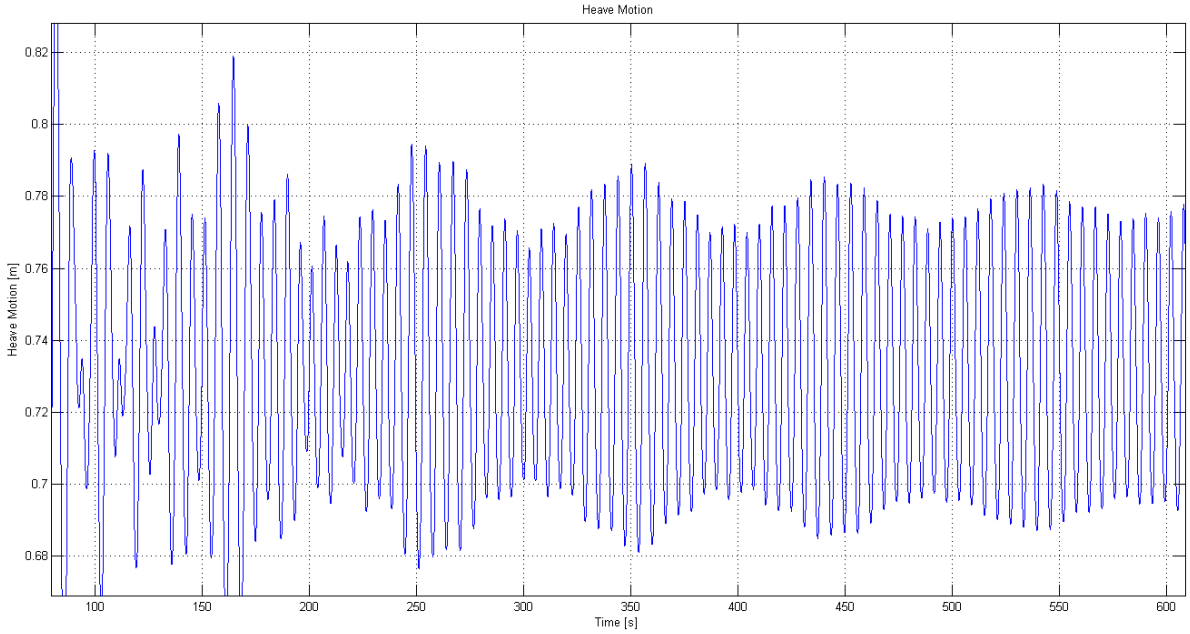

Figure 6.5: Matlab heave results with H=3m and T=6s

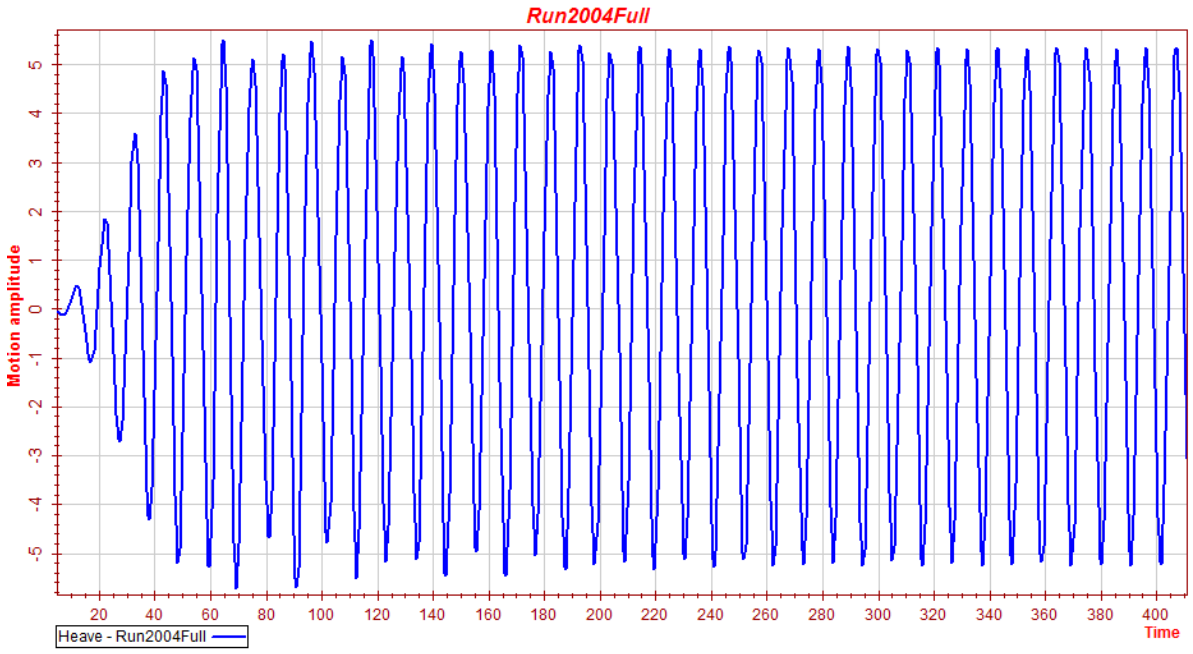

Figure 6.6: Wasim heave results with H=3m and T=6s

The model test result shows a relatively small motion of the buoy. It oscillates around 0.023 m with a mean oscillation of about ± 0.1 m. What is interesting here is that the oscillation is around a positive value. This suggests that the buoy is actually lifted out of the water by the frequent waves. The oscillation period is found to be around 6 seconds which correlates well with the wave period.

We can see some of the same effects in heave results from the numerical model, however the oscillation is around 0.75 m with a mean oscillation of ± 0.08 m. As we can see the oscillation is relatively similar, but the mean offset is very different. The reason for this large difference could lie in the pressure calculation in the numerical model; the wheeler stretching which is applied could cause a slight skewing of the waves in a way which causes more of the wave oscillation to be above the mean water line. The oscillation period is around 6 seconds here as well.

This time the Wasim model is very different from the other models. It oscillates around zero, and the oscillation is ± 0.5 which is much larger than the other two. The oscillation period is also different than the other models, with 10.5 seconds. This period difference coupled with the large difference in response amplitude suggests problems in the Wasim calculations at this "sea state.

Pitch

Lastly, we have the pitch motion (see figure 6.7, 6.8 and 6.9). Pitch is affected by the mooring indirectly as surge is coupled with the pitch motion, this could cause differences in the results, and should be taken in to consideration when examining the figures.

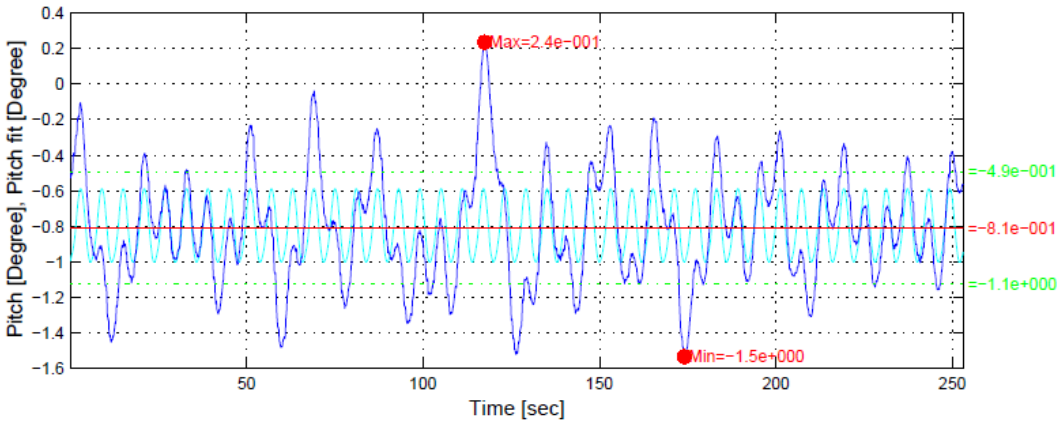

Figure 6.7: Model test pitch results with H=3m and T=6s

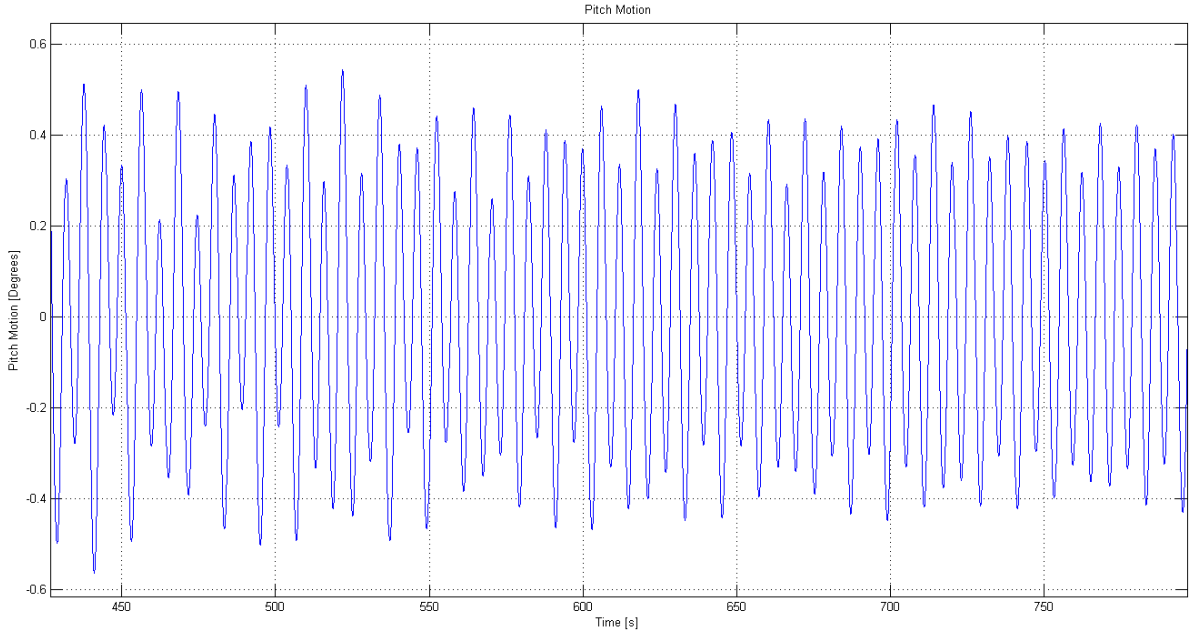

Figure 6.8: Matlab pitch results with H=3m and T=6s

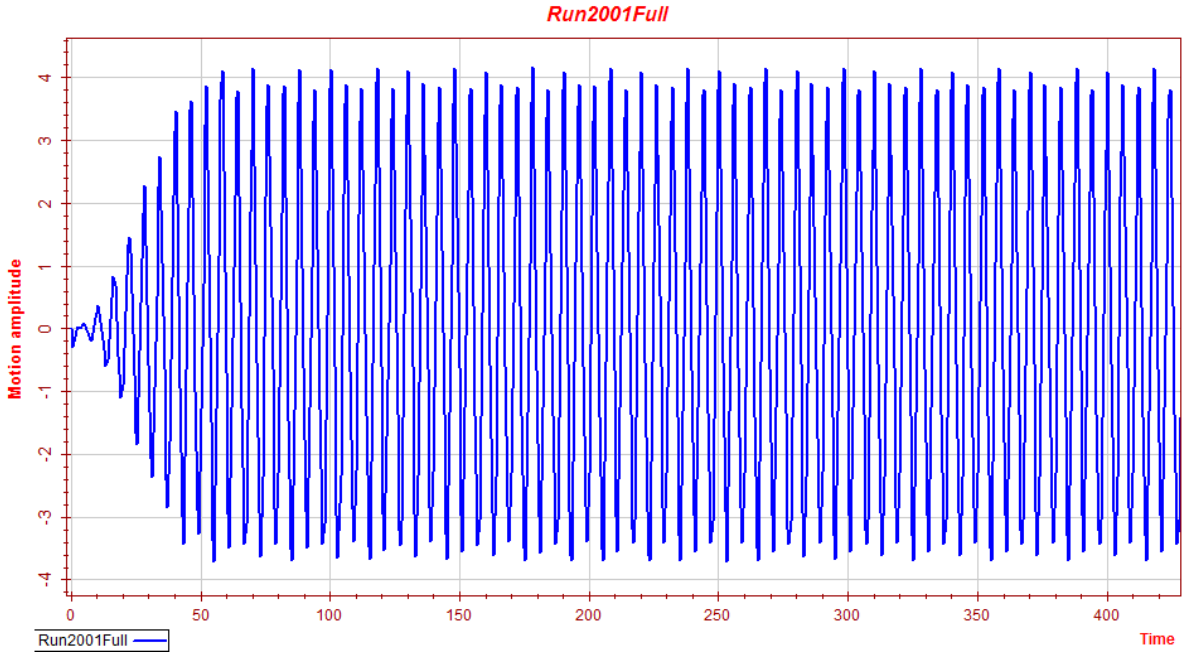

Figure 6.9: Wasim pitch results with H=3m and T=6s

The oscillations in pitch are more erratic than what has been seen in surge and heave, and this makes it more difficult to find the mean oscillation amplitude. The static heeling we observe in the model test results could be influenced by the stiff mooring system in the model tests. In the model tests we see that the buoy will oscillate around a negative angel of -0.81 degrees with an approximate mean oscillation of ± 0.4 degrees. It is also difficult to find the oscillation period in this run because of the erratic behaviour. The result depends on whether or not all the peaks are counted; if all the peaks are counted the result is 6 seconds. If only the largest peaks are counted we get a period of 15 seconds.

In the numerical model we see that the oscillations of the numerical model are also more varied than what has been seen in surge and heave, but not in the same way as in the model tests. The amount of local peaks which is observed in the model tests cannot be found in the numerical model, but the amplitude does vary more. The numerical model does not have a static heeling as we could see in the model tests, but the oscillation is varying in the same range as the model tests of ± 0.4 degrees. The oscillation period is approximately 6 seconds.

We see that the Wasim model gives motions which deviate most from the test results. It oscillates around zero with almost 3.9 degrees in both directions. It is difficult to say why the Wasim model deviates more in this run. There is a possibility that a modelling error is the cause, although no error has so far been discovered. It could also be that Wasim is not able to represent this problem accurately.

6.2 Model Test Run 2004

The second run is a medium "sea state" with a wave height of 10.5 m and a wave period of 10.6 seconds. The motion results are shown in the order of surge, heave and pitch.

Surge

The first motion is surge. Results from the model test, numerical model and wasim are shown in figure 6.10, 6.11 and 6.12 respectively. It is difficult to directly compare with the model tests because of the mooring setup (as mentioned before, see section 5.1) the static drift-off and slow oscillations will probably be most affected, because of this the comparison will only be made between the high frequency oscillations because these have proved to be comparable in run 2001.

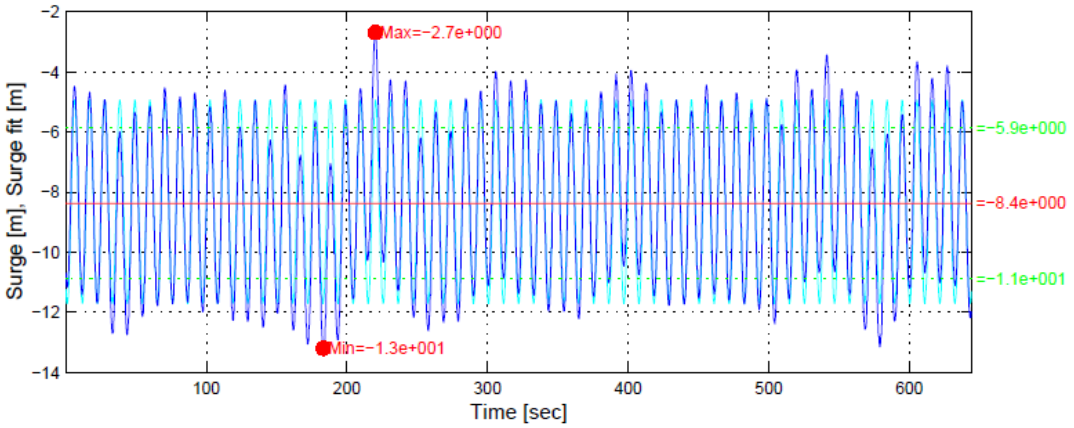

Figure 6.10: Model test surge results with H=10.5m and T=10.7s

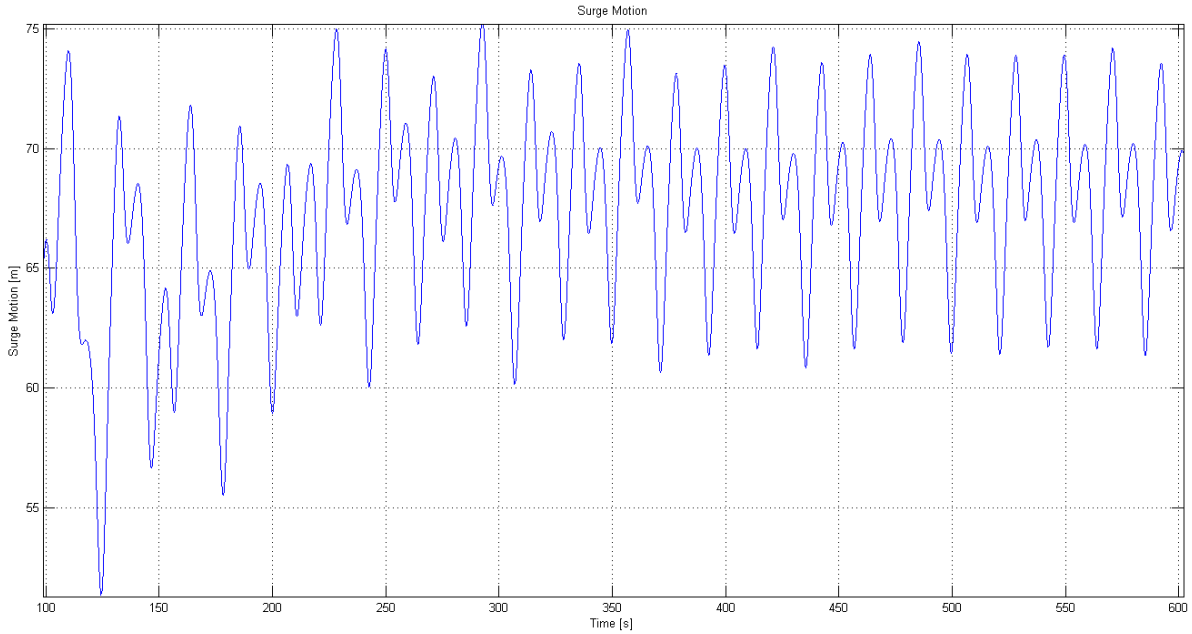

Figure 6.11: Matlab surge results with H=10.5m and T=10.7s

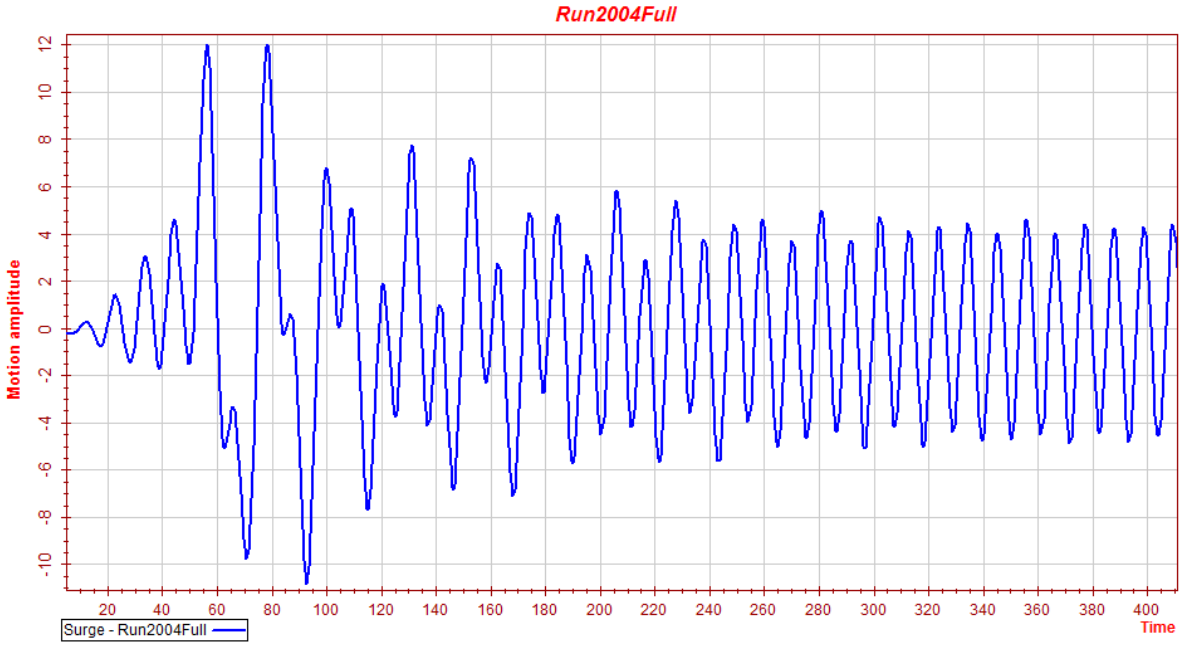

Figure 6.12: Wasim surge results with H=10.5m and T=10.7s

We see that the surge motion in the model test has a static drift-off which is different from zero. We can also see evidence of a low frequency oscillation as we saw in run 2001, but the oscillation is less pronounced. The high frequency oscillation on the other hand is around -8.4 m ± 3 m, although there are larger oscillations when coupled with the low frequency oscillation these are not of interest in the comparisons as mentioned before. The response can be shown to oscillate at a period near 10.7

The numerical model also has a new static value, we see that the numerical model drifts quite a bit more than in the model test, and it oscillates around 67 m ± 5 m. The difference between the two models can be explained by the mooring setup, especially the large static drift-off is most likely due to the long mooring lines. The oscillations do show signs of having two frequencies, but when counting peaks to find the response period it is seen that when counting all peaks we get a period near 10.7

The Wasim model has no static drift-off, but the mean oscillation is close to the numerical model, it is oscillating at roughly ± 4.3. The reason for the lack of static drift-off might be due to the nature of mooring modelling in Wasim. (which is very simplified, and linear) Also in this model we see that the response has a period around 10.7

Heave

The heave results from Run 2004 are shown in figures 6.13, 6.14 and 6.15. The heave results in this run are important, because it was seen in the earlier versions of the program that the area around 10 seconds is close to the natural period. (see appendix section A.1.3 for more details)

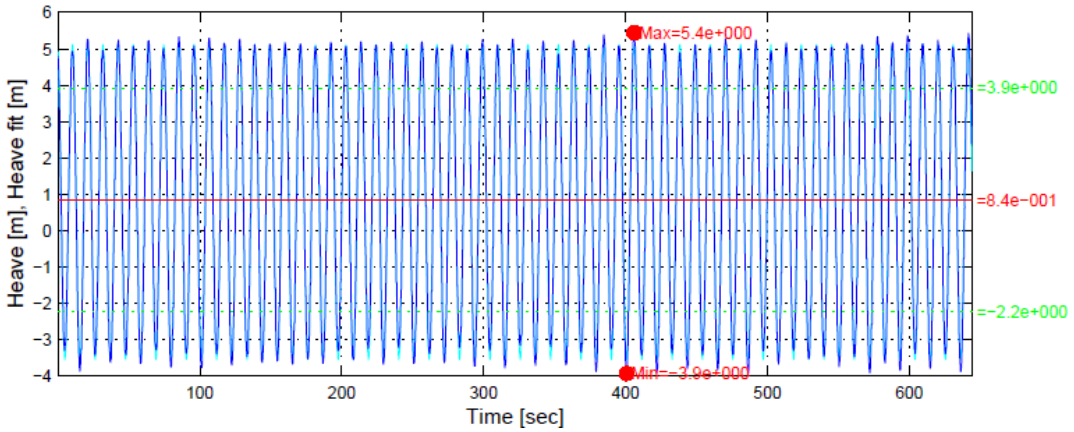

Figure 6.13: Model test heave results with H=10.5m and T=10.7s

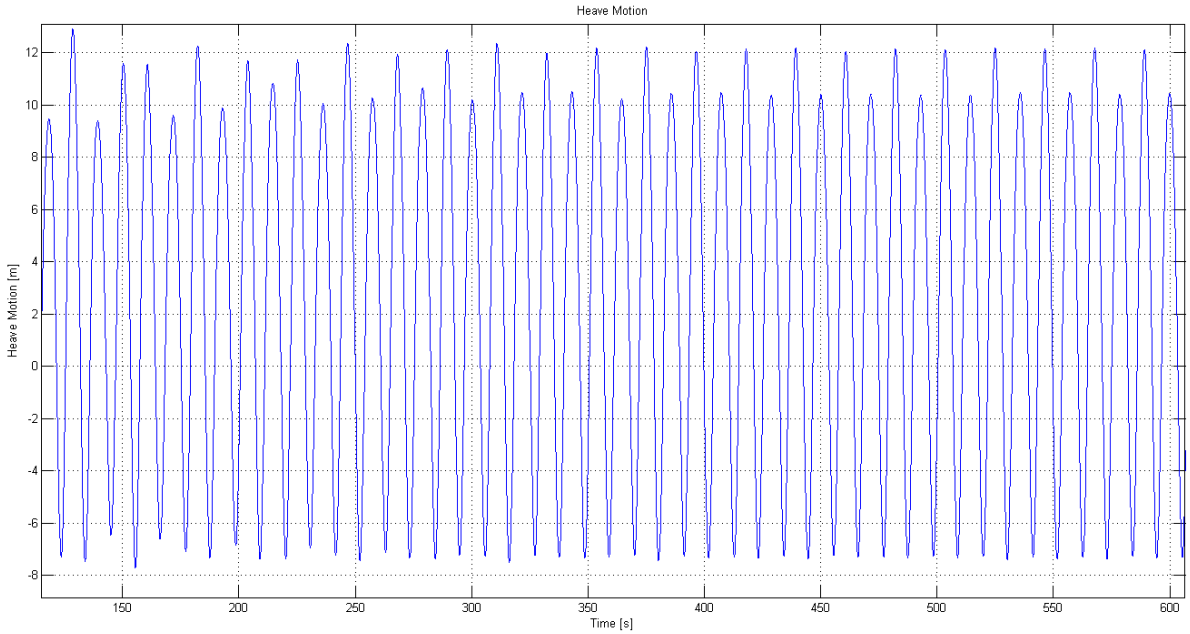

Figure 6.14: Matlab heave results with H=10.5m and T=10.7s

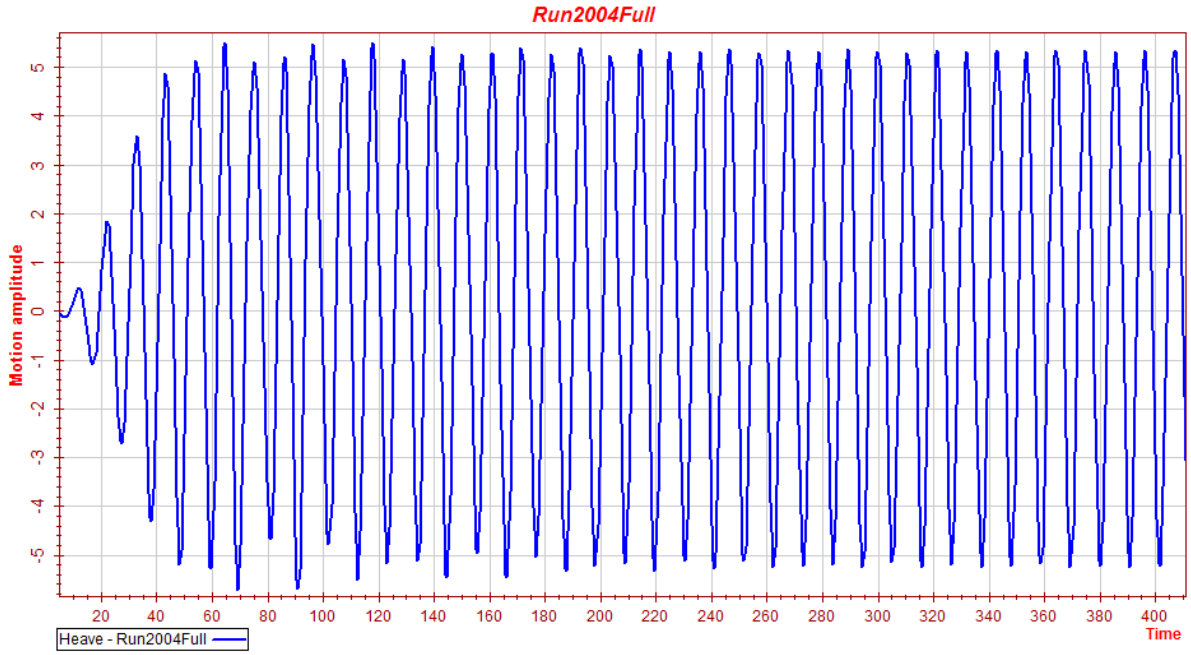

Figure 6.15: Wasim heave results with H=10.5m and T=10.7s

In heave the model test shows an oscillation around 0.84 m, and here the oscillation is about ± 4.5 m. This shows the same positive offset as was seen in run 2001. We do not see any evidence of high responses around this period, even though the response period can be found be around 10.7, which is near the natural period in heave. (see appendixsection A.1 for the decay tests)

The numerical model also shows the same positive offset, but it the oscillation is around 2.8 m ± 9 m. The motions are roughly double compared to the model tests; the explanation for this might be due to a natural period which might be close to the period of this run. It is difficult to say why this effect is shown here, and not in the model tests. The added mass modelling could be the cause of this because the numerical model uses a simple constant added mass model. A change in the added mass will possibly move this peak to a higher or lower period. The numerical model will not be able to account for the total effect of the damping skirt on the buoy due to the proportional damping model. The damping will also be indirectly influenced by added mass through the proportional damping model.

The Wasim model does not show the same positive offset as the two other models. However the oscillation is more in line with the model tests than the numerical model. Here the buoy is oscillating ± 5 m. The response period is also the same. The Wasim model does have a more comprehensive way of calculating the added mass, so this might be the cause of the difference. The added mass in Wasim is most likely found using a BEM as was briefly mentioned in subsection 4.2.3.

Pitch

Finally, we have the pitch results. (see figures 6.16, 6.17 and 6.18). Due to the steepness of the waves, being 0.06, the pitch motion in this run is expected to be large.

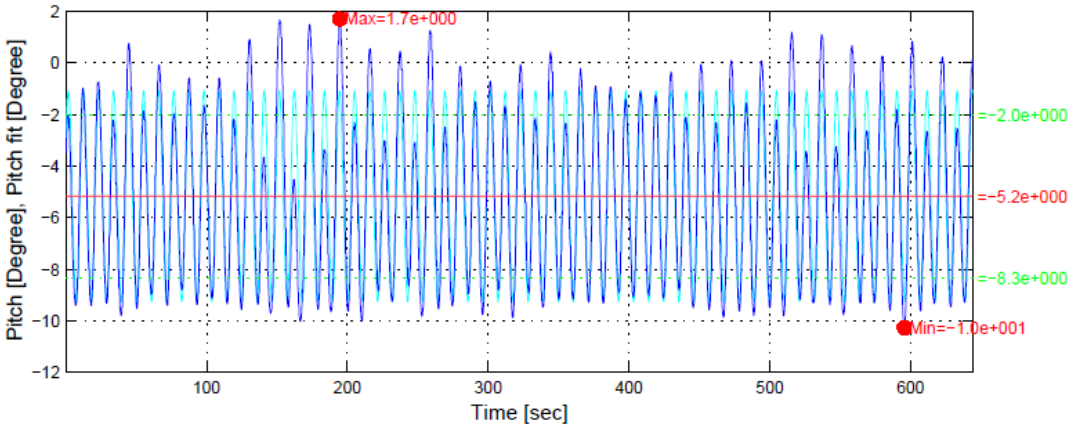

Figure 6.16: Model test pitch results with H=10.5m and T=10.7s

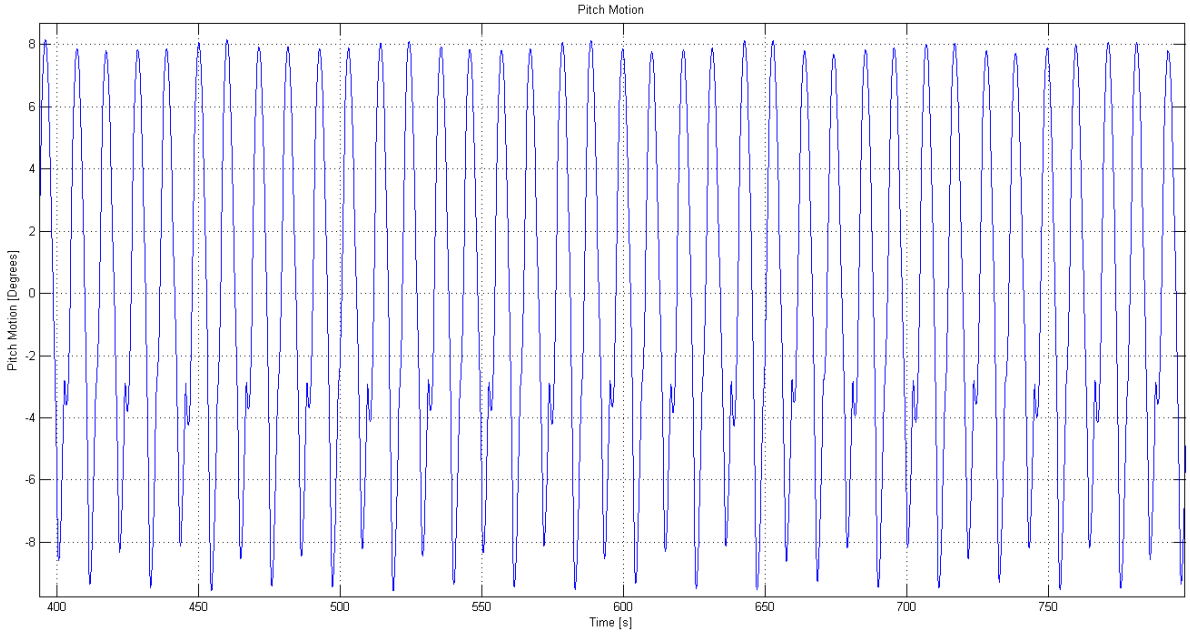

Figure 6.17: Matlab pitch results with H=10.5m and T=10.7s

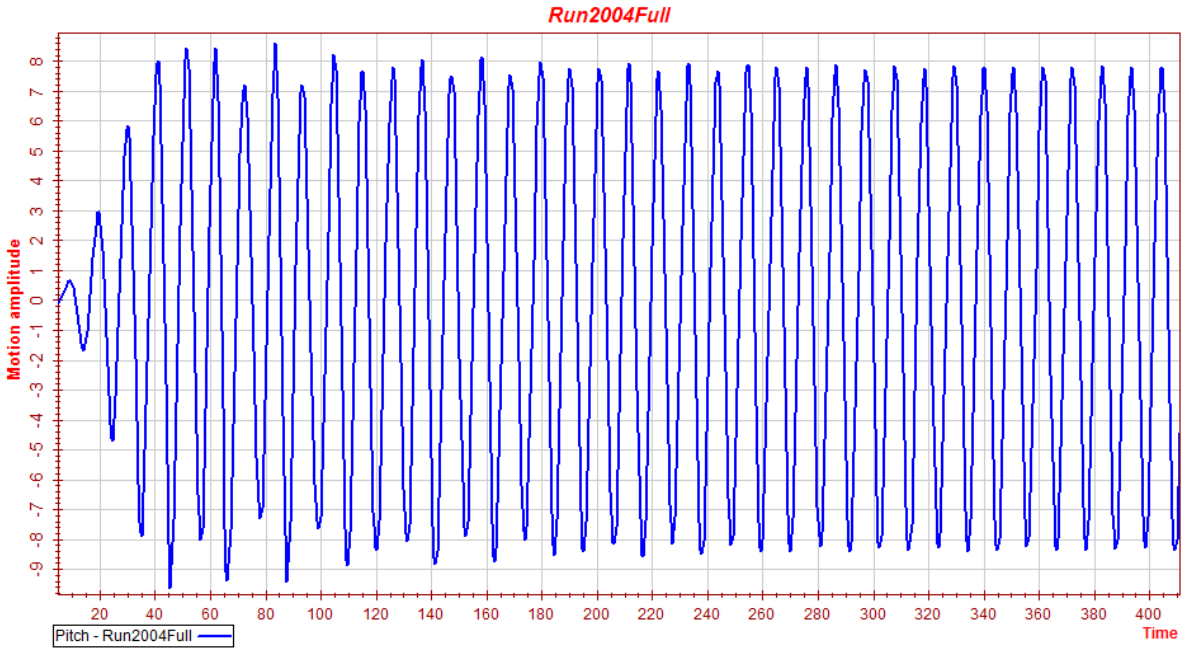

Figure 6.18: Wasim pitch results with H=10.5m and T=10.7s

As expected, the pitch motion is very large here with a maximum value of 10.1 degrees. The model test has a static heeling and this time it oscillates around -5.2 degrees ± around 4 degrees (standard deviation is 3.1 degrees). The pitch motion is a bit noisy so it is difficult to determine the oscillation exactly, but the oscillation period does match the wave period of 10.7 seconds.

When looking at the numerical model we see that there is lack of static heeling, but the amplitude does have the same max value as we can see in the model tests. This makes the comparison more difficult as the static heeling is now so large that to ignore it will be difficult. Therefore it should be better to compare the actual heeling. The heeling in the numerical model is seen to be approximately 8 in the positive direction, and nearly 9 in the negative. Also here we see that the oscillation period does match the wave period.

The Wasim model is looking similar to the numerical model, there is no static heeling, and the amplitude is in the same range, although the oscillation is much more uniform once it has reached a steady state. The oscillation is approximately ± 8 degrees and the period matches the wave period.

6.3 Model Test Run 2015

This run is the severe sea state, it is meant to be at the most critical sea state. The wave height is 19.5 m, and the wave period is 14.6 seconds. This run is also meant to test the stability of the numerical model, because of a stability problem seen in the previous numerical model. (see appendix B for more details)

Surge

The surge motion of the models is shown in figures 6.19, 6.20 and 6.21. Due to the extreme wave height the surge motion in this case might be large.

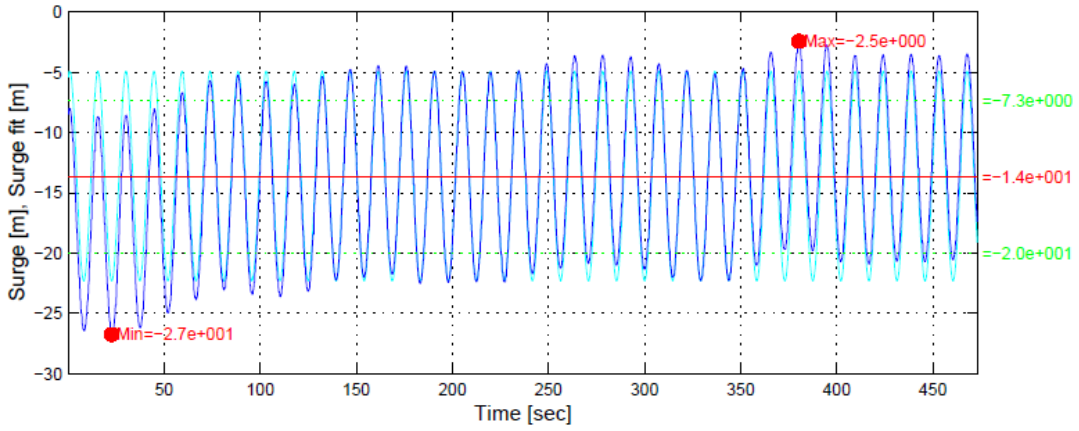

Figure 6.19: Model test surge results with H=19.5m and T=14.6s

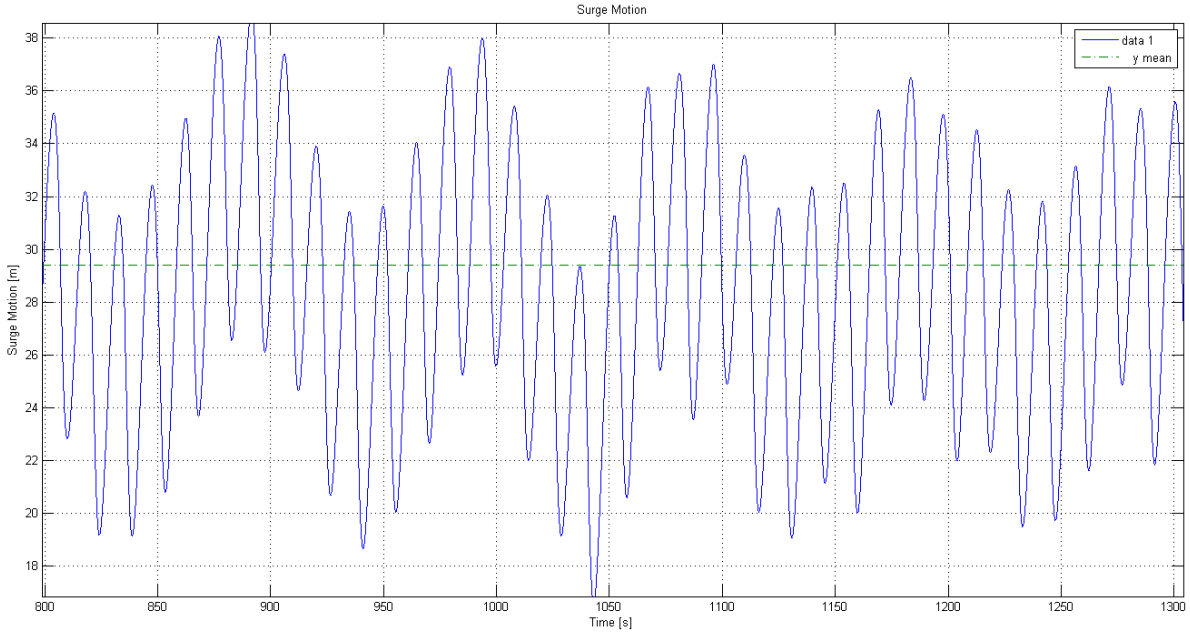

Figure 6.20: Matlab surge results with H=19.5m and T=14.6s

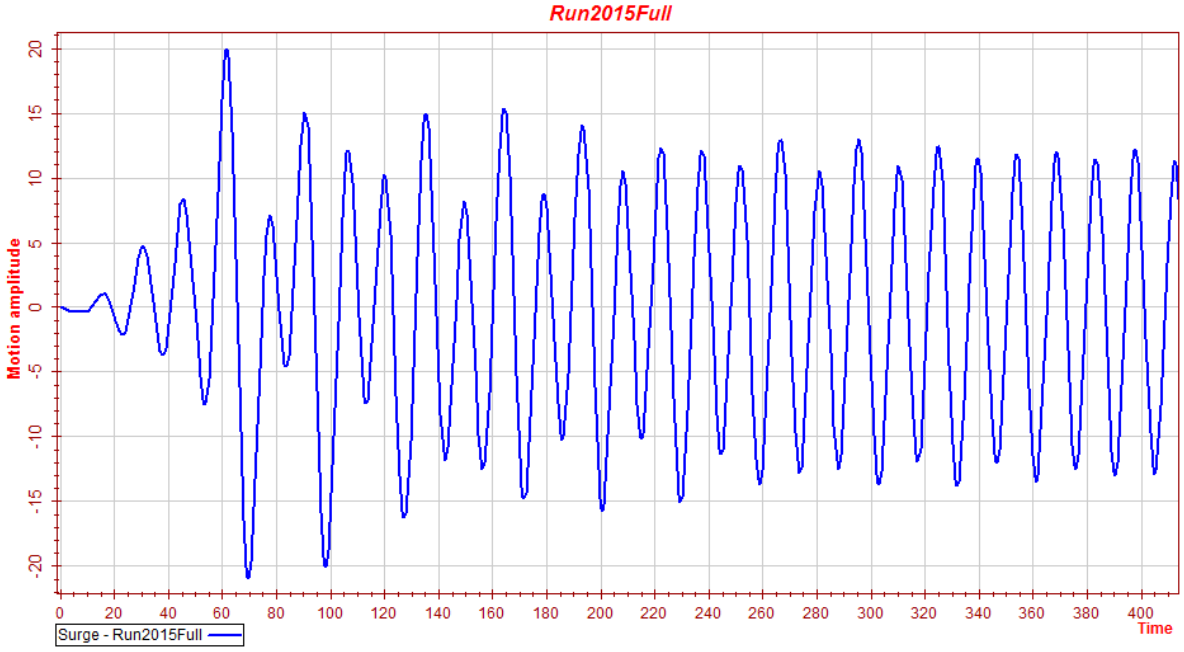

Figure 6.21: Wasim surge results with H=19.5m and T=14.6s

The model tests show a larger static drift-off in this run, the point at which it oscillates is -12 m and it oscillates ± 7 m. (When the oscillations have reached a steady state.) In this run there is little evidence of the slow oscillations which has been seen in the previous runs.

The numerical model has a larger static drift-off, and it oscillates near 30 m. Here we see that there is both a low frequency oscillation with an oscillation of ± 5 m with an oscillation period of approximately 100 seconds. We also have a high frequency oscillation which oscillates ± 7 m with a period matching the wave period of 14.6 seconds.

The Wasim model is once again oscillating around zero, it does show a slightly higher oscillation in this run than what was seen in the previous runs with oscillation of ± 12. The oscillation period is also matching the wave period.

Heave

The heave results for 2015 are shown in figures 6.22, 6.23 and 6.24. The heave motions are expected to be large due to the height of the waves.

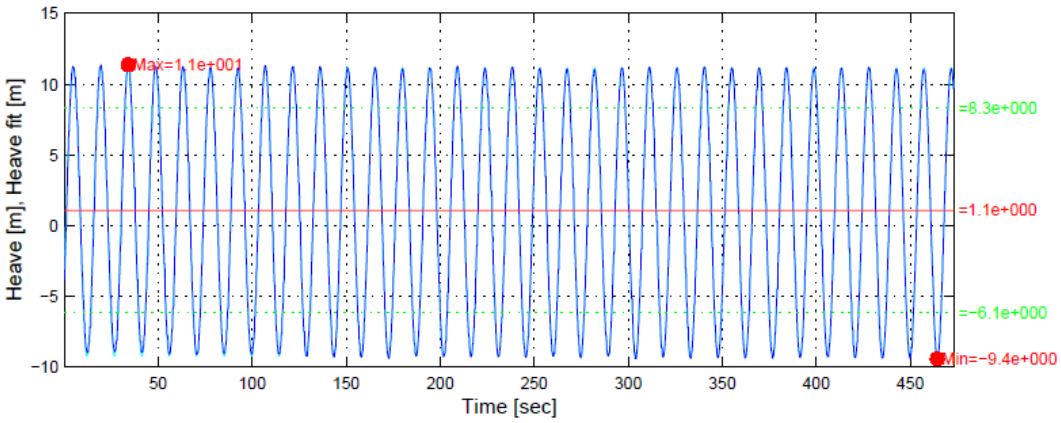

Figure 6.22: Model test heave results with H=19.5m and T=14.6s

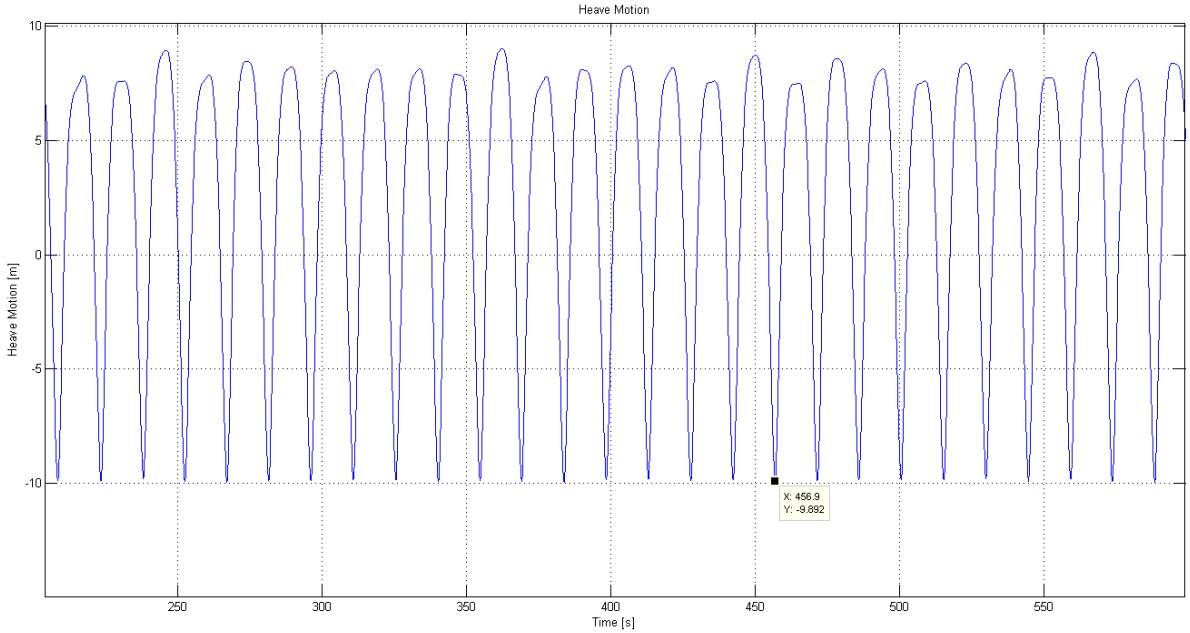

Figure 6.23: Matlab heave results with H=19.5m and T=14.6s

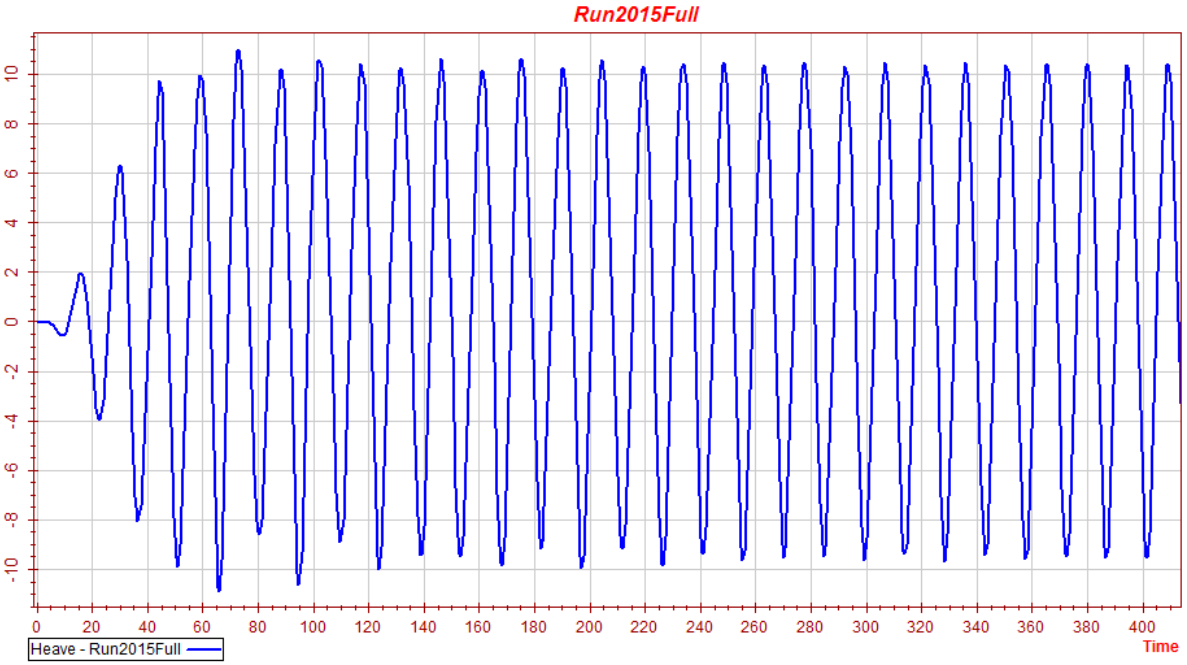

Figure 6.24: Wasim heave results with H=19.5m and T=14.6s

As in the other runs, we can see that model test heave results have a positive offset. In this run the static point is 1.1 m, the oscillation is ± 10 m. We see that the buoy reaches a response amplitude of 11 meters, which is very remarkable as the buoy without the damping skirt only has a draft of 10.5 meters. This indicates that the buoy might be subjected to slamming loads in this type of extreme sea state.

The numerical model is showing a different oscillation. The peaks are rounded and does not reach the same amplitude as the through, the peaks could be rounded due to the rapid decrease of volume from the hull being dry in a wave through. The difference could also simply be that the reference coordinate systems are different, so that the positive amplitude in the numerical model matches the negative amplitude in the model tests. We see that the negative amplitude does match the model test, but the numerical model does not have a offset. The positive amplitude is around 8 meters and the negative amplitude is 10 meters.

Also the Wasim model has a positive offset in this run, although it is less pronounced than in the model test. The middle point is 0.25 m and the oscillation is ± 10 m. The Wasim results are closer to the model tests in heave than the numerical model, although, there is less difference in this run than what has been seen in previous runs. The Wasim model does, however, outperform the numerical model in the heave motions.

We see here that the oscillation is large as was expected, but the motion only has a ratio close to one with the wave amplitude. This is true in all models. This behaviour could be caused by a limiting response due to the extreme wave height of 19.5 m

Pitch

The pitch results from Run 2015 are shown in 6.25, 6.26 and 6.27. In this run the pitch motion could be expected to be large. The waves have the same steepness as in run 2004 (steepness 0.6), this resulted in large perturbations. The most notable feature of the pitch motion was the large off-centre oscillations. Although the waves are longer here, we may still see similarities.

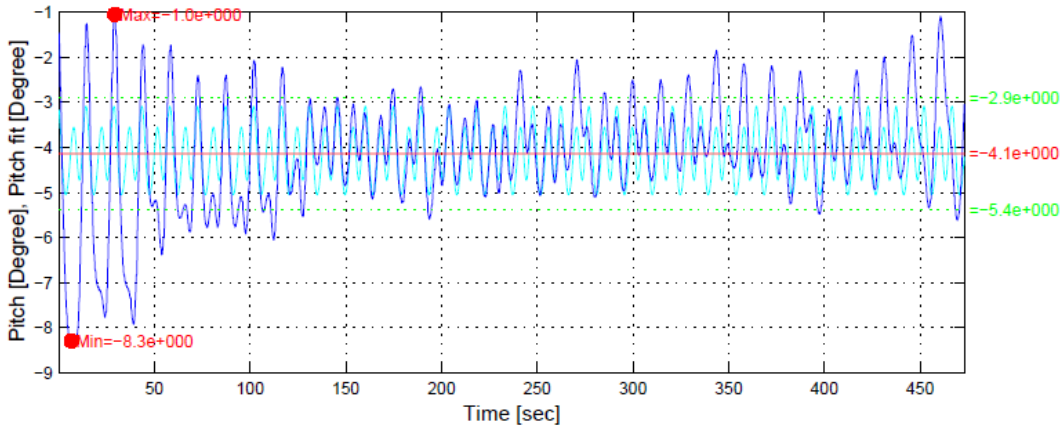

Figure 6.25: Model test pitch results with H=19.5m and T=14.6s

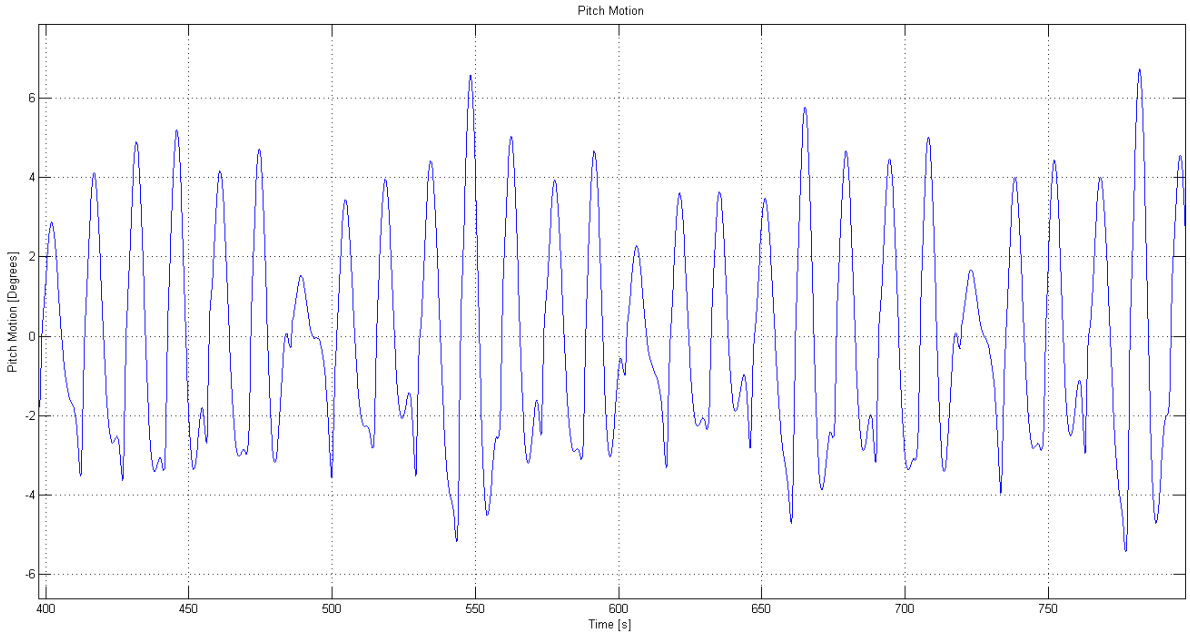

Figure 6.26: Matlab pitch results with H=19.5m and T=14.6s

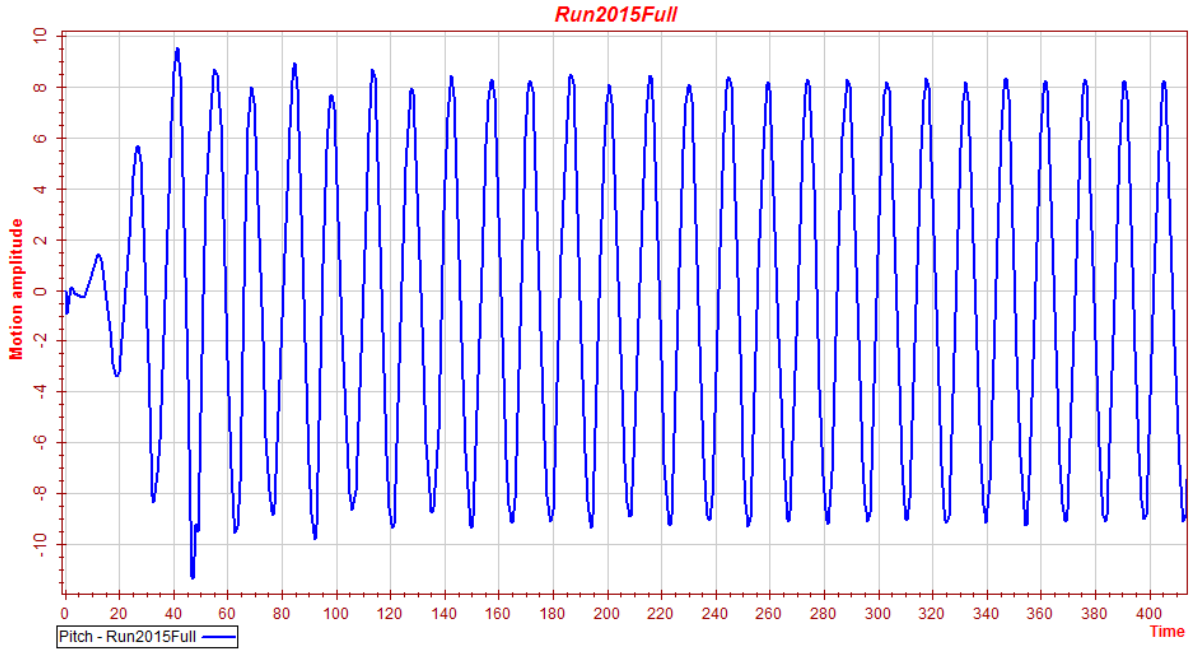

Figure 6.27: Wasim pitch results with H=19.5m and T=14.6s

The model test results does show an off-center pitch oscillation as was seen in run 2004, the oscillation is centred around 4.1 degrees, but he oscillation is really rather small, only ± 1 degree. The reason for this may be that the waves are hitting the structure in a way which hinders oscillation, there is even a possibility that there is green water on the deck, which could keep the structure at a listing angle.

The numerical model is also showing some signs of being affected by the waves hitting the structure in a way which hinders the oscillation. Due to the lack of the static heeling in the numerical model we will have to compare the amplitudes, as was done in run 2004. The positive amplitude varies between 4 and 6 degrees. While the off-center pitch oscillation is not seen here the amplitudes do match very well.

The Wasim model has a very large oscillation compared to the model test, but it is difficult to compare the two due to the off-center pitch motion in the model tests. Looking at the amplitude, we see that the Wasim model has an oscillation which exceeds 8 degrees.

6.4 Model Test Run 2019

We have another medium "sea state" but with long waves, this run has a wave height of 9 m and a period of 20 seconds.

Surge

The surge motion results for this run are shown in figure 6.28, 6.29 and 6.30. Due to the long waves the surge motion can be expected to be smaller in this case than what was seen with the much steeper waves in run 2004 and 2015 where the steepness was 0.06. In this run the steepness is 0.014.

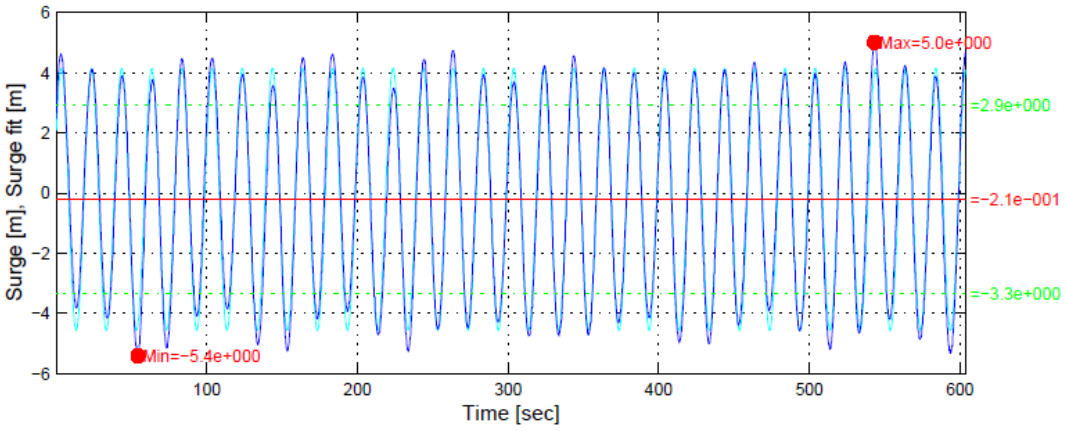

Figure 6.28: Model test surge results with H=9m and T=20s

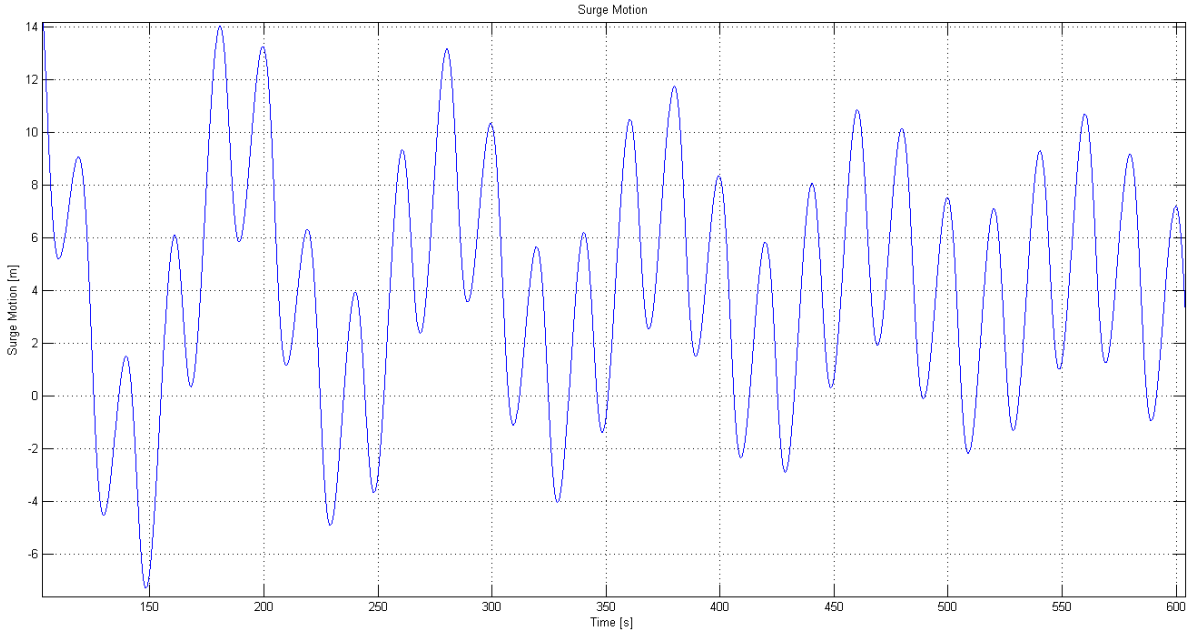

Figure 6.29: Matlab surge results with H=9m and T=20s

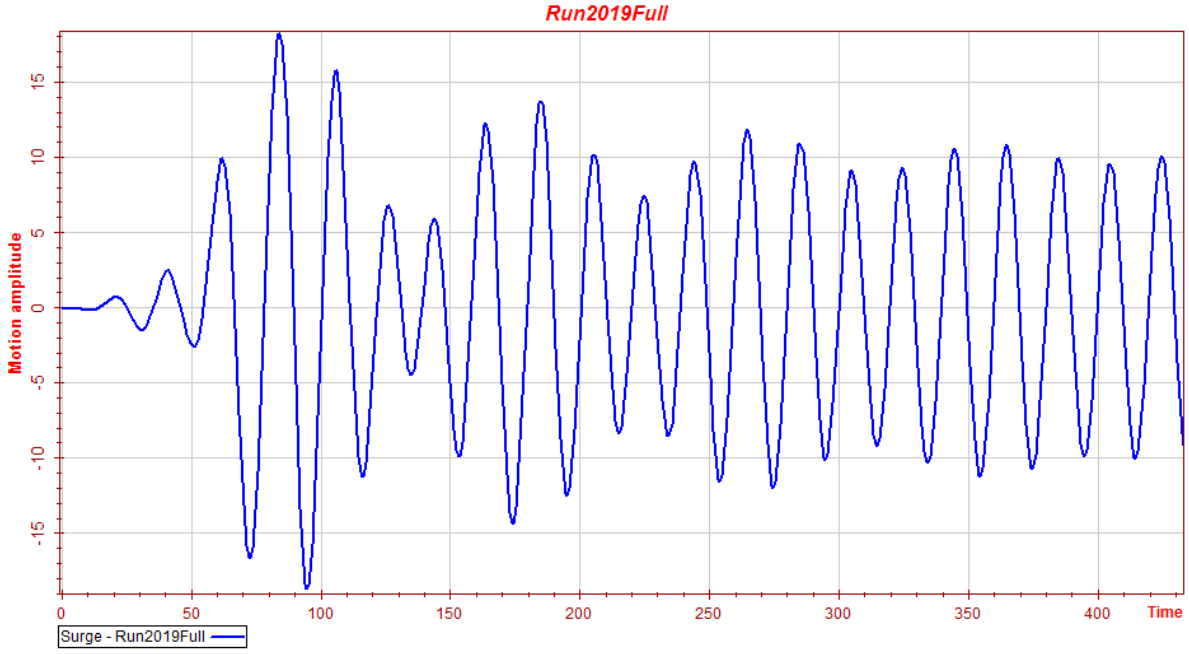

Figure 6.30: Wasim surge results with H=9m and T=20s

The surge motion of the model tests are almost oscillating around zero, (-0.24 meters) the oscillation is ± 4.5 m. We see almost no static drift-off in this run, this is due to the the long waves allowing the structure to restore before the next wave hits.

The numerical model has a small static drift-off, it oscillates around 4 meters ± 4.5 meters. The result is relatively close to the model tests. The low frequency oscillation does damp out, and leaves only the high frequency oscillation.

The Wasim surge motion is once again oscillating around zero, but with ± 10 meters. The result deviates by a factor of two compared to the other models, and no static drift-off is evident.

Heave

The heave results are shown in figures 6.31, 6.32 and 6.33. In this run the heave motion should follow the wave motions exactly due to the long waves.

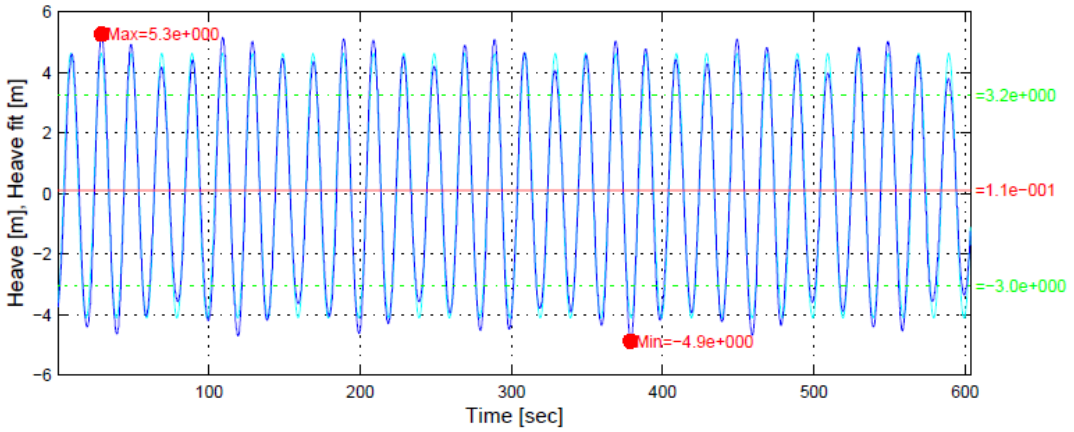

Figure 6.31: Model test heave results with H=9m and T=20s

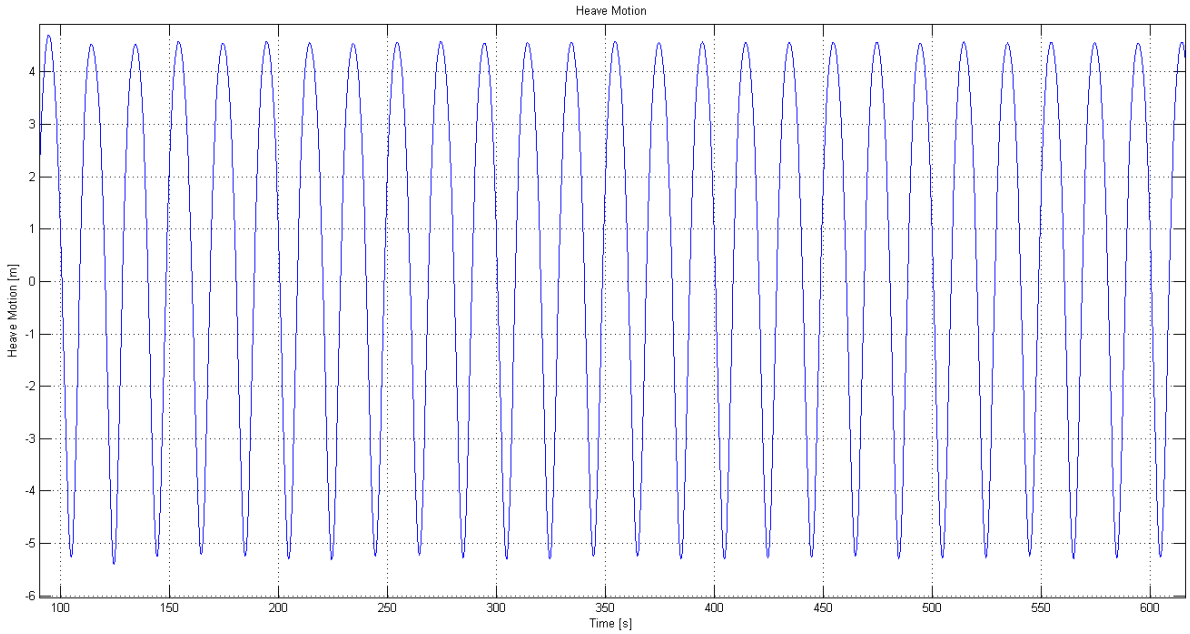

Figure 6.32: Matlab heave results with H=9m and T=20s

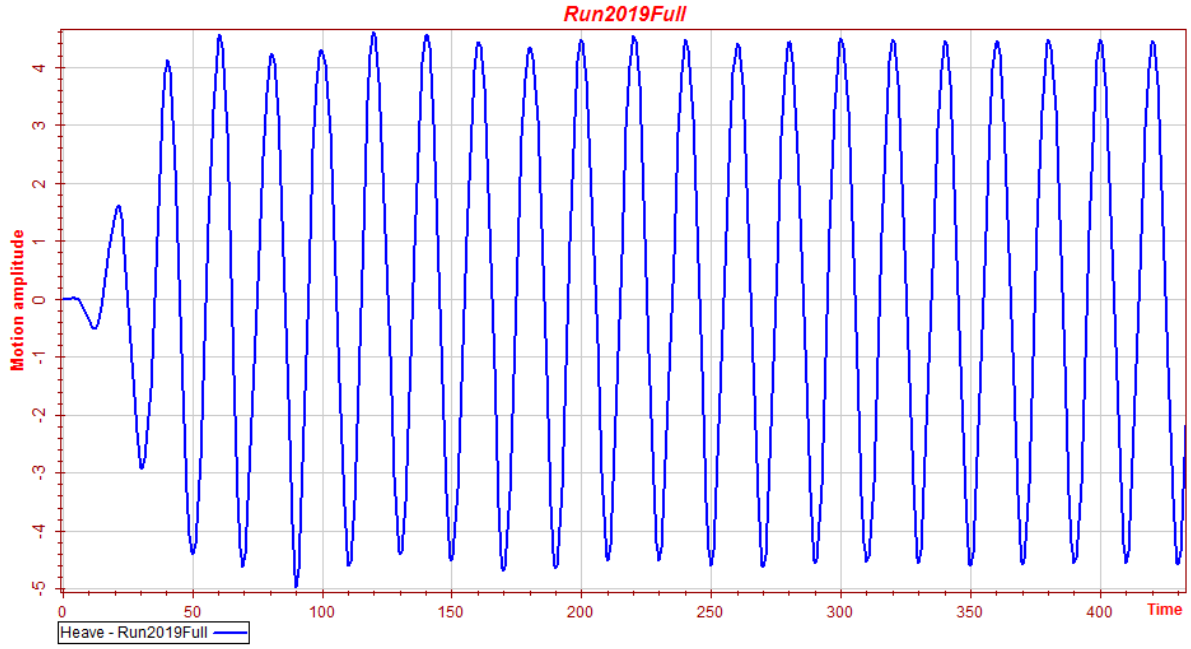

Figure 6.33: Wasim heave results with H=9m and T=20s

In the model tests, we can see almost no positive offset in this run, only around 0.1 meters. The oscillation is close to ± 4.5 meters (the standard deviation is 3.1 meters.). As we see the motion is exactly the same as the wave amplitude.

The numerical model has no positive offset, and the oscillation is roughly ± 4.7 meters. The results are close to the model test.

The Wasim model is also in the same area as the other two models with an oscillation of about ± 4.5 meters.

In this run the heave motion of both models are close to the model tests. This increasing accuracy could be connected to the increasing wave length. As the waves become less frequent the unstable oscillations which often characterises the more erratic sea states disappear, and the structure will be more likely to follow the wave motion. This type of motion is often seen in swells, and the waves will often be more like airy (or first order) waves as they become longer.

Pitch

Finally we have the pitch results of the final examined run. They are shown in figure 6.34, 6.35 and 6.36. Judging by the results in surge and heave we could expect the pitch motion to be approaching a more linear behaviour in this run. While this run still has waves which could induce the non-linear behaviour caused by the geometry this requires the waves to hit significant amounts of the slanted hull, which could be stopped by the heave motion following the wave crest.

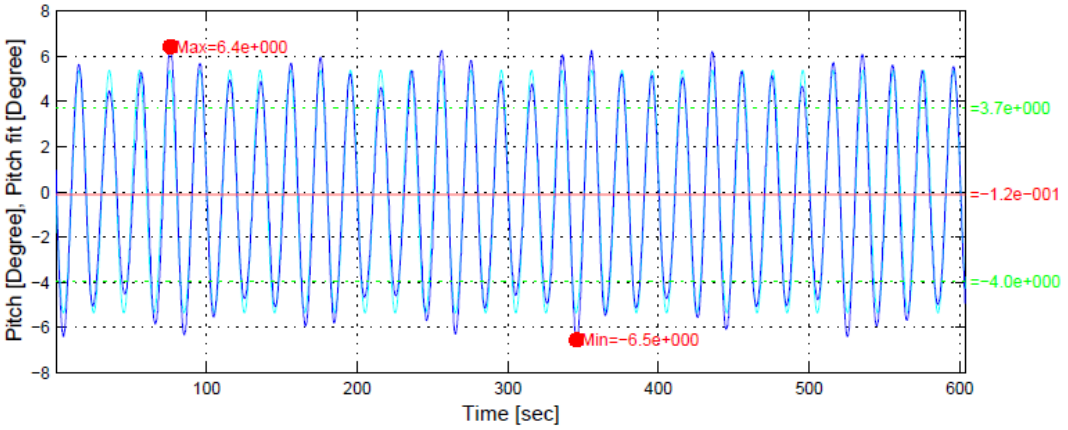

Figure 6.34: Model test pitch results with H=9m and T=20s

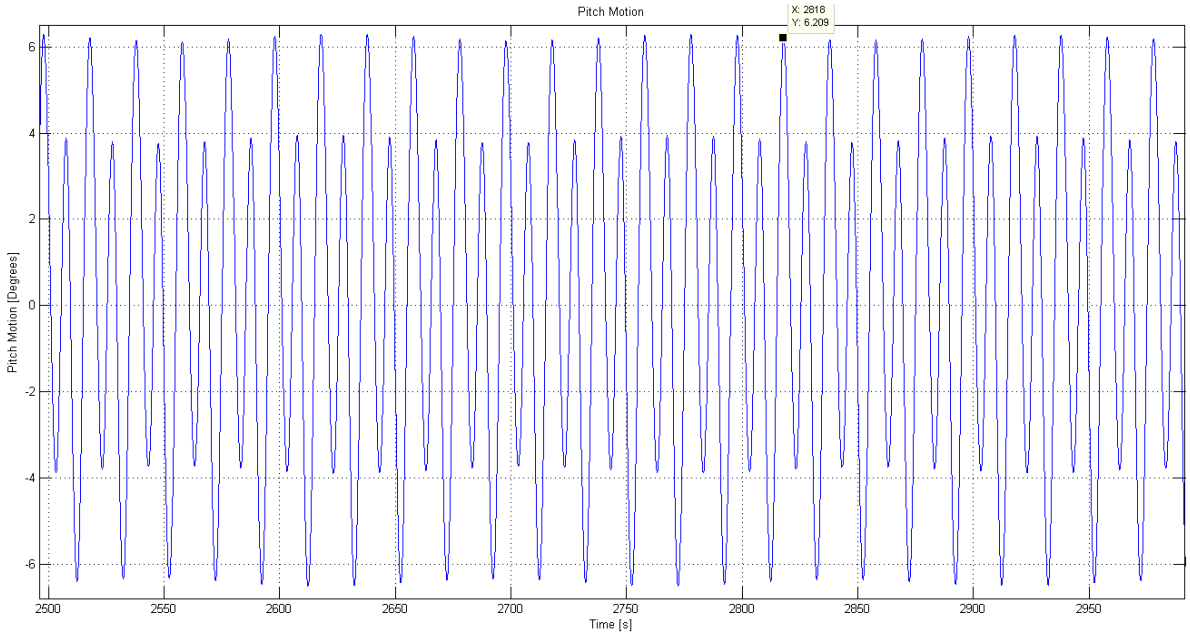

Figure 6.35: Matlab pitch results with H=9m and T=20s

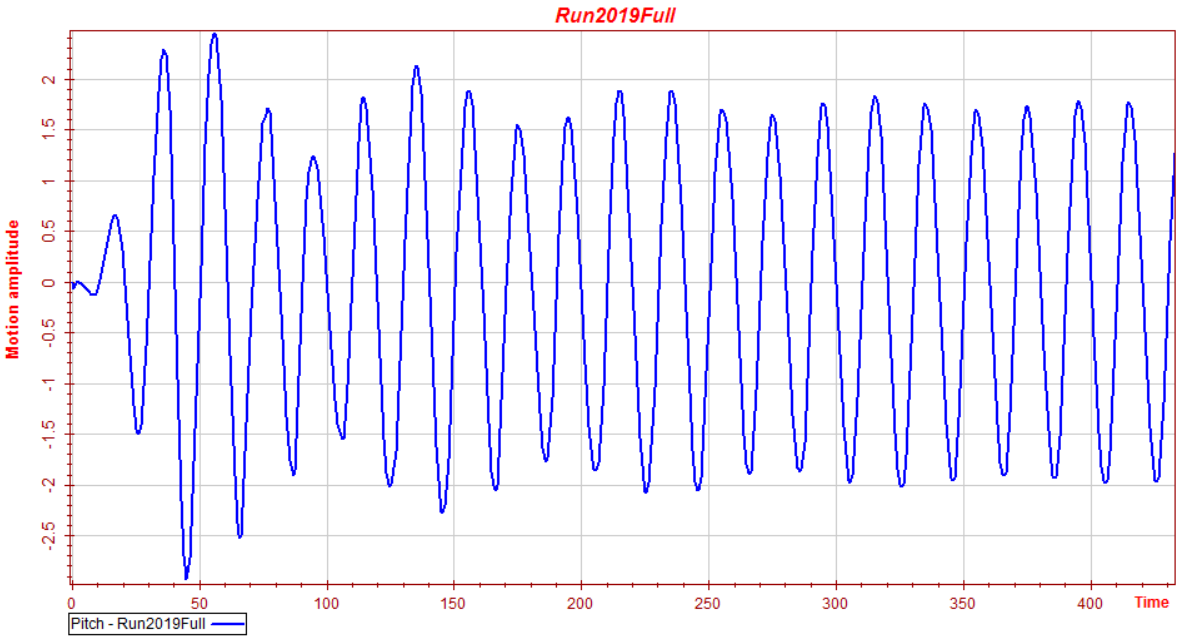

Figure 6.36: Wasim pitch results with H=9m and T=20s

The pitch results of the model tests show an oscillation around 0.12 degrees with a mean oscillation ± 5 degrees. The motion is actually very large for this run, but unlike run 2004 and 2015 there is very little off-center oscillation in this run. The oscillation is also much more undisturbed than what was seen in run 2004 and 2015. This means that the waves are not interfering as much with the motion; this is most likely the reason why we are not seeing the same amount of off-center oscillation here.

The numerical model is also showing a more undisturbed oscillation than what was seen in run 2015. the oscillation varies between two amplitudes ± 4 degrees and ± 6 degrees. These amplitudes are also seen in the model tests, and the mean oscillation and max oscillation is very similar. We can also see that there might be two frequencies in this run.

The pitch motion in the Wasim model deviates from the model tests with a factor of more than two with a mean oscillation of ± 1.8 degrees. This deviation is in line with pitch motion in the earlier runs as will be shown in the conclusion of this chapter.

While the pitch motion can still be considered to be large, we can see that the static heeling in the model tests is almost non-existent in this run. The actual pitch motion in the model tests is still large, but we see a motion which is going towards being linear.

6.5 Model Test Run 2017

This run was added to show that the pitch results from the numerical model does not match the model test perfectly. The runs were originally chosen to include all critical periods, but after an error was corrected in the numerical model the pitch results in run 2001, 2004, 2015 and 2019 seemed to fit the pitch results perfectly. To avoid giving a false impression of the results some effort was made to find results which did not match. Wasim results have not been included in this run.

This run has a wave height of 5 meters and a wave period of 9.9 seconds and considered to be a mild sea state.

Surge

The surge results from this run are not expected to show any significant variations compared to the other runs. The results are shown in figure 6.37 and 6.38, due to the difference in the mooring system only the high frequency oscillations will be compared as they have proven to be comparable in the previous runs.

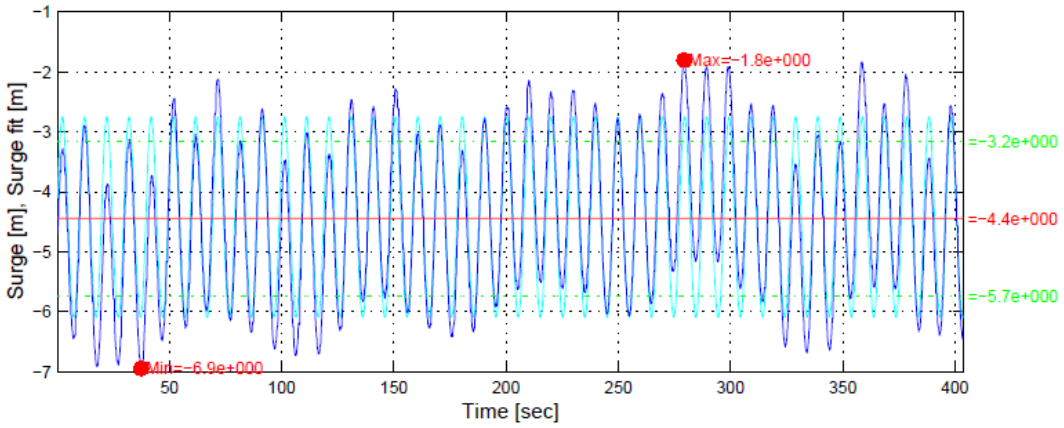

Figure 6.37: Model test surge results with H=5m and T=9.9s

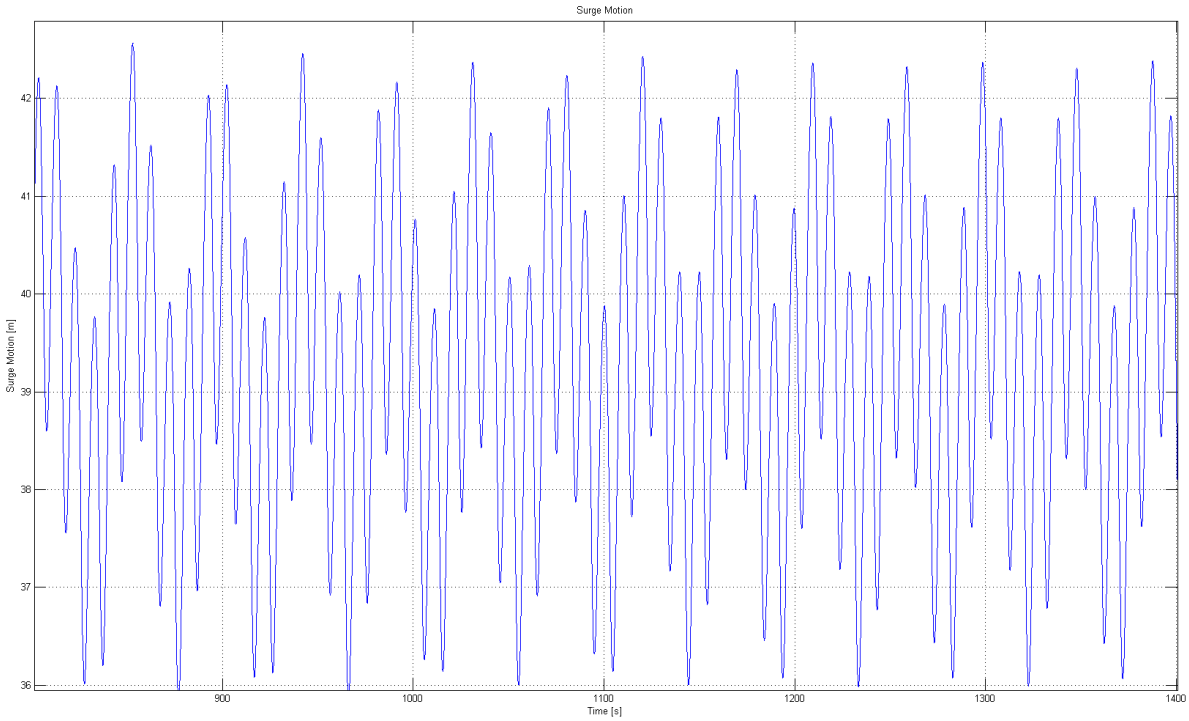

Figure 6.38: Matlab surge results with H=5m and T=9.9s

The model tests have two oscillations as we have seen in previous runs and we also see a small static drift-off of 4.5 meters. The low frequency oscillations are relatively modest in this run with a amplitude of roughly 0.5 meters, and the high frequency oscillations are also small with an oscillation of approximately 1.5 meters.

The numerical model also has two oscillations and a static drift-off, but again this value is much larger with a value of roughly 38 meters. The low frequency oscillations are also larger in this run with a oscillation of 2 meters. The high frequency oscillations are in the same order as the slow drift with approximately 2 meters amplitude.

The periods of the low frequency oscillations are different in the models with the model tests having a period of 80 seconds and the numerical model with a period of 50 seconds, but as with the previous runs the high frequency oscillations in both models are matching the wave period. This is the reason why the low frequency oscillation amplitudes are not compared in this chapter.

Heave

The heave results in the numerical model and model tests have already been shown to be different around this period range. (see run 2004) The results in figure 6.39 and 6.40 should there show a similar difference in this run.

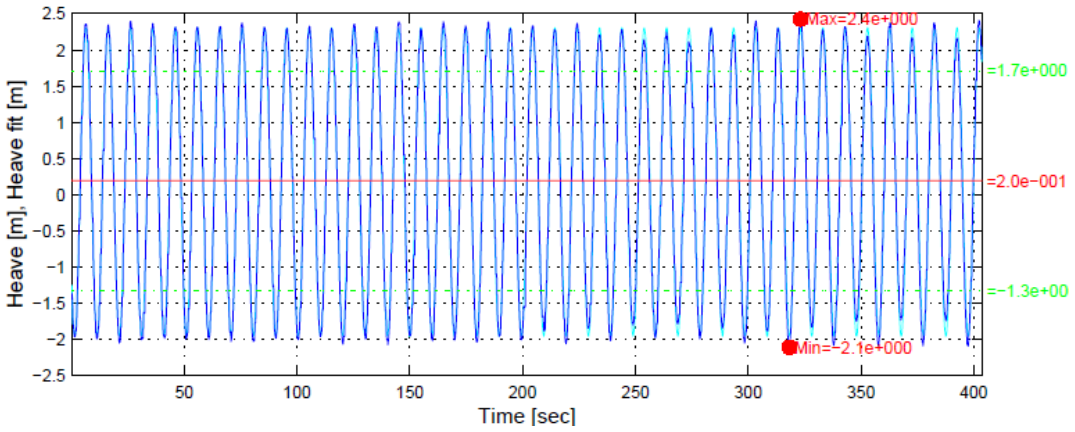

Figure 6.39: Model test heave results with H=5m and T=9.9s

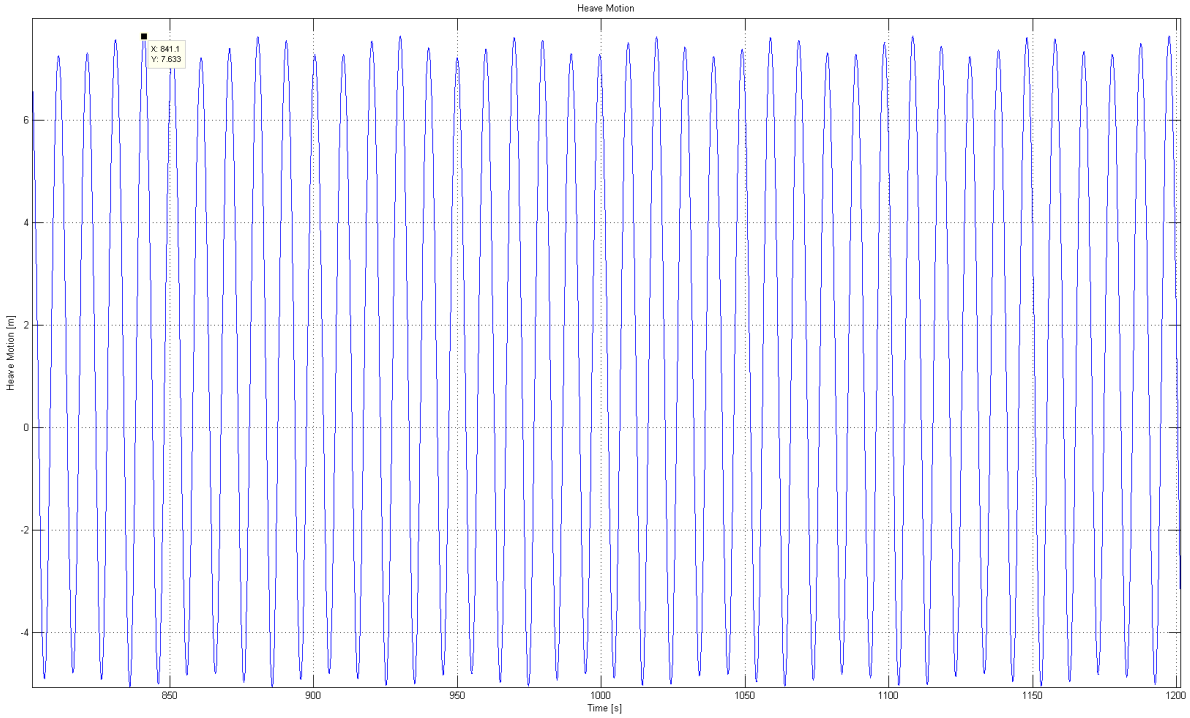

Figure 6.40: Matlab heave results with H=5m and T=9.9s

As we have seen in previous runs this run also has a small positive offset of 0.2 meters in the model tests. The motion in this run is relatively modest with an amplitude of 2.4 meters.

The numerical model on the other hand has a positive offset of approximately 1 meter. The motion is very large compared to the model tests with almost 3 times the response. This shows that the response seen in run 2004 is not even the peak of the response. This error will be discussed more in the summary/conclusion of this chapter.

Pitch

The entire point of this run was to show that the response of the pitch motion in the numerical does not have a perfect correlation with the model test response. In figure 6.41 6.42 the problematic area of the numerical model's pitch motion will be shown.

As we have seen in previous runs the pitch motion has a static heeling value. The oscillation is centred around -2.7 degrees and the oscillation has an amplitude of -5 degrees.

The numerical model does not have a static heeling value, but in this run the oscillation amplitude is nearly twice the value of the model tests with an amplitude of 9 degrees. This shows that the pitch motion also deviates from the model tests in the area of 7-11 seconds, and this suggest that there is some part of the program which cannot properly account for some dampening effects in this area. This will be further examined in the conclusion of this chapter.

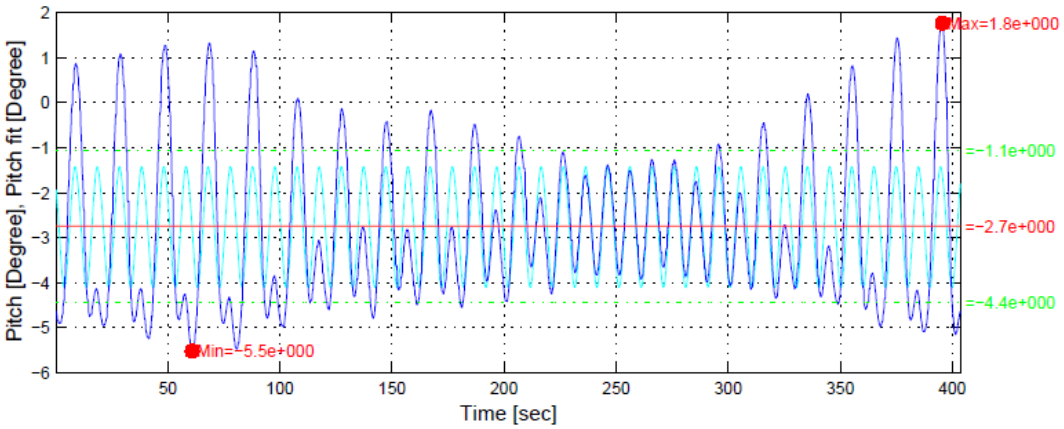

Figure 6.41: Model test pitch results with H=5m and T=9.9s

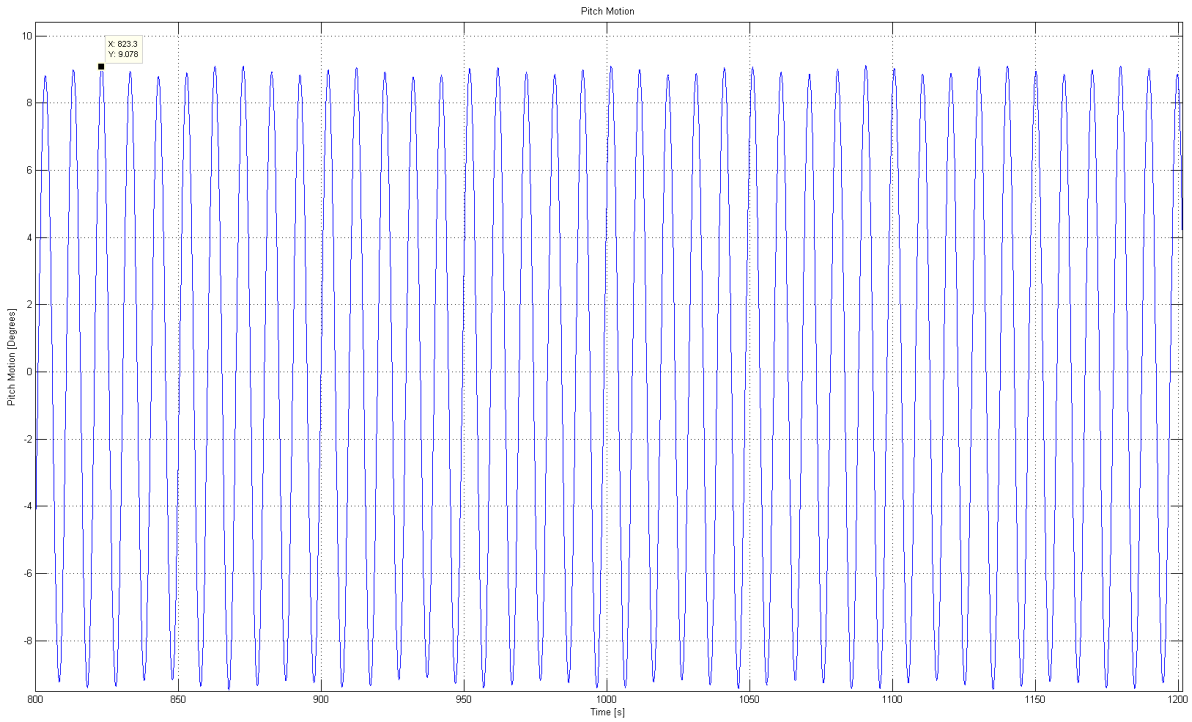

Figure 6.42: Matlab pitch results with H=5m and T=9.9s

6.6 Conclusion from the Comparative Study

To help with this final discussion RAOs have been created from the results of the different runs (figure 6.43, 6.44 and 6.45). The RAOs have been created by dividing the amplitude of the oscillations with the wave amplitude, and they show the response of the Total Buoy in different wave periods.

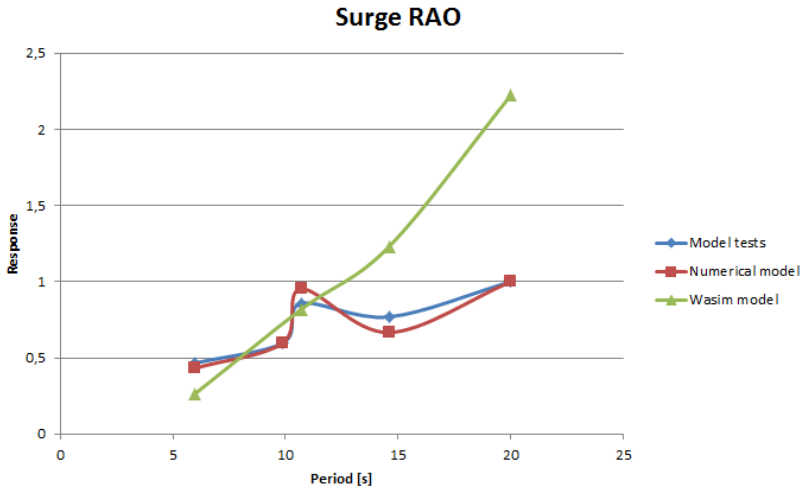

Figure 6.43: Surge results from all models compared in the form of RAOs

In figure 6.43 we see that the numerical model correlates well with the model test i.e. the results are following the same tendency as the model tests. Surge is, as mentioned before, difficult to compare. The biggest difference between the results is the static drift-off, which is larger in most of the numerical model results. In the comparisons of the different runs it was also seen that there were two different oscillations, one low frequency oscillation and one high frequency oscillation, but due to the difference in mooring modelling the low frequency oscillations were found not to be comparable. This difference is made evident by examining the periodic content of the low frequency oscillation in the models, and the large difference in static drift-off. The high frequency oscillations on the other hand did prove to be comparable when it was discovered that the response periods matched the wave periods exactly. It is the high frequency oscillations which are compared in figure 6.43.

The Wasim model does not perform as well as the numerical model. Figure 6.43 shows a near linear correlation in the Wasim results furthermore there is no evidence of the static drift-off or the low frequency oscillations in the Wasim results. The high frequency oscillations do compare well with the other model, but the results with longer waves show that the Wasim model has a larger deviation. The problems in Wasim suggest that the mooring calculations in the model cannot represent the mooring system correctly. There are options which allow a user to fully design a mooring spread in the ocean space, but this requires knowledge of another program in the Sesam package called DeepC. This program can also be used to model risers and other appendages on the structure.

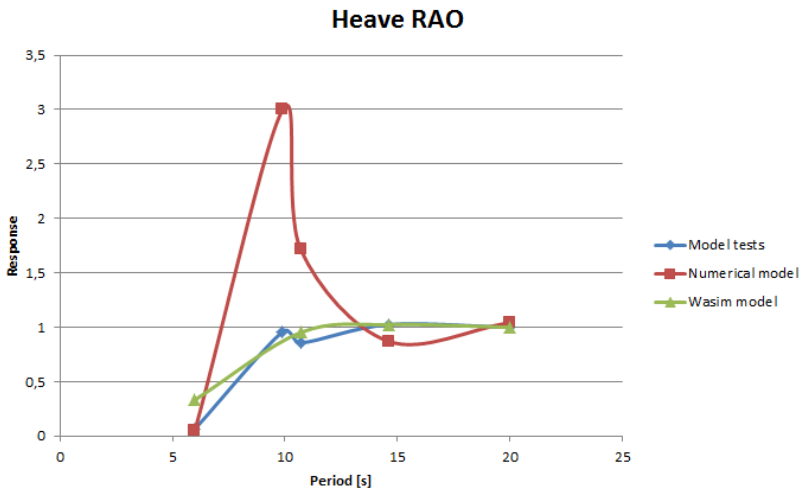

Figure 6.44: Heave results from all models compared in the form of RAOs

In figure 6.44 we see that the numerical model has large discrepancies in the in the period range of 9-11 seconds. It is important to note that the model test curve does have a small peak around 10 seconds. This does suggest that the numerical model has the correct correlation with respect to the model tests, but the amplitude is very different. In the pre-study to this thesis shown in appendix A the natural period in heave was found to be around 9 seconds. This natural period indicates that there should be increased response in the periodic area which is seen in figure 6.44. The large difference in the amplitude could be possibly be caused by problems with the proportional damping model e.g. not accounting for the entire effect of the damping skirt. The results at the moment does suggest that the numerical model is correct in heave for long waves, but until the possible damping problem is solved one should be aware that the natural periods could cause large responses. Another problem with the results which is not shown in figure 6.44, is that both the numerical model, and the model tests have a positive offset when subjected to steep waves. The numerical model has larger positive offset than the numerical model, this difference may be another effect of the damping problem. This problem will be further discussed in Recommendations for Further Work.

The Wasim model is showing much better agreement in heave than the numerical model. The largest difference in the model is the result from the first run which is showing a larger response than the other models. Another difference is the lack of positive offset in the Wasim model. The heave results could be caused by a more accurate representation of the damping force. One possible problem with the numerical model has been identified to be connected to the damping. It is especially the restoring coefficient which has been thought to cause problems in the proportional damping formula.

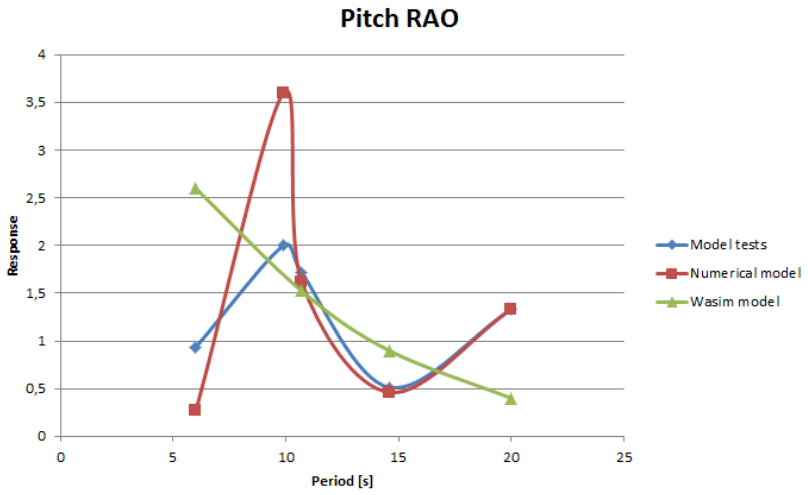

Figure 6.45: Pitch results from all models compared in the form of RAOs

The pitch motion in the numerical is showing the same discrepancies as the heave motion, but the peak is centred more in the period range of 7-9 seconds. The pitch motion is coupled with heave and could be influenced by the large heave motions. Another possibility is that there are damping problems also in pitch, but the most likely reason is that the heave motion is affecting the pitch motion as well. The model tests were also showing tendency to have static heeling i.e. that the oscillations were centred around a value different from zero. This static heeling was not seen in the numerical model, and this could indicate some missing effects or loads. It could also be an indirect effect of the mooring as the model test mooring is much stiffer than the mooring in the numerical model.

The pitch motion in the Wasim has the same linear characteristics as the surge motion. The results from run 2004 are in the same range as the model test, but when looking at the other runs this could be a coincidence.

Based on the observations made in this chapter we can conclude that while the new numerical model does have some good results, there is a discrepancy in the heave and pitch solutions which suggests that further work is needed. The numerical does outperform the Wasim model in this comparison, and the model should either be revised to include more effects or the program should not be used for this type of problem.

Chapter 7

Behaviour of the Total Buoy in Open Water and Level Ice

In this chapter an assessment of the Total Buoy's open water behaviour is to be performed. The best way to show this is to create RAOs (Response Amplitude Operator) from the different motions. The way this can be done is to make a selection of model test runs with different periods and find the unit displacement. (Reaction divided by wave amplitude) The results from these runs will serve as a single data point in the RAO. Surge will not be of particular interest in this chapter as the mooring setup applied in the model tests is not based on reality and therefore cannot be used to assess the real motion.

The effect of ice on the Total buoy is more difficult to examine as the methods of calculating ice/structure interaction is limited, and model tests are not available. Due to the lack of time and possibilities this thesis is rather limited with respect to the examination of ice/structure interaction.

7.1 North Sea and Barents Sea Waves

To be able to do a proper assessment of the open water behaviour of the Total buoy it is important to have a basic understanding of typical sea states in the potential deployment areas. This buoy has been specifically designed to handle ice that excludes the many areas which might be problematic in terms of extreme sea states. One such area is the Norwegian Sea which has one of the most hostile non-ice environments on the planet. In figure 7.1 we can see a map of the Norwegian Sea with ISO-Curves showing the Significant wave heights and maximum peak periods with annual probability of exceedance of 10^{-2}. Areas which are relevant to the Total buoy are around Svalbard and in the eastern Barents Sea. A selection of measurements have been made and from this as scatter diagram has been made for the eastern Barents Sea as shown in table 7.1. (The area in the top right corner in figure 7.1)

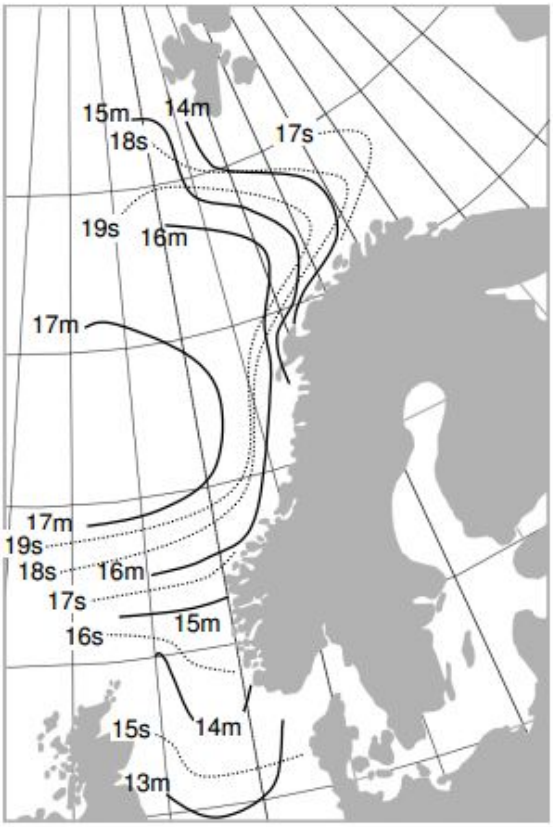

Figure 7.1: Significant wave height Hs and related maximum peak period TP with annual probability of exceedance of $10^{-}2$ for sea-states of 3 h duration. ISO-curves for wave heights are indicated with solid lines while wave period lines are dotted (NORSOK, 2012)

Occurence	Peak Period [s]								
Significant Wave Height [m]	0-2.9	3-5.9	6-8.9	9-11.9	12-14.9	15-17.9	18-20.9	21-23.9	TOTAL
0.0-2.9				0.01	0.05				0.06
3.0-5.9			0.02	0.97	0.45	0.03			1.5
6.0-8.9		<0.01	8.0	6.8	1.9	0.08	<0.01		16.7
9.0-11.9		15.2	48.5	13.5	8.4	0.94	0.12	0.09	81.7
TOTAL	0.0	15.3	51.5	21.3	10.7	1.1	0.13	0.09	100.0

Table 7.1: Typical Hs/Tp scatter diagram for the eastern Barents sea (based on World Waves data) (Fugro, 2005)

As we can see from figure 7.1 and table 7.1 we have very different sea states depending on whether the structure is located near Svalbard or in the Barents Sea. As Svalbard is not open for oil and gas exploration at the present time we shall instead focus on the Barents Sea. The Barents Sea is thought to contain large deposits of oil and gas, and due to the harsh winter climate with temperatures below -30 degrees centigrade it is also difficult to extract the resources continually.

From the scatter diagram we can see which wave peak periods and significant wave heights registered are most prevalent. The significant wave heights are shown to be in the range 0-11.9 m, although most of the waves are in the range 9-11.9. The peak periods are shown to be in the range of 3-23.9 s, but here nearly 99% of the waves are in the range 3-14.9 s. When looking into the RAOs we should now be able to see how the total buoy will behave in this area.

7.2 Heave Motion

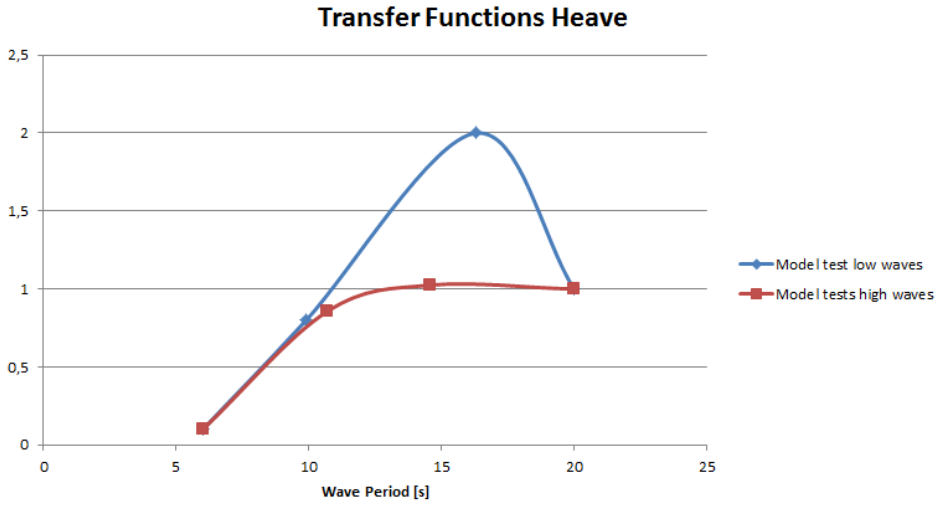

Figure 7.2: Heave RAOs calculated with different wave heights

To assess the open water behaviour the RAOs from runs with low and high waves have been created in figure 7.2. This has been done to show the difference in the structure response with increasing wave height which will demonstrate the non-linearity of this problem. The runs at the ends are the same for both RAOs i.e. only the runs with period near 10 s and 15 s are of different wave heights. It is important to note that there is a possibility that more data points in the RAO could give a different curve, but as there are no available model tests this is not possible.

As we can see from figure 7.2 the heave motion of the total buoy in the model tests is showing significant responses in the range of 11 seconds to 20 seconds. In this range the response from the buoy is actually more than the incoming wave amplitudes. We can see that part of this high response area overlaps with about 12% of the peak periods as

seen in table 7.1. There is also significant difference in the response around 15 seconds between the two RAOs. It suggests that the response of the structure will reach a maximum possible response when the wave heights increase. This does not suggest a non-linearity in the heave motion, because the RAO does not change with increasing waves, but rather reaches a limit response.

7.3 Pitch Motion

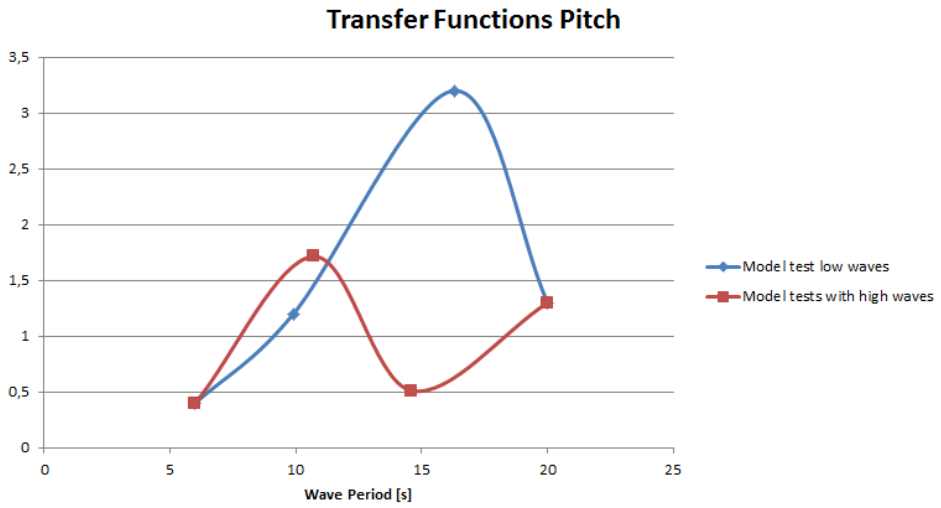

Figure 7.3: Pitch RAOs calculated with different wave heights

Similarly with heave two pitch RAOs have been created for the model tests. It is important to note that there is a possibility that more data points in the RAO could give a different curve, but as there are no available model tests this is not possible

The amount of response seen in the pitch RAO could be a problem, although most of the waves are seen to be of moderate height, some of the larger waves could be problematic due to the high response. Fortunately, as with the heave RAO the most frequent waves does not coincide with the worst responses, and this means that the structure will in most cases have moderate response in pitch. For larger waves we can also see a change in the RAO which causes the high response area to be moved into the high energy area of the sea state. This change in the RAO suggests a non-linear behaviour in the pitch motion connected to the geometry of the structure and the height of the waves.

7.4 Discussion of Open Water Behaviour

As we have seen from the previous sections in this chapter, the RAOs for the Total buoy are showing high responses in the period range of 11-19 seconds. This would be very problematic in North Sea, where the sea states are severe with significant wave

heights ranging from 13-17 meters and with peak periods from 15-19 seconds. (This information can be seen in figure 7.1)

It is, however, very unlikely that the Total Buoy will be subjected to North Sea climate, but far more likely that the buoy will be placed further North in the eastern Barents Sea. This will help immensely on the sea states compared to the North Sea. The wave heights are significantly lower, being in the range of 9-11.9 meters, and the peak periods are seen to be around 9 seconds, which would keep the waves in a one-to-one response or less area on the RAOs.

It should be noted that even if the responses are only one-to-one (meaning that the responses of the structure are matching the incoming waves) the buoy will be ill suited for year round human habitation due to the pitching motion, which could be over 10 degrees in the worst waves. This will be uncomfortable and difficult to work in, so the success of the buoy will depend on the application. If it is intended to be unmanned it should work well in that area, depending of course, on the buoy capability in ice.

Another important factor which may need to be considered is the apparent non-linearity in the pitch motion connected to the increasing wave heights and how this affects the motions of the structure. The mentioned non-linearity will be due to several effects of the geometry in coalition with the tall waves and large motions.

- Waves will hit more of the structure thus increasing wave forces
- Increasing wave heights will change the center of attack increasing the moment arm
- Increasing pitch angles will also increase the restoring moment

This might increase the pitch motion to a dangerous degree even when the buoy is unmanned. The problem could be reduced by designing a mooring system which will counteract the pitch motion as well as the surge motion, and efforts should be made to investigate the effects of mooring on these motions.

7.5 Ice Conditions

When we are looking at the ice conditions in the areas of the Norwegian Sea and the Barents Sea, we see a vastly different environment in the Barents Sea compared to the Norwegian Sea. The Norwegian Sea is considered to be free of sea ice all year. The Barents Sea, However, will have sea ice most of the year except July-September, and in some years ice all year.

First year ice can reach a thickness of 1.5-2 meters (Sakshaug, 2009), and as seen in figure 7.4 this gives a variable loading for the Total Buoy in the eastern Barents Sea in the long term.

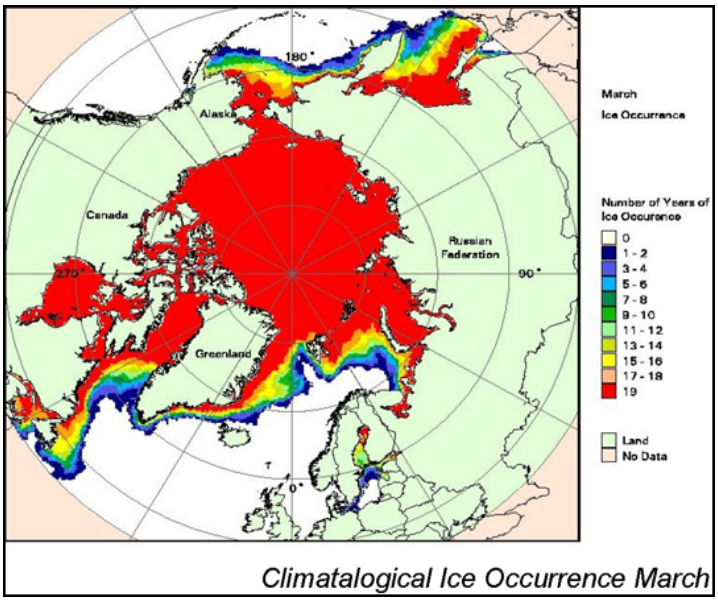

Figure 7.4: Map showing ice occurrence around the northern hemisphere (Fugro, 2005)

7.6 Ice Results

The only results available are from the numerical model, which is based on parametric formulas which are described in more detail in section 2.3. The results are static, and therefore will only give a limited amount of information about the actual loading on the structure. The theory applied also has limitations with respect to ice thickness with a max ice thickness of 1.5 meters, as was shown in section 7.5 to be the lower limit of the actual ice thickness of first year ice in the eastern Barents Sea. The Ice calculations performed by the numerical model returns 4 graphs: the offset in X-direction, the heeling, the force in X-direction, and the heeling moment. (see figures 7.5, 7.6, 7.7, 7.8)

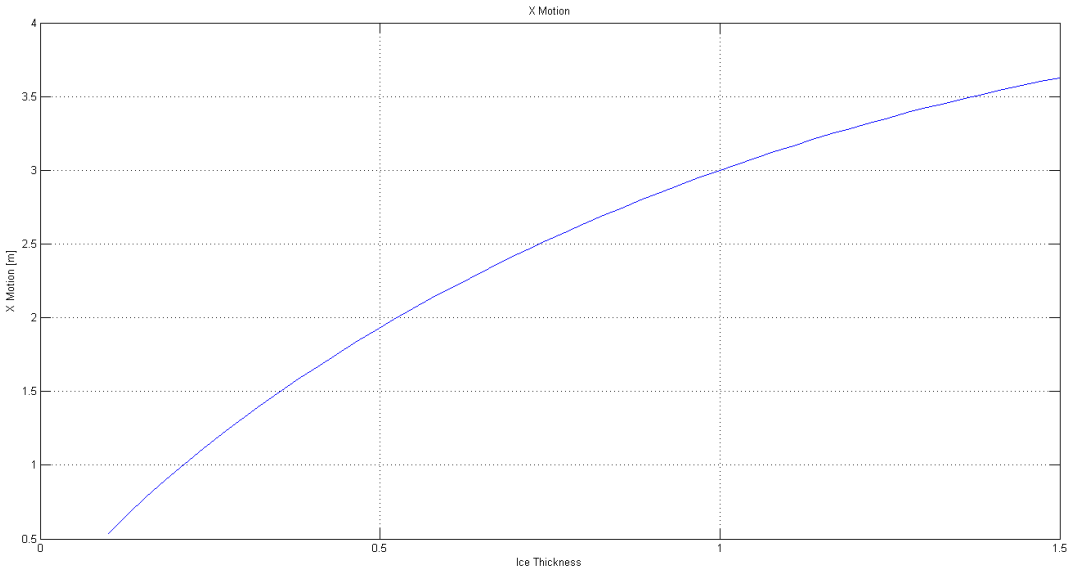

Figure 7.5: Static offset of the Total Buoy in level ice thickness of 0.1-1.5 m

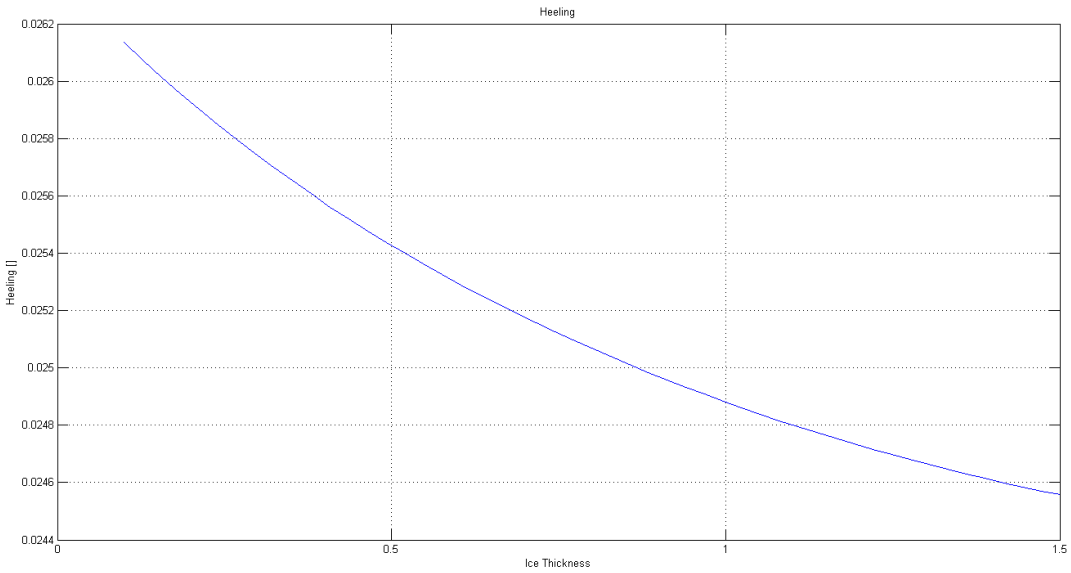

Figure 7.6: Static heeling of the Total Buoy in level ice thickness of 0.1-1.5 m

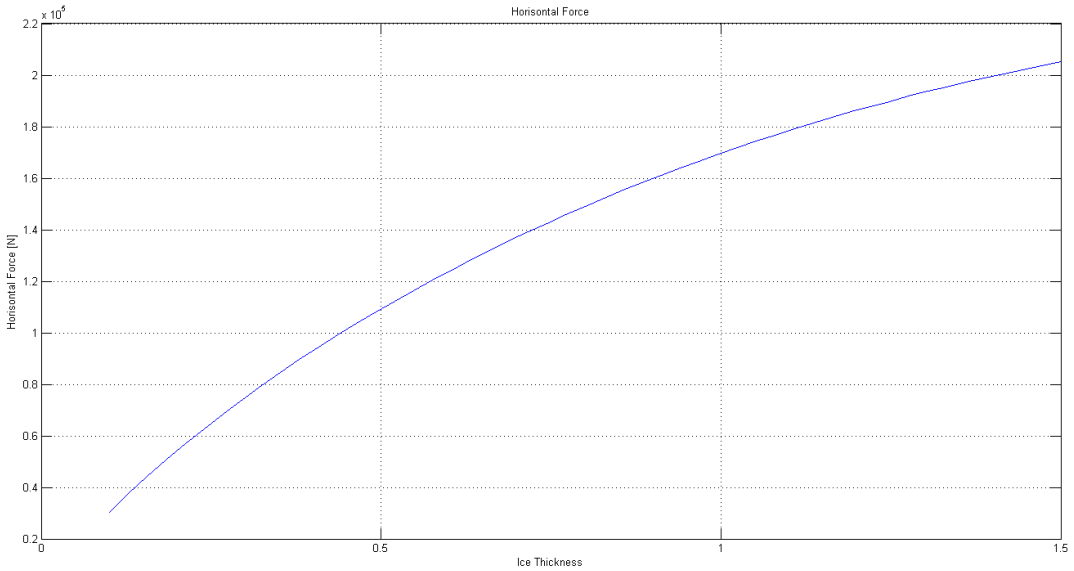

Figure 7.7: Static force on the Total Buoy in level ice thickness of 0.1-1.5 m

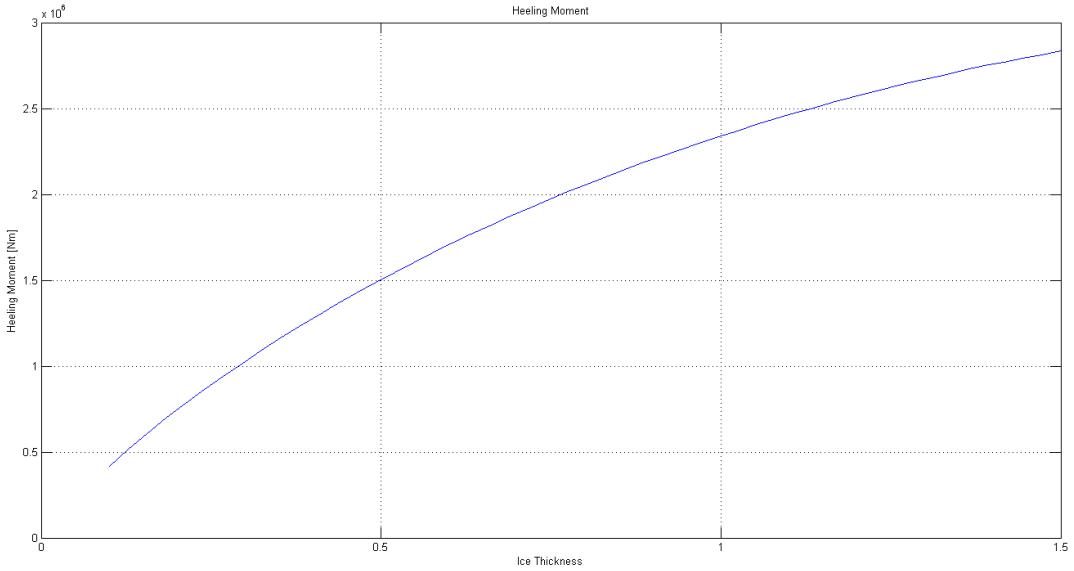

Figure 7.8: Static moment on the Total Buoy in level ice thickness of 0.1-1.5 m

7.7 Discussion of the Capabilities in Ice

The results from the numerical model are, unfortunately, not reliable. This is due to lack of verification through model tests, and the empirical nature of the equations. Even if the results shown in section 7.6 could be proven; they would still not give much aid in the design process. The lack of a dynamic time domain solution is really the largest problem, and it would help the design process more to have a time domain solution.

The Total Buoy does have the capability to deflect ice with the slanted hulls. This helps in breaking the ice sheet in bending instead of crushing which requires less force. S. Loset (2006)

The question which should be examined in relation to the ice capabilities is whether the increase in the ice capabilities is worth the detrimental effect on the motions which have been discussed in section 7.4 or would it be better to design a concept which could vary the waterline depending on whether the loading is from ice or from waves. It is a common assumption that these to loading conditions are mutually exclusive i.e. that one would not expect large ice loads when the structure is experiencing large wave loads and the other way around. This would make it possible to have a buoy with a straight hull configuration in open water condition and by ballasting the structure to a different water level be able to have a slanted section in level ice condition.

Chapter 8

Changes in the New Numerical Model

This chapter will present the improvements in this numerical model over the previous numerical model. This model has focused only on the non-linear motions of the total buoy, and the previous numerical model included several other functions which are not included here. Some of the problems with the previous numerical model are presented in appendix B. The solutions of these problems have been the focus of this development stage, so whether or not the problems have been solved is of interest.

- Problems with sea states
- Problems with accuracy
- Problems with slow time integration
- Presentation of forces

Problems with Sea States

This problem was thought to be due to a simplification made by Glomnes or Viko in the early development of the numerical model. It was seen that the model would fail when waves exceeded a certain point on the buoy. This caused the numerical model to fail when being subjected to moderate waves. The problem was thought to be caused by the assumption that only the slanted part of the total buoy would be subjected to waves, this assumption effectively imposed a wave height limitation which would cause the calculations to fail when it was exceeded.

This problem has been addressed in this new attempt by allowing the possibility of having pressures on the entire surface of the buoy. It is important, however, that the buoy is designed as a closed body. The effects of an opening in the model are unknown, but it will most likely cause problems with the pressure calculations. There have not been any similar problems in the solutions.

Problems with Accuracy

This problem was seen when comparing the Wasim model to the numerical model, and as we saw in chapter 6 the results of the Wasim model cannot be considered to be reliable, this leaves just one comparison with the model tests. The biggest problem with the numerical model was that it did not work for moderate to high waves as mentioned before, and also showed problems for low waves when nearing the natural periods.

This has been attempted to be solved in the new numerical model, although the results are not entirely correct as was seen in chapter 6. The new model does produce results in all sea states tested, so on that point it is performing well. What should be done to solve this model's problems will be addressed in chapter 8.

Problems with Slow Time Integration

This problem was seen in the old model when the run required small time steps, and a short simulation of 200 seconds could take several hours to complete. This problem was largely caused by the time integration scheme which was used. The time integration scheme was a built-in Runge-Kutta solver in MATLAB, and it was thought that a self-produced code could perform better on this specific problem.

In the new numerical model a very simple integration method in the Newmark-β family was chosen for this, and it has shown a very fast solution speed. This does improve the usability of the program, and should be very helpful when trying to determine the differences between input variations. The model is capable of calculating usable results within a few minutes depending on the length of the simulation. The length of the calculations rarely need to exceed 800 seconds to avoid the transient area of the calculations, this length of simulation will take 1-5 minutes depending on the processing power of the computer.

Presentation of Forces

The presentation of force results in the previous model is not very helpful (see figure 8.1). The problem is that all force contributions were presented in one single figure, and the total force on the structure is not shown at all.

In the new numerical model it was decided that only the total force was to be presented (see figure 8.2). This results in a figure which can be easily read, and could be more useful in the pre design than each of the components and their oscillations.

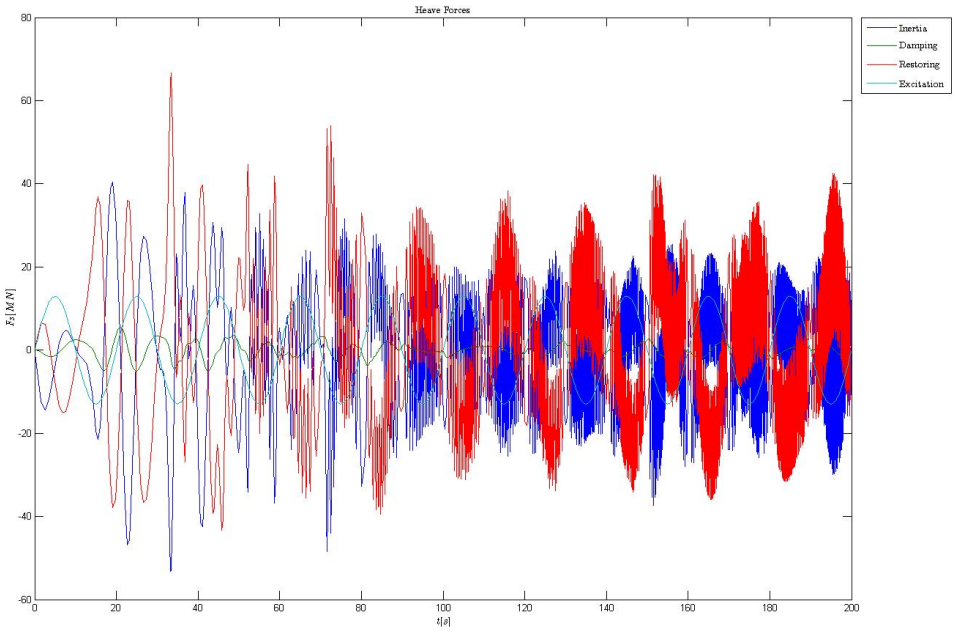

Figure 8.1: Example of force results in the old numerical model

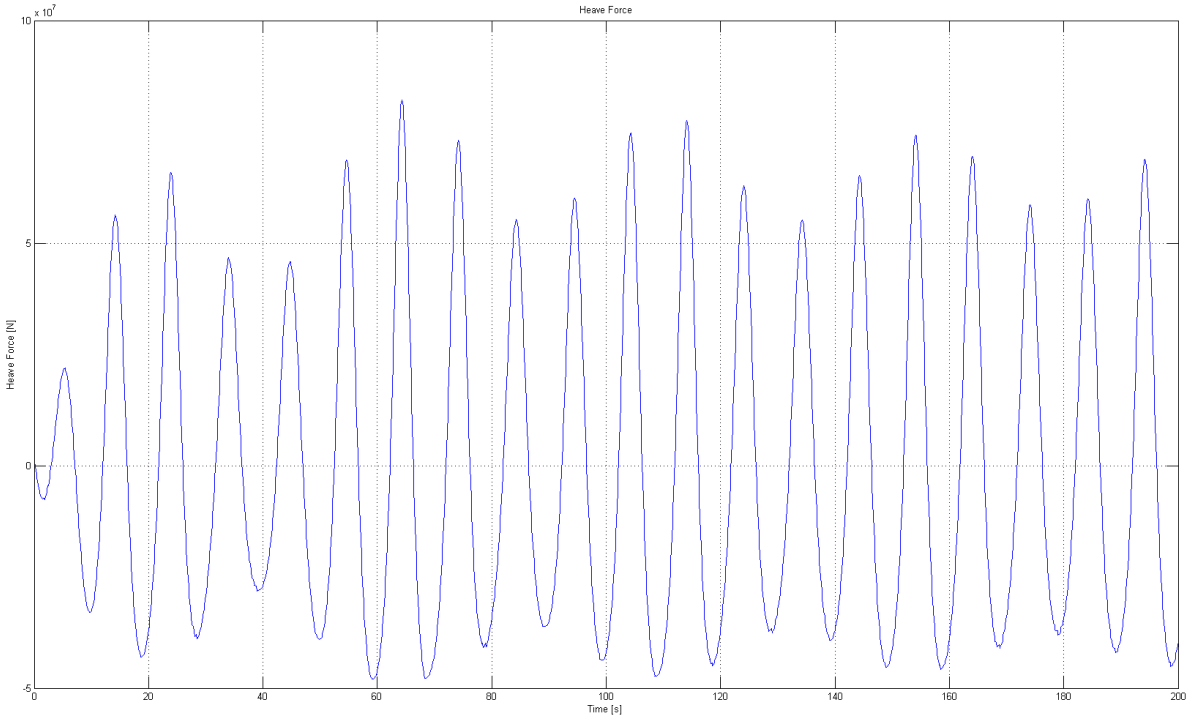

Figure 8.2: Example of force results in the new numerical model

Conclusion

The main objective of this master thesis has been to start the development of a numerical model, which is meant to give aid in the preliminary design of buoy platforms. Compared to the previous numerical model there is some improvement, particularly with respect to stability and speed. Although the new numerical model obviously has some problems, the numerical model is promising because it predicts motions in good agreement with model tests in many cases. In section 6.6 the results from the comparisons were shown as RAOs (smaller versions can be seen in figure 8.3, where the the model test are shown in blue, the numerical model is red, and the wasim model is green)

The surge motion is showing the best agreement with the model tests for the numerical model. One should be aware that the surge figure only shows the high frequency oscillation and not the static drift-off or low frequency oscillations. This is due to a difference in the mooring system due to lack of information pertaining to the model test mooring. This results in a different stiffness, and it was found when comparing the results that the high frequency oscillations were due to similar response periods, but the low frequency oscillations and static drift-off were found not to be comparable.

The heave motion in the model tests is showing a peak in the period range of 8-11 seconds. There is also a very small peak in the same area in the model test RAO which could mean that the peak itself is correct, but the amplitude is too large. This problem is thought to be related to the damping in the numerical model. Except for this peak the results in general are close to the model tests. The possible solutions to this problem, amongst others, will be presented in the Recommendations for Further Work chapter.

The pitch motion results are in general very good, but once again the numerical model has a peak in the period range of 8-11 seconds. This peak is probably due to the coupling effects between heave and pitch, and the results in pitch should improve if the heave solution is improved.

When looking at the results from the Wasim solutions in figure 8.3 we see that while the heave results have good agreement the results from surge and pitch are not correlating with the model tests at all. Due to this difference the Wasim model does not achieve results which can be used in design of these types of structure.

The comparisons also highlighted the motions of the Total Buoy in the model tests, and it was thought necessary to perform an analysis of the open water and level ice behaviour. The Total Buoy was seen to have poor open water behaviour for the Norwegian Sea, but much better suited for the Barents Sea, which is the most likely location for the

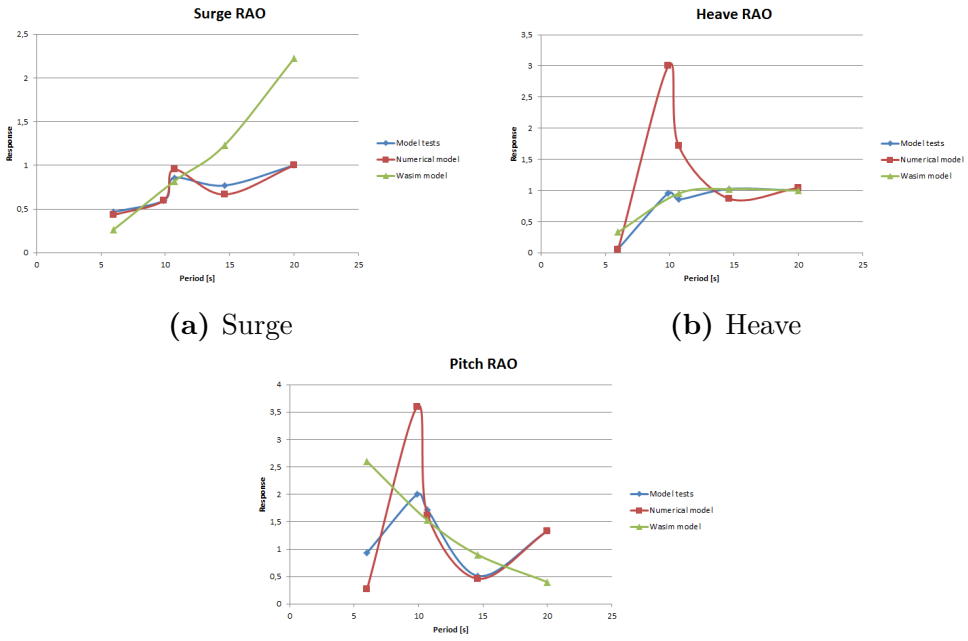

(a) Surge

(b) Heave

(c) Pitch

Figure 8.3: Miniature versions of comparison RAOs from chapter 6

Buoy. This is due to the sea states in the Barents sea having smaller wave periods and wave heights. When looking at the RAOs we can see that the response will be around one-to-one with the incoming waves. In the case of pitch motion this means one degree of heeling per meter incoming wave, and this will be very uncomfortable for any humans inhabiting the buoy. For this reason the Total Buoy would perform poorly as a regular manned platform concept, but will be good for partially manned or unmanned operations. Unfortunately, due to the lack of time the ice capabilities are only explored with the static solution from the numerical model, which does not give much useful information apart from the static drift-off and heeling which the buoy will be subjected to. These results are further not possible to verify due to lack of alternative solutions at this time e.g. model tests.

The Total Buoy as a concept does depend heavily on the results from ice model tests, because the structure takes a penalty to the open water behaviour because of the slanted hulls. Thus the gain from having the slanted hulls in ice must be greater than the disadvantage of the open water behaviour. However, if the pitch motion could be improved by introducing mooring lines the concept could be much more viable.

Recommendations for Further Work

As we have seen, there are some problems with the new numerical model, and this is where possible solutions will be proposed. The reason these solutions have not been performed during the course of this thesis is due to the time consuming nature.

The largest problem with the non-linear motions in the numerical model is the large amplitude which was seen in heave and pitch. This could have several different solutions, which will be presented here.

Restoring Coefficient Calculation

This part of the program was reused, but it is a very complicated subroutine, and it might be beneficial to simplify this. In the numerical model this had to be taken out of the iteration process because the restoring calculation proved to be unstable and slow. This calculation is now being used to calculate a static restoring coefficient, and unfortunately this restoring coefficient also had to be used in heave to calculate the damping, and could be influencing the results in such a way that the peaks in heave and pitch in the period range of 8-11 seconds is caused by a bad restoring coefficient. This is considered the most likely source of the high amplitudes in heave and pitch.

Damping and Added Mass Frequency Dependence

This difference in the results needed more explanation, and though some suggestions were made in chapter 6 it was thought that a more thorough investigation could help with the further work on this model. There were two areas in particular which needed more investigation; the damping and added mass.

The pitch results are thought to be influenced by the coupling with heave. The theory is that the pitch results will improve if the heave solution is improved. The focus will therefore be centred on heave. The damping and added mass are both frequency dependent which has been shown by (Faltinsen, 1990, p. 49-55). This leads to damping and added mass coefficients that could change with wave frequency (or period as is most commonly used in this thesis). An example of a frequency dependent added mass and damping can be seen in figure 8.4. The Total Buoy might not have the same relation, but it is good approximation for the illustrative purpose here. We see from figure 8.4a that the damping peaks are in the mid-range frequencies, which could correspond to

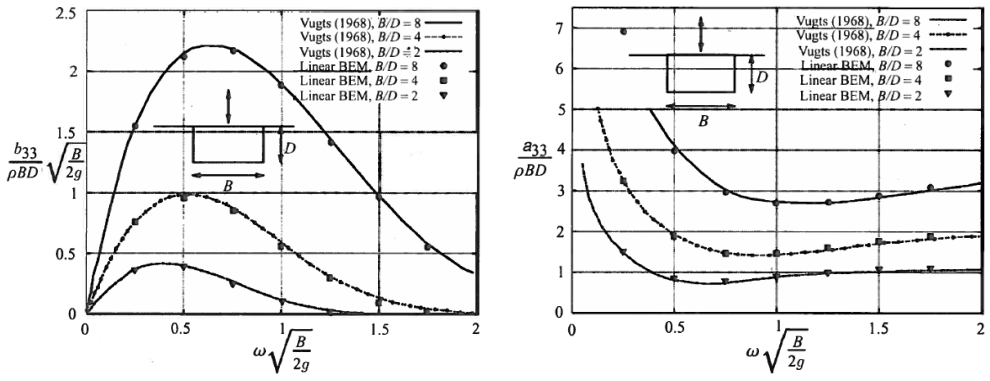

(a) Damping **(b)** Added Mass

Figure 8.4: Two-dimensional added mass and damping in heave for a rectangular cylinder oscillating on the free surface, for different B/D ratios. B is the beam of the cylinder and D is the draft. Infinite water depth is used. As shown in (Faltinsen, 2005, p. 237)

the same problematic period range which was seen in the heave RAO. It is difficult to calculate any values corresponding to the Total Buoy from these curves, due to the varying width of the structure over the draft and the damping skirt also adding further confusion.

The added mass is also varying with respect to frequency, but due to the nature of the curve related to the frequency (if one assumes similar correlation for the Total Buoy) one can see that the added mass will stay more or less the same value except for small periods. This could affect the values seen in run 2001 (Wave Period 6 seconds), but is unlikely to affect the peak seen in the range 8-11 seconds.

The inclusion of the frequency dependence in damping and added mass could be achieved by finding similar curves as in figure 8.4 or confirming that these curves are also reasonable with respect to the Total buoy and could be applied more or less directly to the same problem. If one is able to find the frequency dependence; they should be included as input and the damping and added mass functions should be expanded to include them. This is to keep the calculation as general as possible so that the program can be applied to other problems.

Another possibility for including the frequency dependence is with the aid of convolution integrals in the solution of the motions. This is explained in detail in (Faltinsen, 2005, p. 257-). One should be aware, however, that as the motion calculation applied in this model is very simplified the method might not be directly applicable. An important difference is the way the coupling between heave and pitch is achieved. The coupling is achieved through the pressure calculation and updating the coordinates accordingly. The method shown in (Faltinsen, 2005, p. 257-) uses coupling coefficients. Another problem which will need to be addressed is how to apply the convolution integral in the Matlab code, but this is only a matter of further studying the method in question. The choice of how the frequency dependence is included should be based on which is the simplest and fastest with respect to the programming.

Ice Model

Another problem which will need more work is the ice calculations, because the static solution provides very little helpful information for the design of these structures. The numerical model will need to be able to do a dynamic ice analysis on the buoy with focus on the time domain solution of the buoy motion in varying level ice thickness. This should be the main focus of the continued development of this numerical model. The development of a time domain ice calculation necessitates model test results to compare with. If model test results on the total buoy are not available one should instead try to develop the ice calculations from other similar fixed or floating structures with either force results or motion results.

Include Options to Calculate Coefficients Directly

Finally, one should consider expanding the program to be able to calculate added mass, damping and restoring coefficients with only geometric input. The program is very dependent on good input to be able to calculate good results, and while the program itself has been written in a way which allows the user to calculate any cylinder based structure there are input values which are required that are not easily obtained.

These include damping percentages and added mass correction coefficients, which are difficult to find for arbitrary shapes. These values can now only be approximated by table values and empirical formulas. Otherwise one can do a forced oscillation model test to gain some value, use a potential theory based computer program, or, in the future use Computational Fluid Dynamics (CFD).

Include Linear Numerical Calculation Written By Glomnes and Viko

When doing the comparisons in the pre-study (see appendix A) parts of the linear calculations in the numerical model were seen producing good and fast results. It could be a good idea to include these into the present numerical mode, and expand the GUI (see MathWorks (2012) for help with GUI) to include these calculation options. This has not been done due to focus on getting the non-linear calculations to work.

Include Free Oscillation Tests

Another option which could be included is free oscillation tests. This option can be run by manipulating the present code, but the option has not been included in the GUI due to lack of time to ensure a good quality.

References

Amdahl, e. a. (2010). *USFOS - Hydrodynamics - Theory - Description of Use - Verification*. USFOS.

Ditlevsen, O. (2002). Stochastic model for joint wave and wind loads on offshore structures.

Faltinsen, O. M. (1990). *Sea Loads on Ships and Offshore Structures*. Cambridge University Press.

Faltinsen, O. M. (2005). *Hydrodynamics of High-Speed Marine Vehicles*. Cambridge University Press.

Fenton, J. (1990). Nonlinear wave theories. *Ocean Engineering Science*, 9.

Flow3D (2009). Fifth-order stokes wave. www.flow3d.com.

Force Technology (2006). Force technology 2006017.2 seakeeping tests on ice-breaking offshore buoy. Technical report, Force Technology.

Fugro (2005). Regional reference: Barents sea.

G. W Timco, A. M. C. (1997). The influence of variable-thickness ice on the loads exerted on sloping structures. *Cold Regions Science and Technology*, 26:39–53.

Glomnes, E. B. (2006). Conceptual design of conical buoy for arctic conditions. Technical report, NTNU.

Glomnes, E. B. (2007). Surface buoys and jack-ups for arctic conditions. Master's thesis, NTNU.

Hedges, T. (1995). Regions of validity of analytical wave theories. *Proceedings of ICE - Water, Maritime and Energy*, 112:111–114.

Ivar Langen, R. S. (1979). *Dynamisk Analyse Av Konstruksjoner*. SIT TAPIR.

MathWorks (2012). Matlab - documentation. http://www.mathworks.se/help/techdoc/.

Newmark, N. (1959). A method of computation for structural dynamics. *Journal of the Engineering Mechanics Division*, 85(7):p.67–94.

NORSOK (2012). Norsok - n-003 actions and action effects.

S. Loset, K. N Shkhinek, O. T. G. K. V. H. (2006). *Actions From Ice on Arctic Offshore and Coastal Structures*.

Sakshaug, E. (2009). *Ecosystem Barents Sea*. Tapir Academic Press.

Steen, S. and Aarsnes, J. V. (2010). *Experimental Methods in Marine Hydrodynamics*.

Viko, N. G. (2006). Conceptual design of conical buoy for arctic conditions. Master's thesis, NTNU.

Appendix A

Comparison of Previous Numerical Model

The focus of this chapter will to check the functionality of the numerical model compared to the model tests and the corresponding Wasim runs. In the cases where the numerical model fails then only Wasim will be compared to the model tests. If the Wasim results are close to the model tests then comparisons shall be made between Wasim and the numerical model for a sea state in which the numerical model does not fail. As the Wasim model includes integration to the true surface, the comparison should be able to point out the significance of integration of pressure to the true surface. Unfortunately many of the graphs in (Glomnes, 2006) have been destroyed (as shown in figure A.1, so there will only be a limited number of figures from that thesis, due to the time it takes to decipher.

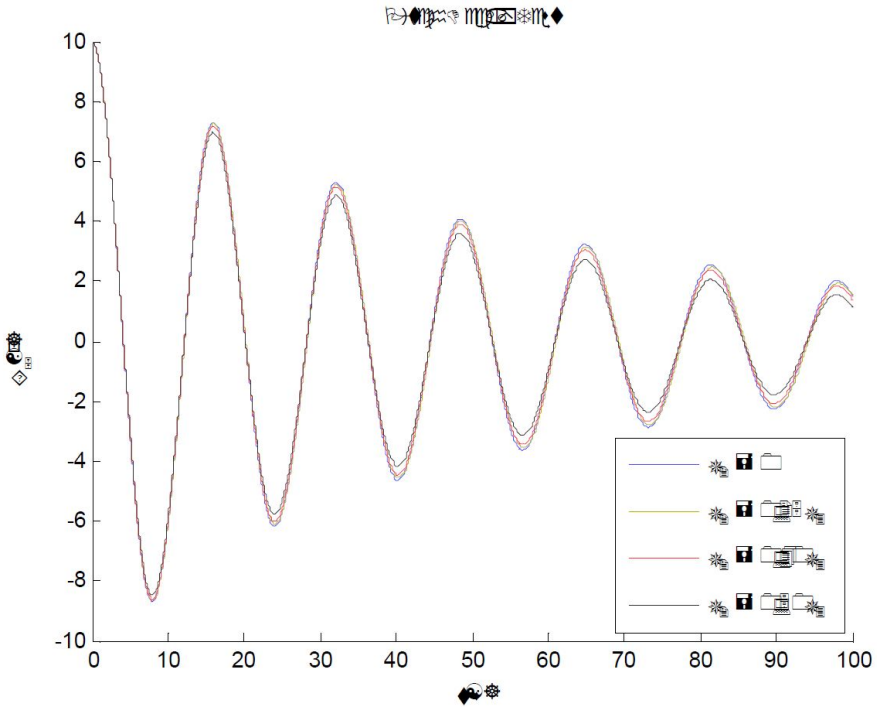

Figure A.1: Example of contaminated plots

A.1 Decay Tests

Because of the complex nature of the problem a good way to begin the comparison is to do decay tests. The decay test is a still water test where the structure is given a displacement in one or more degrees of freedom. The resulting motion makes it possible to calculate damping ratios and eigenvalues. (In this case the damping ratios are of little interest because the critical damping ratios have been selected to be the same in all cases based on the original model test results (see chapter 4))

A.1.1 Pitch Decay Test Results

The results from decay tests are shown in the following graphs. These have been calculated with the numerical model which was appended to (Glomnes, 2007) with no mooring lines specified and with the Wasim model as defined in Chapter 4

Heave

From figure A.2 and figure A.3 we can see a significant difference in these results. The amplitude from the numerical model is more than twice as large as the Wasim and the natural period is also different here. (see table A.1)

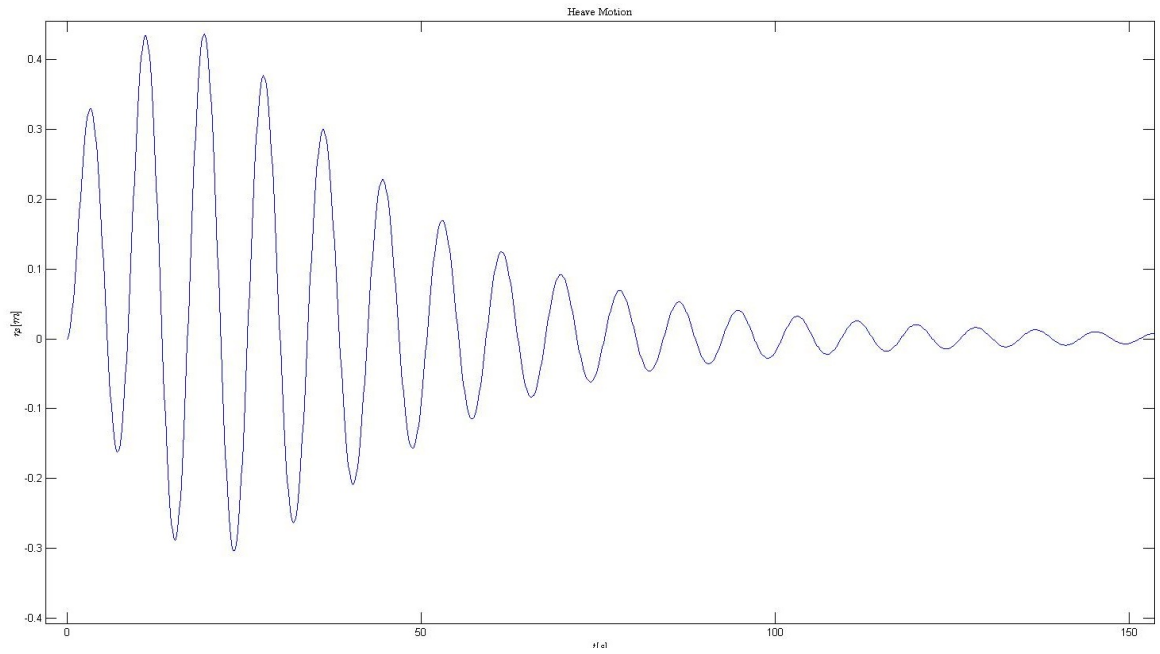

Figure A.2: Pitch decay test results in heave from numerical model

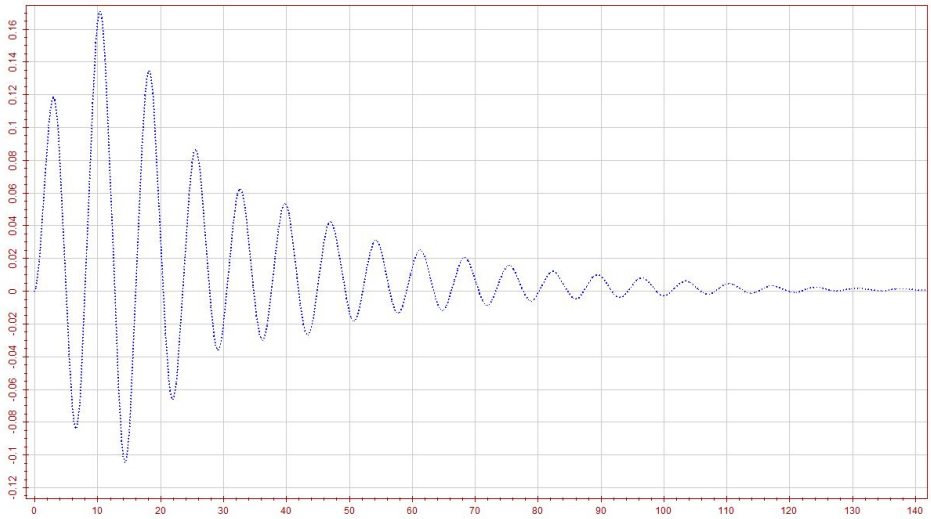

Figure A.3: Pitch decay test results in heave from Wasim

Pitch

As we can see by comparing the graphs in figure A.4 and figure A.5 there is smaller difference between the pitch results. The amplitude from the numerical model is in general a bit lower than the Wasim results but in this case the difference is very small. The natural period in the numerical model is higher than the value from Wasim. (see table A.1

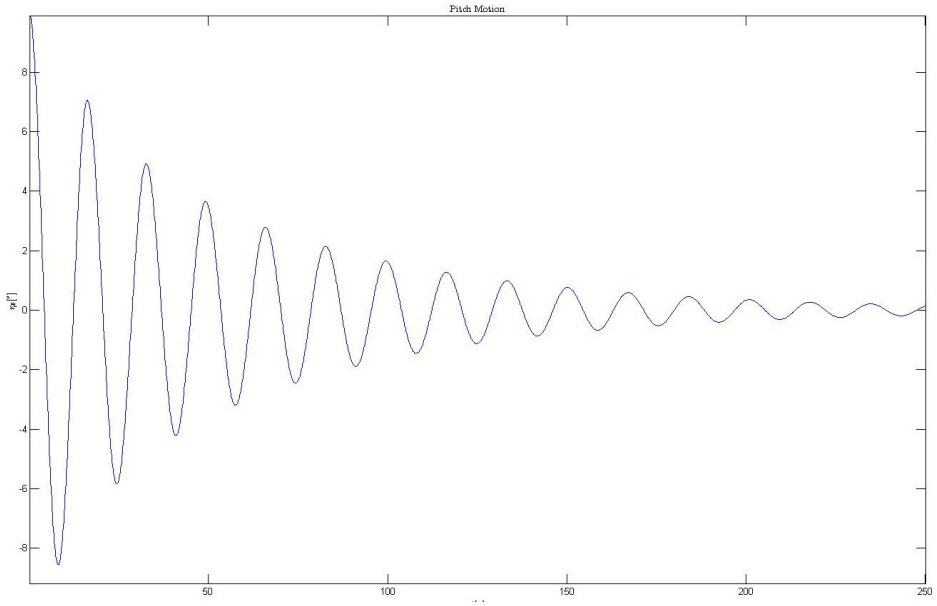

Figure A.4: Pitch decay test results in pitch from numerical model

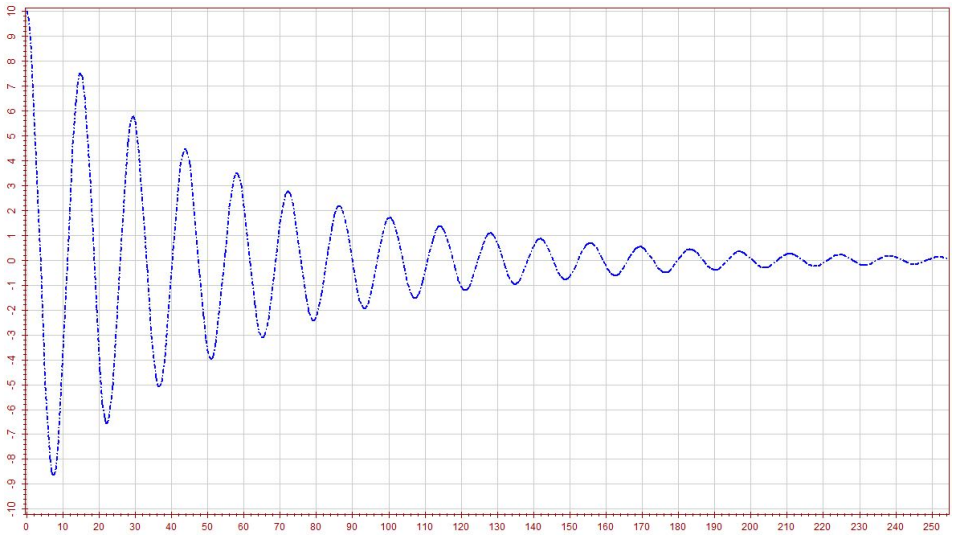

Figure A.5: Pitch decay test results in pitch from Wasim

A.1.2 Heave Decay Test Results

In figure A.6 and A.7 there is a difference in the results. In this case the amplitude of the numerical model is about 50% higher than the Wasim results but the natural periods is very similar (only about 2.5% difference)

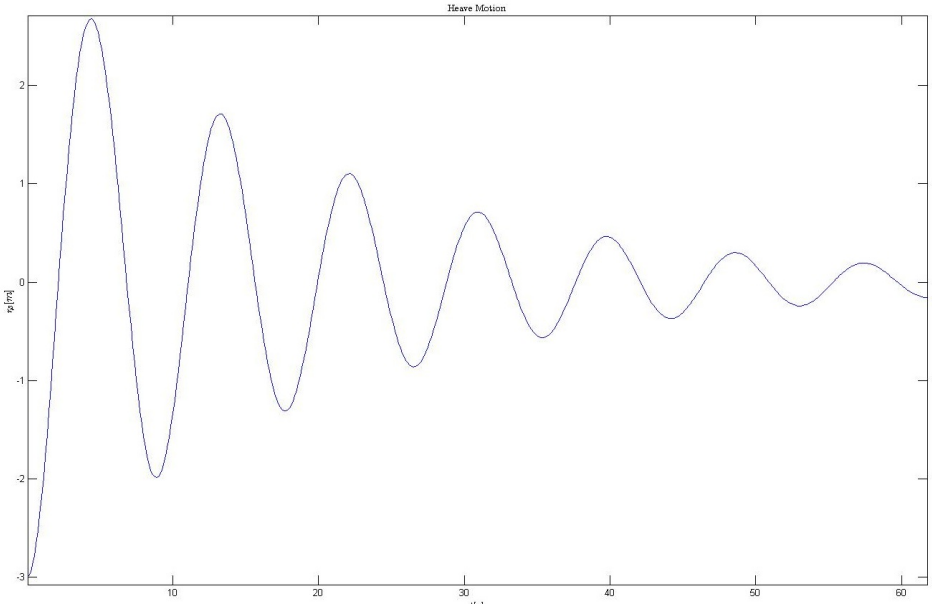

Figure A.6: Heave decay test results in heave from numerical model

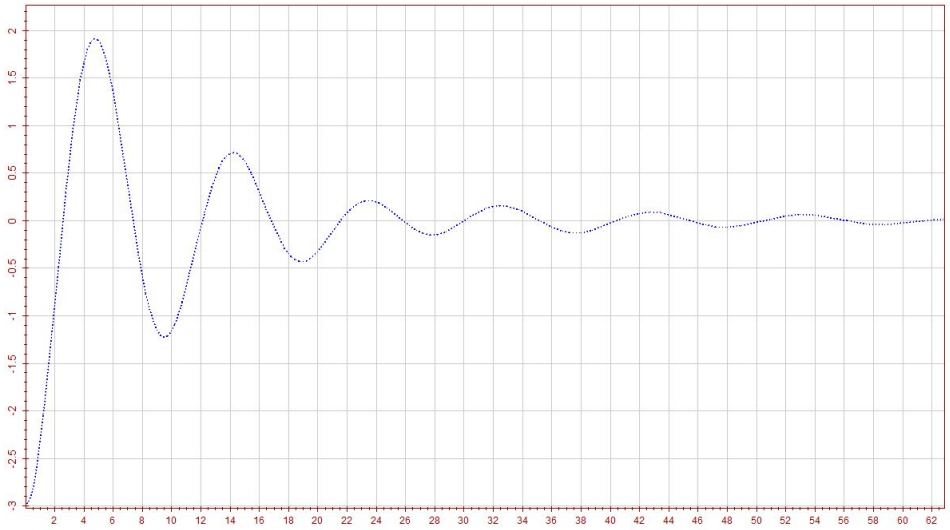

Figure A.7: Heave decay test results in heave from Wasim

A.1.3 Natural Periods Comparison

Table A.1 shows the different natural periods from model tests, the numerical model and Wasim. The model test results have been found in (Glomnes, 2006) but are originally

from a Force Technology report. (Which is unavailable at this time) The other values have been found by analysing the decay test results. The natural periods can be found by reading the difference between two peaks in the decay tests presented in the figures in this section. (Steen and Aarsnes, 2010)

	Pitch[s]	Heave[s]
Model Test Results	16.3	8.8
Numerical Model	16	9.1
Wasim	15	8.9

Table A.1: Natural Periods Comparison

The largest difference can be seen in the pitch results. The numerical model has a closer fit to the model test results than the Wasim results. The heave results are very close to the model tests in both cases. There might be several explanations for this:

- The added mass or mass calculated in Wasim might be higher than the numerical model.
- The stiffness calculated in the numerical model might be lower than calculated in wasim

A.2 Linear Regular Waves

To determine the functionality of the numerical model it is necessary to test the linear part of the numerical model compared to the model tests. Wasim also ran with linear theory to check if the linear solution is worth the modelling time. In table A.2 we can see the chosen model test runs and the corresponding wave parameters.

Run	Wave Height	Wave Period
2010	9.0 m	13.4 s
2019	9.0 m	20.0 s

Table A.2: Model test runs(Glomnes, 2006)

A.2.1 Comparison of Run 2010

Model Test Results

In the figure A.8 and A.9 we can see the results from the model test runs(From Force Technology) as presented by (Glomnes, 2006).

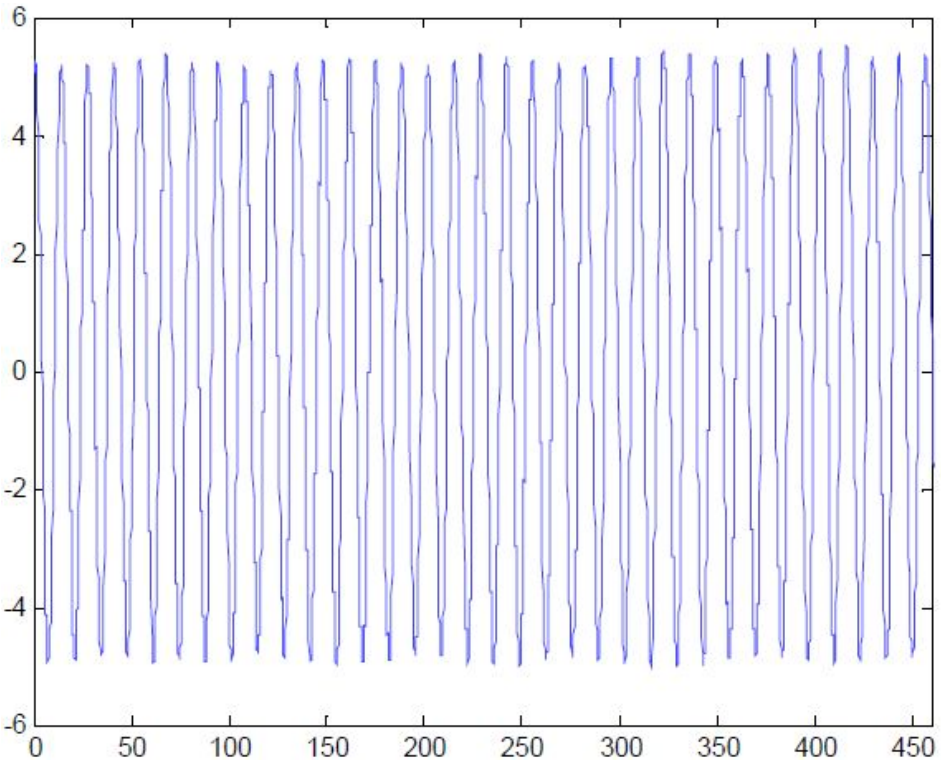

Figure A.8: Heave response from model test run 2010(Glomnes, 2006)

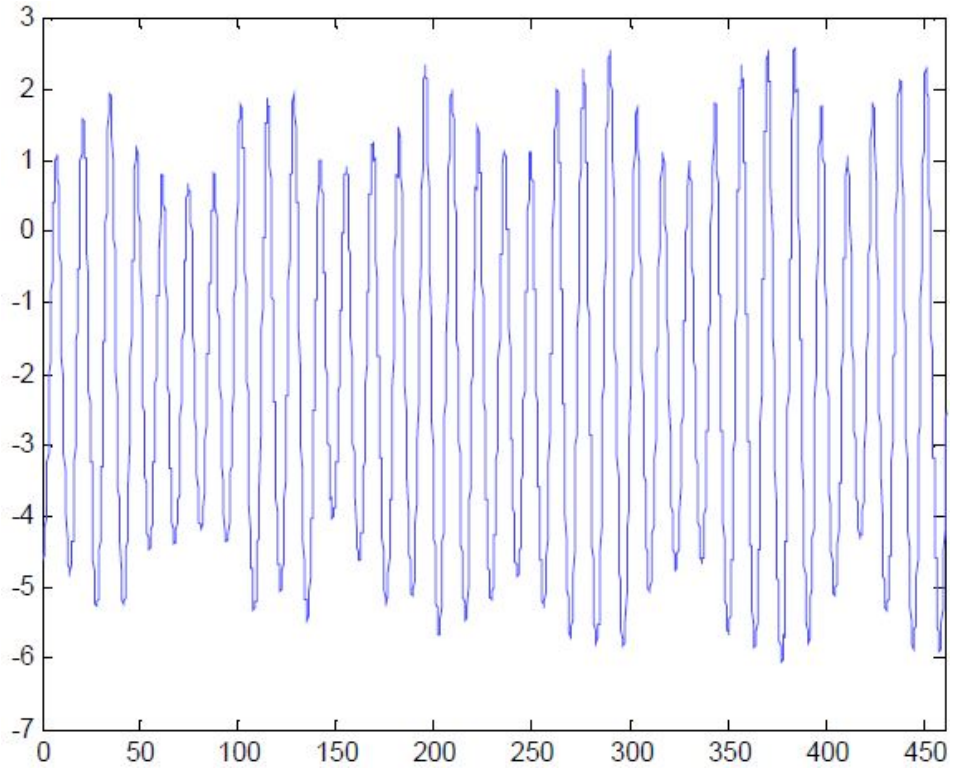

Figure A.9: Pitch response from model test run 2010(Glomnes, 2006)

Numerical Model results

When comparing the results in figure A.10 and A.11 to the model test we can see that the heave response is very close to the model test response. This indicates that the heave motion of the buoy is close to linear. In the case of pitch motion we can see that the relative difference between maximum and minimum is the same, however there is a large difference in the positive and negative amplitude in the model test. In the numerical model the amplitude is the same. It is also important to note that the amplitude is varying in the model test but not in the linear model, this points to a non-linearity in the pitch motion of the buoy.

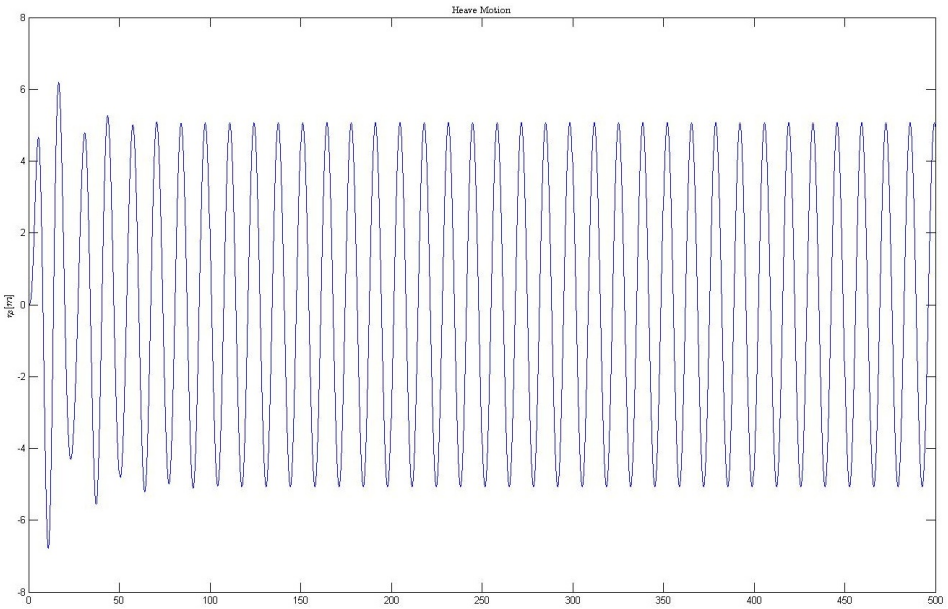

Figure A.10: Heave response from Numerical Model run 2010

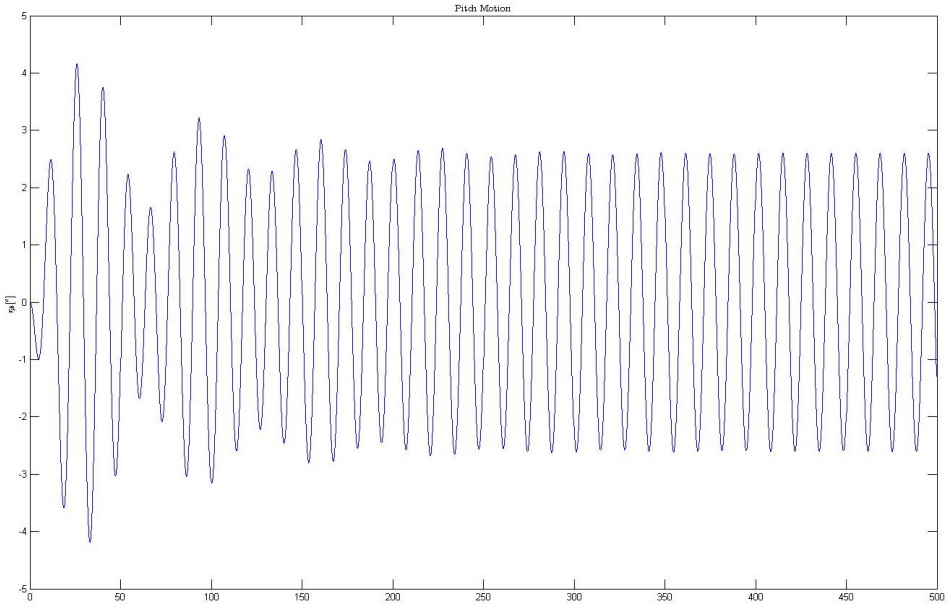

Figure A.11: Pitch response from Numerical Model run 2010

Wasim Results

Heave is again very similar to the model test, but Pitch is not close to the other results, it is about six times larger than the numerical model. The explanation of this might be seen in the linear decay test given in figure A.13. The natural period in pitch is just below 14 seconds for this run which is very close to the wave period, this is a possible explanation for the extreme response as seen in figure A.12, but it also shows that Wasim might not be a good choice for linear calculations. Another important aspect of this is that the linear model does not integrate pressure to the true surface, and this is a possible effect of just integrating to the mean surface.

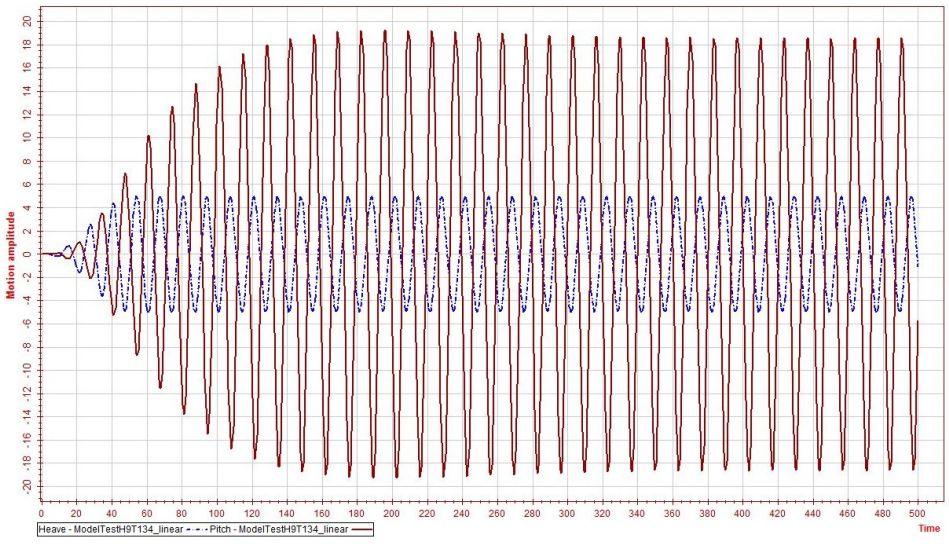

Figure A.12: Heave response from Wasim run 2010

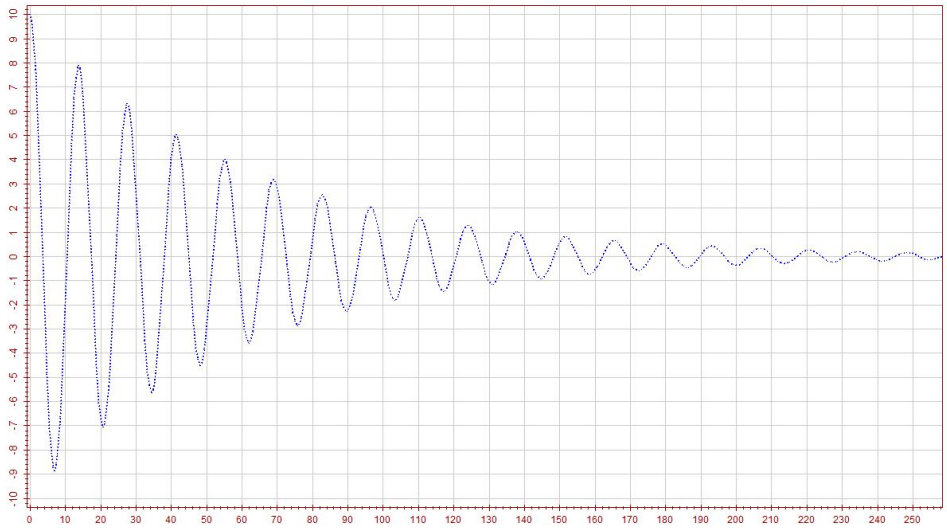

Figure A.13: Linear pitch decay test

A.3 Non-linear regular waves

In the case of non-linear motion the numerical model fails during both runs. First the comparison will only be between Wasim and the model test run(see figure A.8) and if the model test and Wasim run is similar then Wasim can be used for comparison with the numerical model.

Wasim Results from run 2010

The heave results seen in figure A.14 are much the same as in the linear runs. The pitch results are much closer to the model test, however the amplitude is still larger and the amplitude skewness cannot be seen in the Wasim run. The difference in amplitude might be due to the natural period difference which was seen in the decay tests in section A.1 although the natural period is further from the wave period in this it is still within 2.5s. This might be the cause of the difference in the amplitudes.

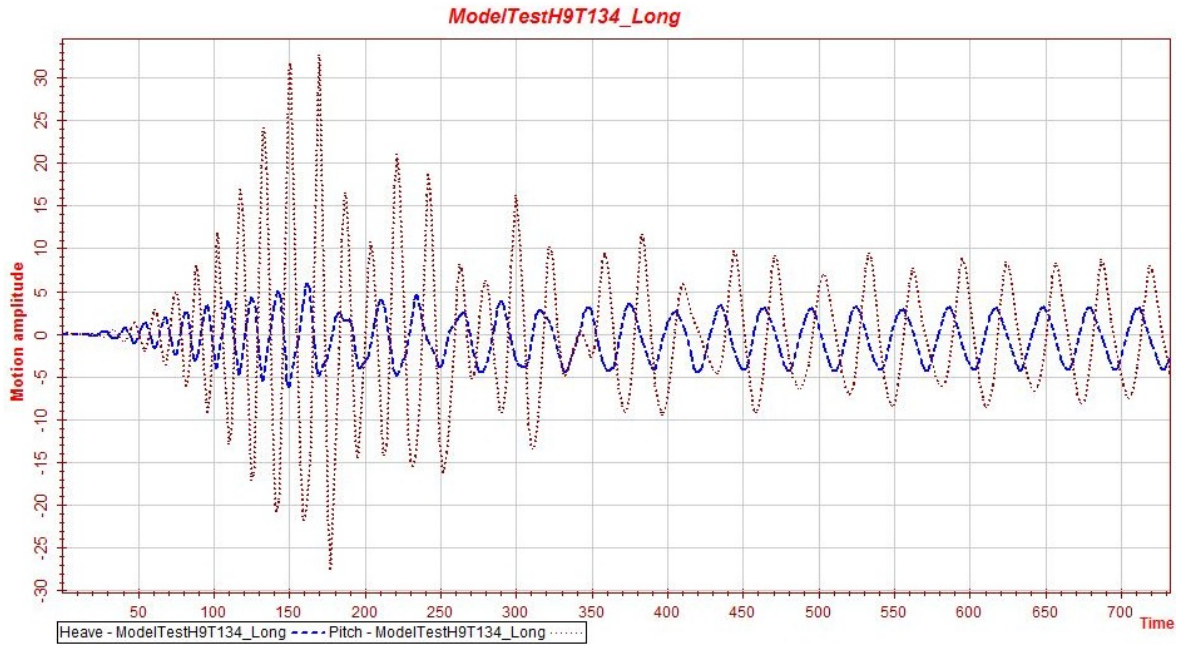

Figure A.14: Non-linear response from Wasim run 2010

A.3.1 Comparison of run 2019

As the pitch motion above has a difference in amplitude a test of the other model test run must be done to ensure that there is a close enough fit outside of the resonance area.

Model test results

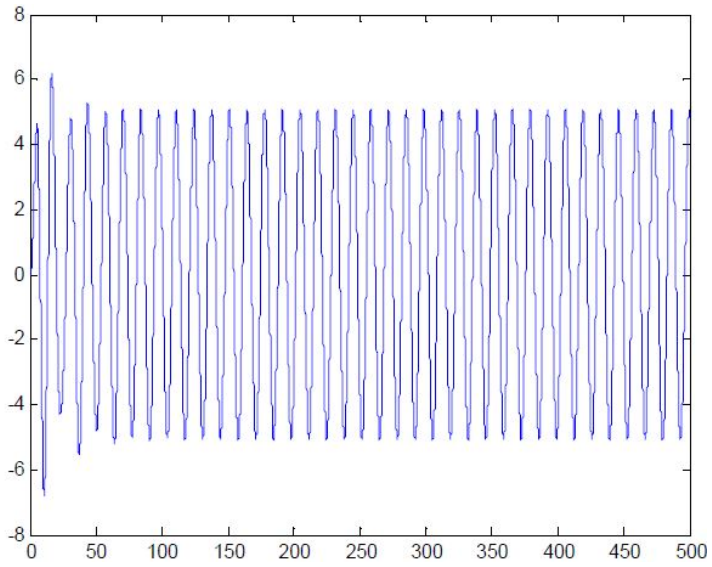

Figure A.15: Heave response model test run 2007

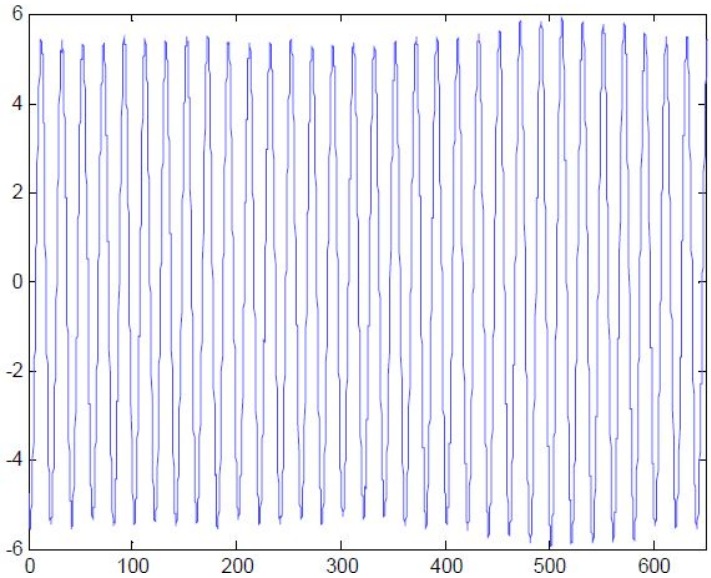

Figure A.16: Pitch response model test run 2007

Wasim Results from run 2019

As can be seen from the graphs (in figures A.15, A.16 and A.17) there is lot less difference in this case. The heave motion is once again very similar and the pitch motion is much closer than what was seen in the linear runs, but in this case Wasim actually gives a lower estimate than the model test. It is difficult to explain this difference but in this case the model test is closer to its natural period so once again this might be a possibility. The difference is not that significant so in preliminary design this difference can be neglected

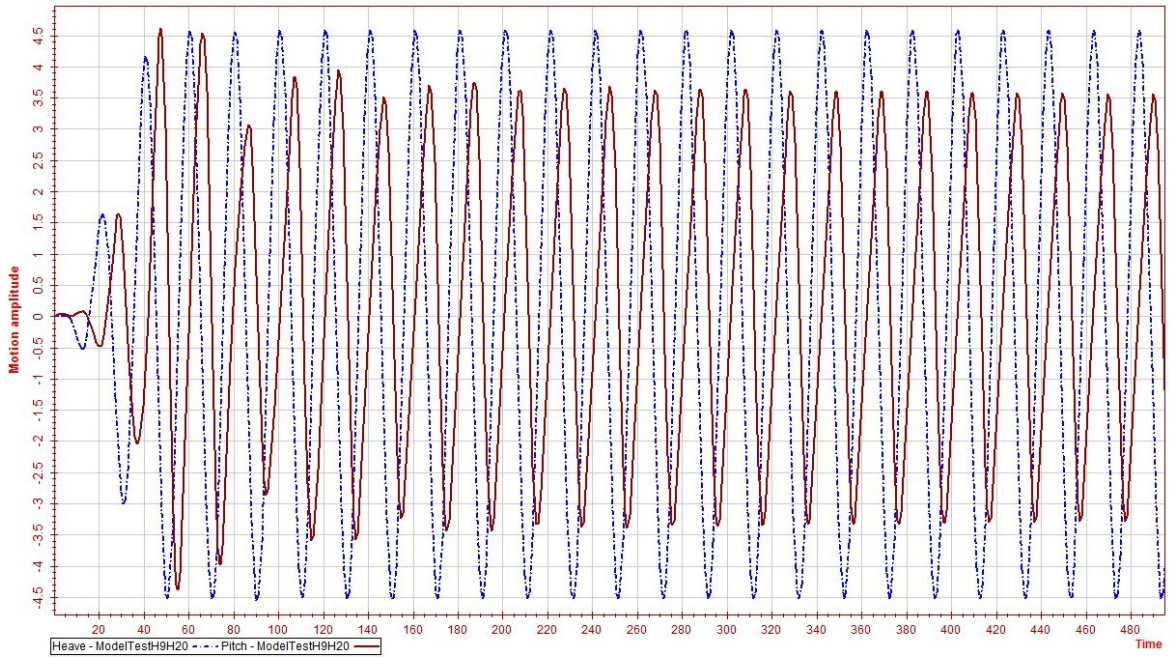

Figure A.17: Non-linear response from Wasim run 2019

A.3.2 Comparison between numerical model and wasim results

As the numerical model fails for the model test waves a different approach must be utilized. As Wasim is close to the model test solution it should be possible to check a milder sea state.(in which the numerical model does not collapse)

H=3 T=15

The intention with this sea state was to check the results for a reasonable low wave height in combination with a long period. The numerical model is partly based on a long wave approximation and should therefore have a good result with the chosen wave.

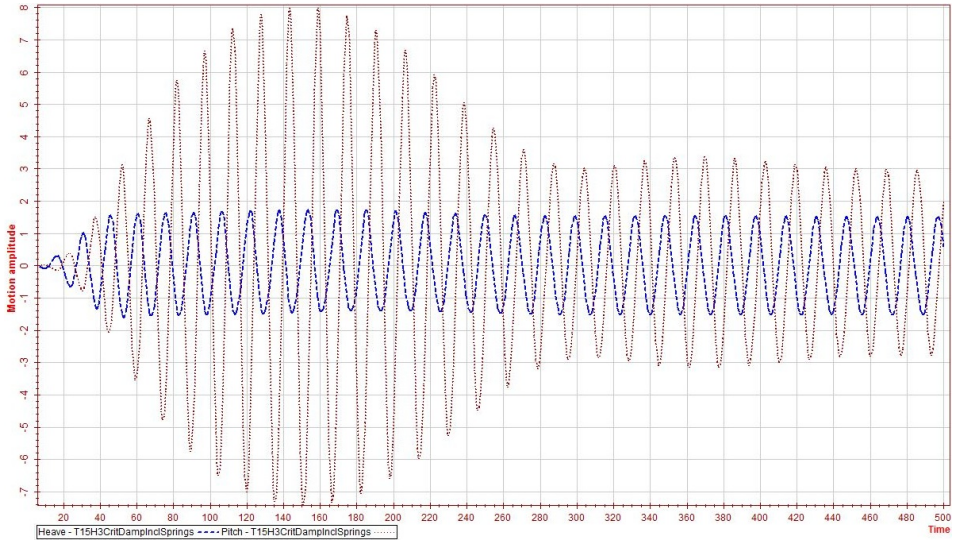

Figure A.18: Wasim Run H=3 T=15

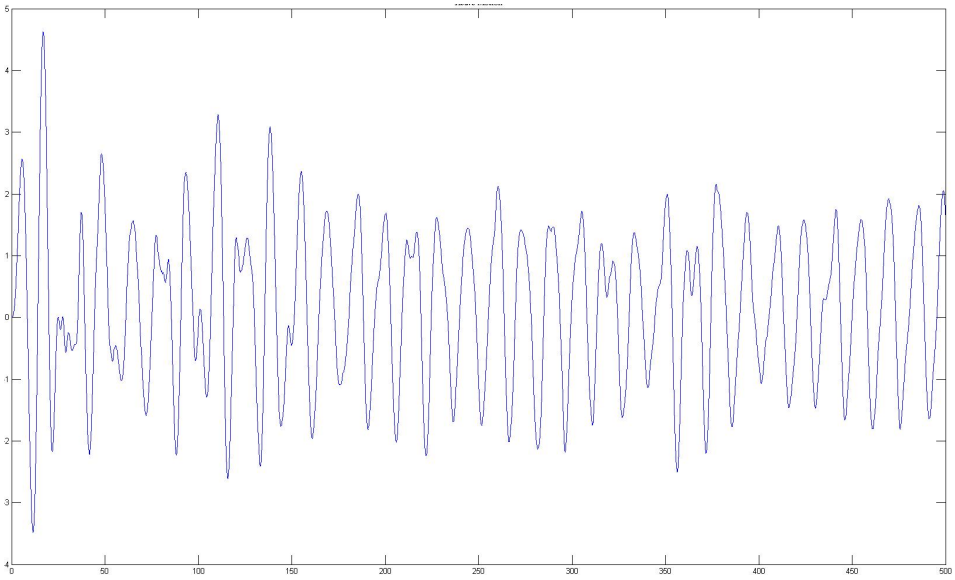

Figure A.19: Numerical Model Run H=3 T=15 Heave

When comparing the results from figures A.18, A.19 and A.20. We can see that there is in general more noise in the numerical model solutions. The heave amplitude has a difference of up to 100% and for the pitch motion we there is about 67% difference in the amplitude.

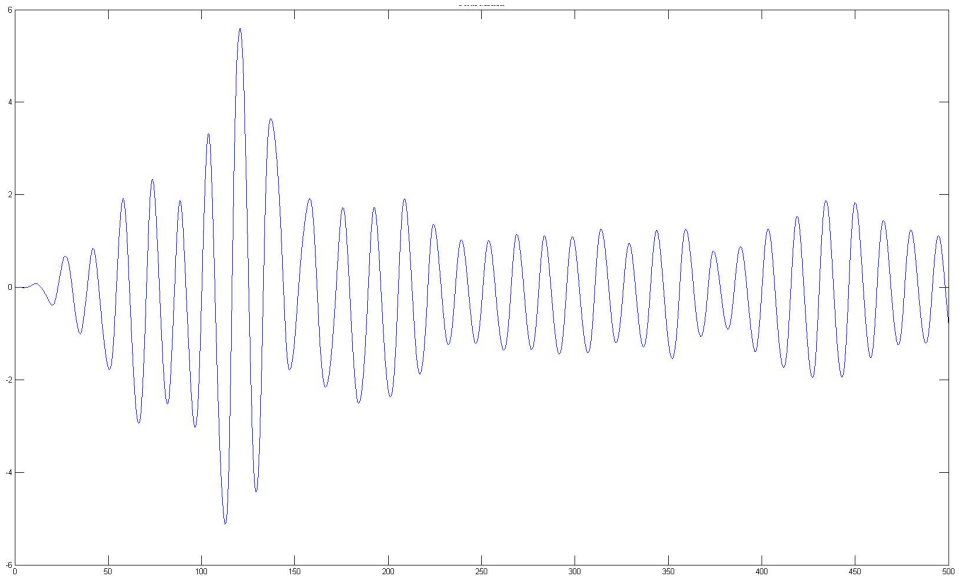

Figure A.20: Numerical Model Run H=3 T=15 Pitch

H=6 T=12

This sea state was chosen to see a generally tougher sea state which is closer to the natural periods of pitch and heave. The results of the runs can be seen in figures A.21, A.22 and A.23

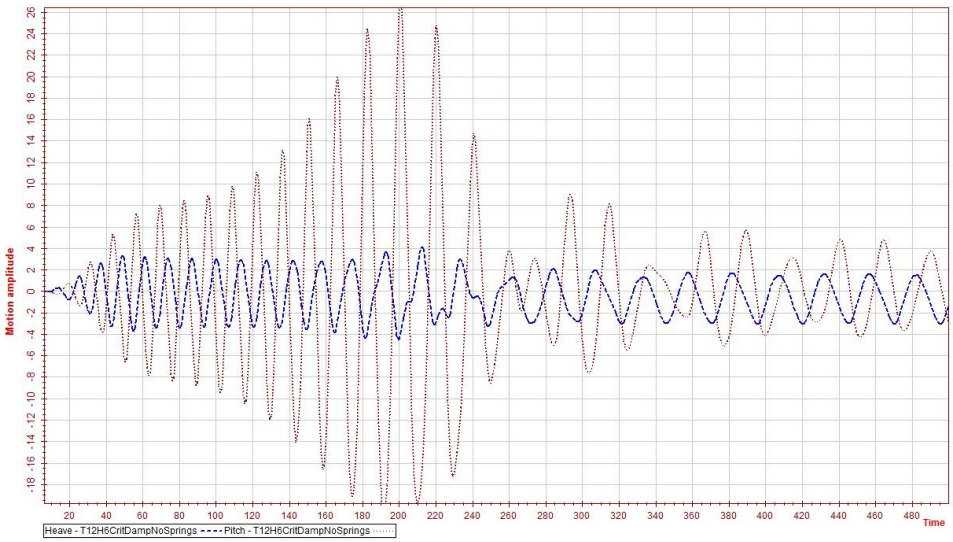

Figure A.21: Wasim Run H=6 T=12

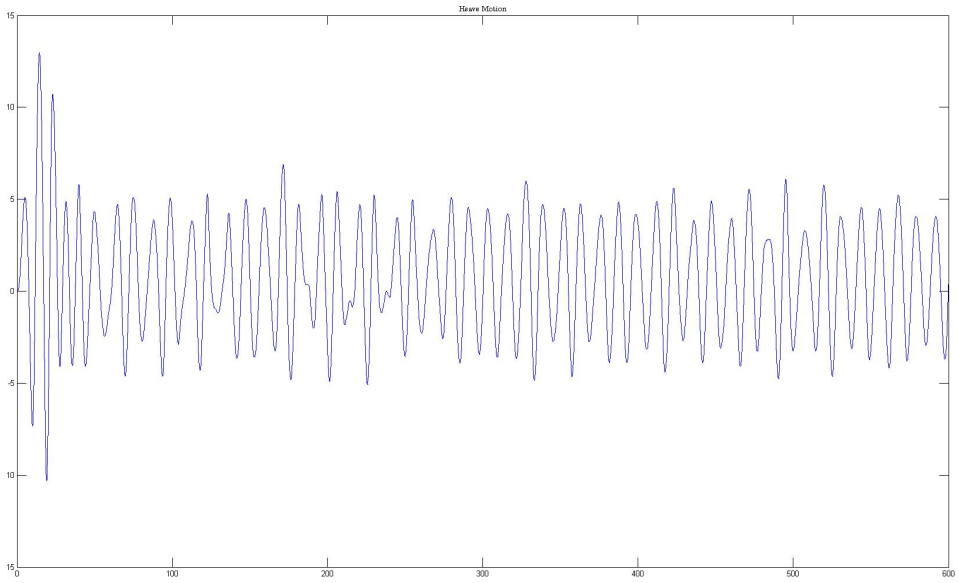

Figure A.22: Numerical Model Run H=6 T=12 Heave

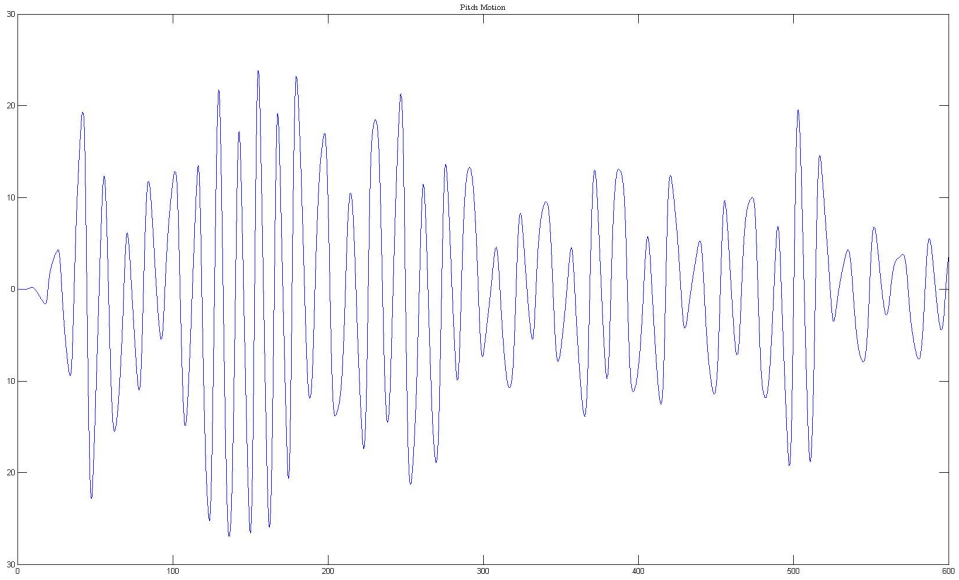

Figure A.23: Numerical Model Run H=6 T=12 Pitch

This result is rather poor for the numerical model solution as even the heave motion, which in general has been close, is very far from the Wasim solution. The difference is about 100% for the pitch motion, for the heave motion we see that there are points where the solutions are very close and some other points where the fit is not quite as good.

A.4 Short Result Conclusion/Summary

The main intention was to check the general solutions of the programs and compare them with model tests. The reason for checking all motion calculations and not just the non-linear part was to remove these from further examination and focus on a specific part of the numerical model in the future. (Wasim was also compared to give insight into the differences in the models)

The non-linear module of the numerical model could not be compared to the model test due to failure while running the numerical model. To check the results of the numerical model it was necessary to use Wasim as an alternative, but this required a confirmation of the results. Comparisons were made between the model tests and Wasim and it can be seen from the graphs given in section A.3 that there is reasonable correlation between the results, and Wasim can therefore be applied as a reference with respect to reliable comparison data.

Finally a couple of comparisons were made between Wasim and the Numerical Model. For a low wave height we can see that the heave and pitch motion is underestimating the response by 50-100%. When doubling the wave height and lowering the period the difference in percentage is very much the same as the previous run except that in this case the numerical model is overestimating the responses. As the numerical model is thought to be giving reasonable answers for low wave heights, this is an indication of the difference between instantaneous pressure integration and the mean surface pressure integration. When the model is tested with a more severe sea state it shows tendencies to give large overestimations of motions. This is most visible in the pitch results, where motions could be as large as 20 degrees.

Appendix B

Problems With the Previous Numerical Model

After comparing the different program results in appendix A. The purpose of this chapter is to highlight the problematic areas and also propose possible solutions. The problems are mostly in the non-linear time integration part of the model. According to (Glomnes, 2006), (Glomnes, 2007) and (Viko, 2006) this has been problematic since the first version of the program. Unfortunately this is still the case. Another difficulty which has been encountered is the presentation of the force results, which at its best can called noisy. An example of this can be seen in figure B.1

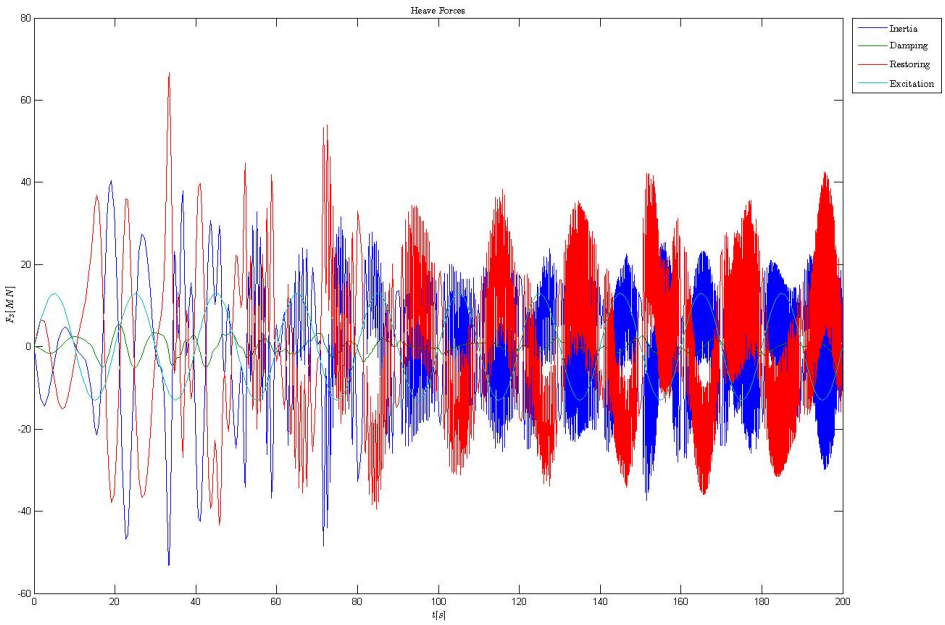

Figure B.1: Example of Force Results

B.1 Identified Problems

B.1.1 Problems With Sea States

The largest problem with the non-linear calculations is the fact that it fails when the wave height is above a certain limit. The output from MATLAB in these runs are complex numbers and near singular values, an example of this can be seen in figure B.2. In this run the structure has been "fixed" by increasing the hydrostatic coefficients, in essence the structure will then be close to motionless, thus eliminating the relative motion between the structure and waves. The point of this exercise is to test the limits of the structure due to steep waves and tall waves. In reality the actual "max" wave height could be lower than this when the structure is allowed to move. This is very likely to happen near the natural periods of the buoy, which makes the wave period an important factor as well.

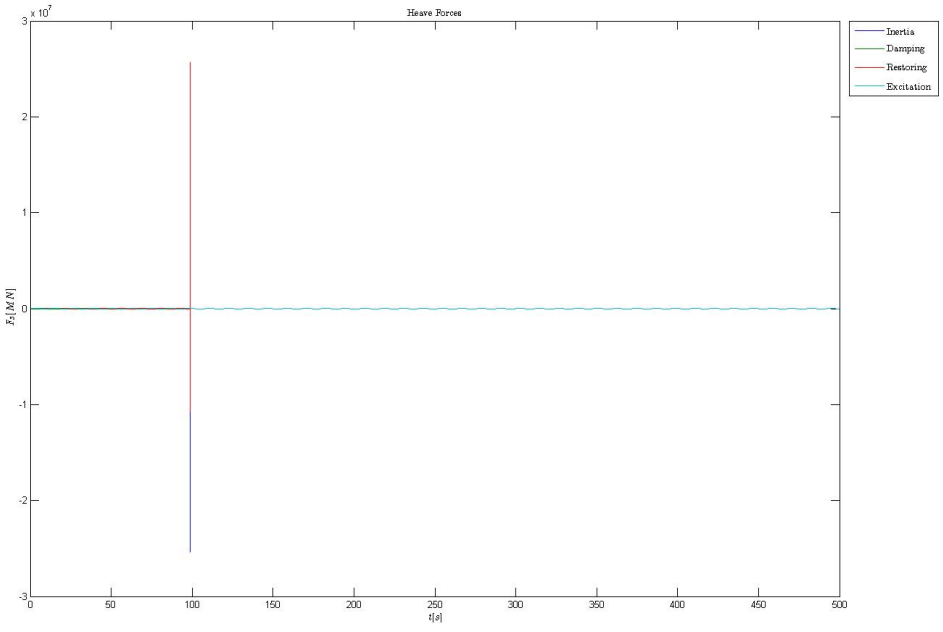

Figure B.2: Results from "fixed" structure in 6 meter waves

This phenomenon occurs when the wave height is high enough, the limit seems to coincide with the height of the slanted part of the hull. This problem is due to a assumption made by (Glomnes, 2006), in which he assumed that the only part of the buoy affected by waves are the slanted parts. This is effectively limiting the maximum wave height which can be applied.

Possible Solution

Review of the initial assumptions made in the non-linear calculation, and try to change the assumptions to include more of the structure in the wave calculations. This could include integration of pressure to the real surface, and other higher order calculations, not just simplifications based on geometry.

B.1.2 Problems With Accuracy

As previously stated in appendix A there are problems with the accuracy of the numerical model with as much as 50-100% difference between the Wasim results and the numerical model. (where the numerical model gives the higher estimates) This problem is particularly difficult to reason out, because it requires a lot of trial and error with the code, and given the generally slow computing time of the numerical model in general makes it a very time consuming task.

The fact that the motions are both underestimated and overestimated depending on the size of the waves might be indicative of an error in either inertia, damping, restoring or excitation forces. As the damping in the numerical model is given as a percentage of critical damping, which of course is dependent on the stiffness and mass as shown in equation 4.8. This means that an error in either the stiffness or mass terms will also affect the damping.

Another problem might be in the way the new time integration function works. Ode45 needs to solve the problem as a system of linear equations, and there are some inconsistencies in the way the force is calculated. The restoring force does not seem to be included in the actual time integration and the inertia force is calculated by enforcing equilibrium after the integration has been completed. The accelerations are then found from the calculated inertia force.

Possible Solution

Assuming that this is not simply due to the problem stated in B.1.1 then this problem might be solved by examining all of the coefficient calculations with a focus on the added mass formulae which are used in Inertia.m. It is specifically the calculations of A(1,5),A(5,1) and A(5,5) which should be investigated further.

It is also important to check the way ode45 solves the problem, this has not been a particular focus of this thesis so it might be correct. However it might be a good idea to solve this problem with a numerical integration scheme which has been written specifically for this problem, thus giving more control of the calculation steps.

Solver	Problem Type	Order of Accuracy	When to Use
ode45	Nonstiff	Medium	Most of the time. This should be the first solver you try.
ode23	Nonstiff	Low	For problems with crude error tolerances or for solving moderately stiff problems.
ode113	Nonstiff	Low to high	For problems with stringent error tolerances or for solving computationally intensive problems.
ode15s	Stiff	Low to medium	If ode45 is slow because the problem is stiff.
ode23s	Stiff	Low	If using crude error tolerances to solve stiff systems and the mass matrix is constant.
ode23t	Moderately Stiff	Low	For moderately stiff problems if you need a solution without numerical damping.
ode23tb	Stiff	Low	If using crude error tolerances to solve stiff systems.

Table B.1: Alternative Runge-Kutta solvers in Matlab

B.1.3 Problems With Slow Time Integration

Finally the time integration scheme chosen is not a very good choice. It does seem to be stable over a larger area compared to the Newmark-β method written by (Viko, 2006), even though this method is supposed to be unconditionally stable. The problem is that ode45 is exceptionally slow, the solver took around 4 hours to complete a 50 second run with a time step of 0.01.

Possible Solution

A possible solution is to change the solver from Ode45 to an alternative which is more applicable to this stiffness dominated problem. The other possible solvers are shown in table B.1

The stiff solvers ode15s and ode23s increases the speed of the solution significantly. The same test yields a run time of a few seconds. It also gives the same answer as ode45 so there is no penalty to the accuracy.

Another option is to return to the previous Newmark-β solver, or write a new one. Theoretically the Newmark-β should be able to handle this problem and yield completely stable results so if the problem described in B.1.1 is solved then this method might work.

B.1.4 Presentation of Forces

As mentioned in the introduction to this chapter the force presentation could be better, first of all is the noise level, second is the fact that every single component is presented in the same graph. The noise level is probably due to poor solutions or accuracy problems as mentioned in the previous sections, so this problem will most likely be solved if the program in general is improved. The second is problematic because it is difficult to process that much information in a single plot. It might be better to present the total force and have the components as optional plots if the user should desire to see them.

Electronic Appendices

Zip File containing

- Last version of the new numerical model
- Last version of the old numerical model
- PDF of Thesis
- Javascript file from WASIM which can be used to recreate model in HydroD